(12) LEVEL II

NSWC TR 80-339

AD A106485

CRITICAL PARAMETERS FOR DETONATION PROPAGATION AND INITIATION OF SOLID EXPLOSIVES

BY DONNA PRICE

RESEARCH AND TECHNOLOGY DEPARTMENT

10 SEPTEMBER 1981

Approved for public release, distribution unlimited.

DTIC
ELECTE
NOV 2 1981
S D
B

DTIC FILE COPY

NAVAL SURFACE WEAPONS CENTER

Dahlgren, Virginia 22448 • Silver Spring, Maryland 20910

81103003 8

UNCLASSIFIED

SECURITY CLASSIFICATION OF THIS PAGE (When Data Entered)

REPORT DOCUMENTATION PAGE		READ INSTRUCTIONS BEFORE COMPLETING FORM
1. REPORT NUMBER (14) NSWC/TR-80-339	2. GOVT ACCESSION NO. AD-A106 485	3. RECIPIENT'S CATALOG NUMBER
4. TITLE (and Subtitle) (4) Critical Parameters for Detonation Propagation and Initiation of Solid Explosives		5. TYPE OF REPORT & PERIOD COVERED
		6. PERFORMING ORG. REPORT NUMBER
7. AUTHOR(s) (10) Donna/Price		8. CONTRACT OR GRANT NUMBER(s) (16) R0C001, R01309
9. PERFORMING ORGANIZATION NAME AND ADDRESS Naval Surface Weapons Center (Code R10) White Oak Silver Spring, MD 20910		10. PROGRAM ELEMENT, PROJECT, TASK AREA & WORK UNIT NUMBERS 61152N; ZR00001, ZR01305; R0116
11. CONTROLLING OFFICE NAME AND ADDRESS (11) ZR01305, ZR0130401		(11) 12. REPORT DATE 10 September 1981
		13. NUMBER OF PAGES 101 (12) 105
14. MONITORING AGENCY NAME & ADDRESS (if different from Controlling Office)		15. SECURITY CLASS. (of this report) Unclassified
		15a. DECLASSIFICATION/DOWNGRADING SCHEDULE

16. DISTRIBUTION STATEMENT (of this Report)

Approved for public release, distribution unlimited

17. DISTRIBUTION STATEMENT (of the abstract entered in Block 20, if different from Report)

18. SUPPLEMENTARY NOTES

19. KEY WORDS (Continue on reverse side if necessary and identify by block number)

Detonation, Shock Sensitivity, Critical Initiating Pressure, Critical Diameter, Failure Diameter, Shock to Detonation Transition (SDT), Critical Particle Size, Critical Density, Critical Temperature

20. ABSTRACT (Continue on reverse side if necessary and identify by block number)

The complicated relations and interdependence of the various critical parameters are demonstrated. In particular, the critical diameter is determined by charge temperature, initial particle size, density, confinement, composition, and shock sensitivity. The critical initiating pressure is also a multivariant function and depends on the same set of variables. Relations between different gap (shock sensitivity) test results and between those of gap and wedge tests are also shown.

DD FORM 1 JAN 73 1473 EDITION OF 1 NOV 65 IS OBSOLETE S/N 0102-LF-014-6601

UNCLASSIFIED

SECURITY CLASSIFICATION OF THIS PAGE (When Data Entered)

411563

JOB

FOREWORD

This report was prepared under Task ZF0130901, IR-159. It is concerned with the complicated relations and interdependence of the various critical parameters as well as relations between the results of various shock sensitivity tests. The same material was presented in a series of eight lectures in 1980-81. It should be of interest in the areas of explosive sensitivity and propellant safety.

JAMES F. PROCTOR
By direction

Accession For	
NTIS GRA&I	☑
DTIC TAB	☐
Unannounced	☐
Justification	
By	
Distribution/	
Availability Codes	
Dist	Avail and/or Special
A	

CONTENTS

ILLUSTRATIONS

ILLUSTRATIONS (CONT.)

ILLUSTRATIONS (CONT.)

TABLES

CRITICAL PARAMETERS FOR DETONATION PROPAGATION AND INITIATION OF SOLID EXPLOSIVES

INTRODUCTION

It is the purpose of this report to examine the available relevant information and to elucidate the very complicated relationships and interdependence of the various critical parameters for detonation propagation and initiation in solid HE. In particular, the role of test diameter relative to critical diameter in affecting the critical pressure for initiating detonation (and vice versa) will be described and illustrated. Comparisons will also be made between experimental values of shock sensitivity from different gap tests and the wedge test. Critical density (in the form of % TMD), critical particle size, and critical temperature for propagation, and critical pressure for shock initiation will also be considered.

Since there will necessarily be cross references to critical diameter and gap test values, these will be defined here, and later described and discussed in separate sections. The critical diameter (d_c) is defined for a cylindrical solid charge as the minimum diameter at which a steady state detonation can propagate. The gap test is a widely used measure of shock sensitivity. In its simplest form, it consists of a cylindrical donor, attenuator, and acceptor. We shall consider only those tests in which the shock attenuator (gap) is a solid material. The test arrangement is that of Fig. 1. In a series of test firings, the gap thickness is varied until the 50% point is reached, i.e. that gap thickness for which detonation occurs in 50% of the trials. That 50% point gap is defined as the test value. If the test has been calibrated, the test value can also be given as shock pressure at the end of the gap (P_g). If the Hugoniot of the explosive acceptor is known, this can be converted to P_{ci} the transmitted pressure which is the minimum initiating or critical pressure to initiate detonation in that acceptor in that test.

To achieve steady-state detonation, a cylindrical charge must have $d \geq d_c$ and the initiating shock must have an amplitude $P \geq P_{ci}$. Together these conditions are necessary and sufficient for steady-state detonation. This report will consider each in turn.

CRITICAL DIAMETER

Historical

Sometimes the critical diameter is defined as the smallest diameter of a charge at which propagation of an undamped detonation wave is still possible. This definition has been avoided here because it includes the case of gases and liquids in which a constant velocity front appears, but the propagation is by means of fading and re-ignition. In other words, the steady-state detonation structure is absent. At the present time, this phenomenon has not been observed in solids and it is believed that the sustained front in detonating solid HE has the Zeldovitch-von Neumann-Doering (ZND) model structure. According to this model, the detonation wave with one-dimensional flow has the structure:

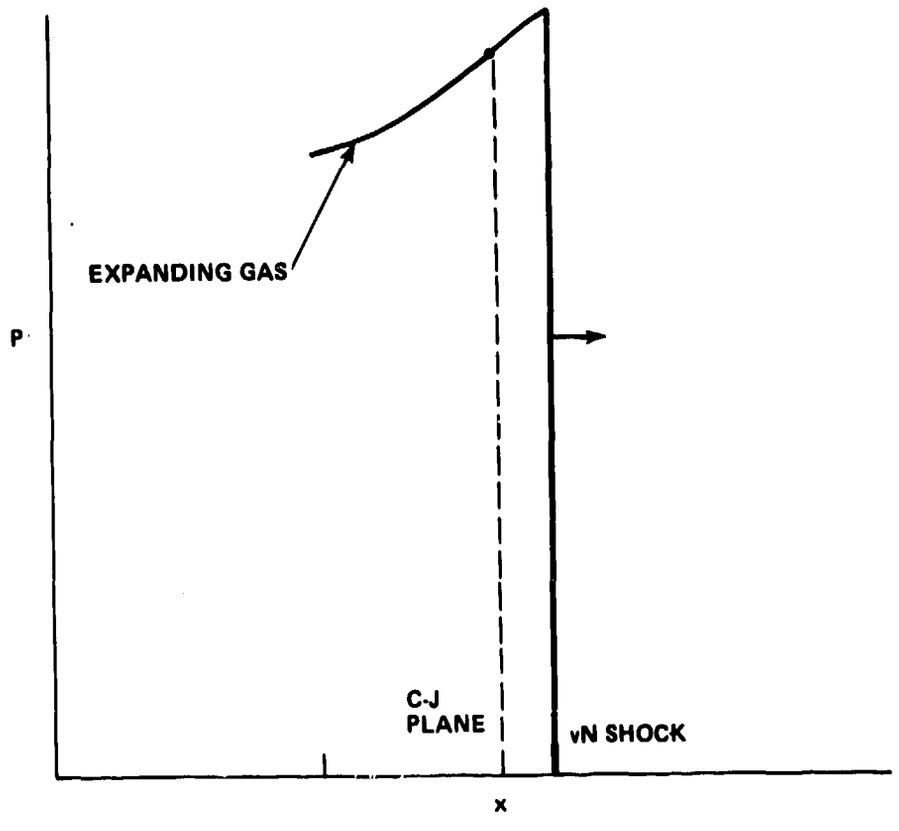

The plane of the von Neumann shock is separated from the Chapman-Jouguet (C-J) plane by a distance called the reaction zone length. Reaction can start at the shock front; it must be completed at the C-J plane. The pressure drop between these two planes results from a combination of heterogeneous (hot spot) and homogeneous reactions; in the latter, the von Neumann pressure is maintained for the induction time (i.e. throughout most of the reaction zone) after which the pressure falls very rapidly to the C-J value. In the case of heterogeneous reaction, the pressure starts to drop immediately after the von Neumann shock and reaches the C-J value with a less steep gradient.

The structural unit bounded by the C-J and von Neumann planes is propagated unchanged in a steady state detonation. On the other hand, the gas products follow the C-J plane in a continuously changing structure as the wave propagates.

According to the definition chosen, the critical initiating pressure for cylindrical charges at the critical diameter is then the von Neumann spike pressure, and the critical initiating pressure pulse is that between the von Neumann and C-J planes of the detonation front. These two planes are separated by a distance $\underline{a}$ (reaction zone length) and a time $\underline{\tau}$ (reaction time).

Another way of saying this is that at the critical diameter, a cylindrical charge can be cut in two cylinders of half length. One half can be used as the donor, the other as an acceptor in a gap test. The 50% point should then be zero gap.

For essentially voidless materials of 95% or greater theoretical maximum density (TMD), the detonation velocity at critical conditions (D_c) is, of course, less than the ideal detonation velocity (D_i). However, it is not a great deal less at high % TMD. For example, pressed and cast TNT at 98% TMD have D_c/D_i values of 0.95 and 0.94, respectively[1]. DNT at 99% TMD has a D_c/D_i value of 0.85[2]. On the other hand, high porosity, granular charges exhibit much

[1]Price, D., "Shock Sensitivity, A Property of Many Aspects," 5th Symposium (International) on Detonation, ONR ACR-184, U.S. Gov. Printing Office, Washington, DC, 1972; pp 207-217.

[2]Price, D., Erkman, J. O., Clairmont, Jr., A. R., and Edwards, D. J., "Explosive Characterization of Dinitrotoluene," Combust. Flame, Vol. 14, 1970, pp 145-148.

lower values; e.g., TNT at 50% TMD has a D_c/D_i value of 0.65[1] and 25μ AP at 51% TMD, about 0.45[3]. These values are given for illustration only, not for generalization. D_c, like d_c, is a function not only of the chemical composition of the charge, but also of its initial particle size (δ), temperature, and % TMD.

In the conventional 1-D, plane theory, the C-J pressure (P_j) is given by

$$P_j = \rho_o D_i^2/(\gamma+1) \qquad (1)$$

This theory does not, of course, consider diameter effect; that can be treated only with a 2- or 3-D model with a reaction zone of finite thickness. However, we can use Eq. 1 to obtain estimates of the orders of magnitude involved. Thus at $D_c/D_i = 0.95$, $(P_j)_c \sim 0.9\ P_j$. In the case of high density TNT, $P_{vN} = 1.25\ P_j$[4]. Hence $(P_{vN})_c \sim 1.25(P_j)_c \sim 0.9 \times 1.25\ P_j = 1.125 \times 189$[4] = 213 kbar.

Khariton[5,6] evidently first attempted to express the diameter effect on detonation velocity D and the critical diameter d_c quantitatively. Like earlier workers, he explained the effect by energy losses caused by rarefactions entering the reaction zone from the lateral surfaces. And the principle he proposed was:

$$d_c \sim 2\tau c \qquad (2)$$

where c is the average sound velocity in the detonation products and τ is the detonation reaction time. Thus $\tau c \sim$ distance traveled (one radius) by the rarefaction before it quenches the reaction.

---

[3]Price, D., Clairmont, Jr., A. R., and Jaffe, I., "Explosive Behavior of Ammonium Perchlorate," Combust. Flame, Vol. 11 No. 5, 1967, pp 415-425. Also ibid. Vol. 13, No. 1, 1969, pp 104-108.

[4]Coleburn, N. L. and Liddiard, Jr., T. P., "Hugoniot Equations of State of Several Unreacted Explosives," J. Chem. Phys., Vol. 44, No. 5, 1966, pp. 1929-1936.

[5]Khariton, Yu. B. and Rozing, V. O., Dokl. AN SSSR, Vol. 26, 1940, p. 360. Through Ref. 7 and 8.

[6]Khariton, Yu. B., Collection: "Problems of the Theory of Explosives," Izd-vo AN SSSR, Moscow, 1947. Through Ref. 7 and 8.

From Eq. 2, Kharitor derived

$$\frac{d_{c_1}}{d_{c_2}} = \frac{\tau_1}{\tau_2} \tag{3}$$

for the same explosive under different conditions, e.g. different initial particle size. He also derived

$$\frac{d_c}{D_c} \propto \tau_c \tag{4}$$

His derivation is described in Ref. 9, but an estimate can be obtained from the 1-D theory. There

$$c = (\gamma/\gamma+1)D \tag{5}$$

Hence $c \propto D$ and Eq. 2 produces Eq. 4. The latter must be applied cautiously, however, because γ and hence the proportionality function can differ from explosive to explosive; γ is also a function of the density.

Khariton's principle stimulated a great deal of experimental work on d_c in Russia. But since the advent of the electromagnetic method[7] to measure mass velocity as a function of time, and to estimate τ, it has been recognized that Eqs. 2-4 are certainly not quantitative[7,10] and cannot be used to estimate even relative values of τ.

[7] Dremin, A. N., Savrov, S. D., Trofimov, V. S., and Shvedov, K. K., "Detonation Waves in Condensed Media," Izd-vo Nauka, Moscow, 1970. Translation AD 751417.

[8] Dremin, A. N. and Trofimov, V. S., "Nature of the Critical Detonation Diameter of Condensed Explosives," Combustion, Explosion, and Shock Waves, Vol. 5, No. 3, 1969, pp. 208-12.

[9] Rybanin, S. S., "Effect of Inhomogenties in an Explosive on the Critical Detonation Diameter," PMTF, Vol. 10, No. 4, 1969, pp 141-144, through a translation journal.

[10] Kravtsov, V. V. and Silvestrov, V. V., "Effect of Low Temperature on Detonation Parameters of Cast Trotyl," Combustion, Expl. and Shock Waves, Vol. 15, No. 3, 1979, pp. 387-390.

Slightly later, Jones in England[11] and Eyring et al.[12] in USA introduced analytical expressions for D as a function of d. The latter, for unconfined charges, is

$$\frac{D}{D_i} = 1 - \frac{a}{d} \tag{6}$$

where "a" is the reaction zone length, assumed a constant. This is a linear relationship between the ratio of detonation velocities and d^{-1}. It fits D(d) data of most explosives well at large d and not at all as d approaches d_c[13]. Jones' relationship is more complicated; it fits the data somewhat better, but not well[13].

Recently Campbell and Engelke[14] have added a correction term to Eq. 6 to obtain:

$$\frac{D}{D_i} = 1 - \frac{A}{(R-B)} \tag{7}$$

where A and B are length parameters and R is the charge radius. Eq. 7 fits the D(d) data of more than a dozen essentially voidless explosives down to $d = d_c$.

---

[11]Jones, H., "The Theory of the Dependence of the Rate of Detonation of Solid Explosives on the Diameter of the Charge," Proc. Roy. Soc., Vol. A189, 1947, p. 415.

[12]Eyring, H., Powell, R. E., Duffey, G. H., and Parlin, R. H., "The Stability of Detonation," Chem Revs., Vol. 45, 1949, p. 69.

[13]Malin, M. E. and Campbell, A. W., "Particle-Size Effects in Explosives at Finite and Infinite Diameters," J. Appl. Phys. Vol. 28, 1957, pp. 63-69. Also Malin, Campbell and Mautz, "Particle Size Effect in One- and Two-Component Explosives," 2nd ONR Symposium on Detonation, 1955, pp 360-381.

[14]Campbell, A. W. and Engelke, R., "The Diameter Effect in High Density Heterogeneous Explosives," Sixth Symposium (International) on Detonation, ACR 221, ONR, U.S. Gov. Printing Office, Washington, 1978; pp. 642-663.

Dremin, et al.[7,8] considered that Jones' nozzle theory[11], Eyring's curved front theory[12], and subsequent work[15-19] based on "extremely simplified schemes of flows" have produced little or no advance. In other words, a rigorous theory of detonation limits for condensed explosives has not yet been developed. Dremin[8] formulated the problem and described the fundamental physical principles which he believed could be the basis for constructing such a theory. His discussion is the most helpful reference for failure limits encountered in the literature. Another hopeful initial treatment has been recently published by Chaiken and Edwards[20].

Measurement

The critical diameter can be measured in several ways. The explosive can be cast or machined into a right cylindrical cone. When it is initiated at the base, d_c is the cone diameter at which detonation fails. The detonation can be followed optically or electronically[21]. This method has the disadvantage that propagation from larger to smaller diameters along the cone results in overboosting which may show quenching at a diameter somewhat less than the

[15] Wood, W. W. and Kirkwood, J. G., "Diameter Effect in Condensed Explosives. The Relation between Velocity and Radius of Curvature of the Detonation Wave," J. Chem. Phys., Vol 22, No. 11, 1954, pp 1920-23.

[16] Cook, M. A., "The Science of High Explosives," Reinhold, New York, 1958.

[17] Dubnov, L. V., "Losses in a Detonation Wave," Russian J. Chem. Phys., Vol. 30, No. 10, 1960, pp 1124-5.

[18] Evans, M. W., "Detonation Sensitivity and Failure Diameter in Homogeneous Condensed Materials," J. Chem. Phys., Vol. 36, No. 1, 1962, p. 193.

[19] Rempel, G. G., collection: "Explosives" No. 52/9, 39, through Ref. 7.

[20] Chaiken, R. F. and Edwards, John C., "A Kinetic Lattice Approach to Detonation in Heterogeneous Explosives," Sixth Symposium (International) on Detonation, ACR 221, ONR, U.S. Gov. Print. Office, Washington, D. C., 1978; pp 344-351.

[21] Jaffe, I. and Price, D., "Determination of the Critical Diameter of Explosive Materials," ARS Journal, Vol 32, 1962, pp 1060-1065.

true d_c. Another method is to use a stepped cylinder with long enough segments to allow any overboosting to die out. At $d \gg d_c$, a charge length $\ell \geq 3d$ is quite adequate; but as $d \to d_c$, the Russians use ℓ of 10-12 d. Finally, a series of cylinders of varying diameter can be used, and D(d) determined. Then Eq. 7 can be used to select d_c in the interval between the diameter at which detonation failed (d_c^-) and the next larger d where it propagated (d_c^+). This last method seems the best although the value of d_c so obtained may differ very little from the average of d_c^+ and d_c^- if the experimental increment ($d_c^+ - d_c^-$) is small.

There are insufficient data in the literature to compare conical and cylindrical determinations of d_c from the same charge by the same investigators. If the angle of the cone is kept very small, it is doubtful that the difference in the method of measurement could be distinguished from the effect of differences in charge preparation that would inevitably occur in two different laboratories. Consequently, no distinction has been made in the method used to obtain the d_c values listed in the later tables.

Because it is difficult to prepare charges as cylinders of very small diameter, it is much simpler to measure a critical layer height of an explosive slab. For a confined layer this thickness was designated h_c and its relation to d_c was given as

$$d_c \simeq 2h_c \tag{8}$$

by Belyaev and Sukoyan[22] for a flat plate of thickness h of TNT (ρ_o = 1.57 g/cm^3, δ_o = 400 - 800μ); the explosive was confined on the underside by a 5 mm thick witness plate of lead. It is reasonable to expect some such relationship between d_c and h_c, but how general and how quantitative it may be is an open question. In a recent LASL report[23], the results of critical wedge thickness tests are given; these tests too had a confining witness plate (brass) as well as some lateral confinement. Data for four cast and four pressed explosives

[22] Belyaev, A. F. and Sukoyan, M. K., "Detonability of Some Explosives with Increase in External Pressure," Comb., Expl., and Shock Waves, Vol. 3, No. 1, 1967, pp 11-13.

[23] Urizar, M. J., Peterson, S. W., and Smith, L. C., "Detonation Sensitivity Tests," LA-7193-MS, April 1978.

on which d_c values are also available are given in Table 1. Since the ratio d_c/h_c varies from 1.2 to 7.6, it does not appear that Eq. 8 or a similar one can now be used for anything except establishing an order of magnitude. However, a more controlled study, e.g. identical preparation and charges (ρ_o, composition, particle size) might improve this situation.

In addition to being a function of the chemical composition of the charge, the value of the critical diameter is a strong function of 1) degree of compaction/porosity, 2) initial particle size of a granular charge or the nature of the casting of non-granular charge, and 3) the test temperature. These variables will be considered in turn.

Porosity/% TMD Effect (Critical Density)

If we represent the theoretical maximum density by TMD, then the percent porosity is (100 - % TMD). For TNT-like materials, d_c decreases as % TMD increases (see Fig. 2); for materials like ammonium perchlorate and its mixtures, d_c increases as % TMD increases (See Fig. 3). These curves, dividing the d-% TMD plane into detonation and failure areas, are called detonability curves. For any given HE, at a specific % TMD, there is a critical diameter for detonation, d_c. Similarly for any fixed charge diameter, there is a critical value of % TMD (or ρ_{oc}) for propagation of detonation. Hence one may speak of either critical diameter or critical density. Other critical parameters described later must also be considered in parallel although these two are probably the most studied.

At the time data of Figs. 2 and 3 were determined, their trends were used to classify HE into Group 1 (TNT-like) and Group 2 (AP-like) explosives[27]. However, further work revealed that there was an upturn in the Group 1 curve at high % TMD, and in the Group 2 curve at low % TMD. In other words, the general failure curve appears to be U shaped although both branches are not generally found in easily accessible experimental ranges. Fig. 4 shows the reversals for NQ (Group 1) at 80-85% TMD and AP (Group 2) at 40-25% TMD. Materials showing Group 2 behavior at high % TMD are those likely to dead-press, i.e. become subcritical at high density.

[27] Price, D., "Contrasting Patterns in the Behavior of High Explosives," Eleventh Symposium (International) on Combustion, Combustion Inst., Pittsburgh, 1967; pp 693-702.

TABLE 1

Critical Heights and Diameters for Various Charges

Material	ρ_o (g/cm^3)	Critical Values: Wedge Ht.* h_c (mm)	d_c (mm)	d_c Ref.	d_c/h_c
		Cast Charges			
50/50 Pentolite c	1.700	1.39	6.7	21	4.8
Comp B(A) c	1.713	1.42	4.3	14	3.0
Comp B-3 c	1.728	0.82	6.2	21	7.6
75/25 Cyclotol c	1.752	1.51	6.0	14[a]	4.0
			8.0	21	5.3
		Pressed Charges			
DATB	1.724	0.73	5.3	25[b]	7.3
PBX 9404	1.78-1.85	0.46	1.18	14	2.6
Comp A-3	1.63	0.56	<2.2	24	<3.9
TNT	1.63	2.16[d]	2.62	14	1.2

*Ref. 23. If density range was short, values of replicate runs were averaged; large ranges in ρ_o are indicated.

a. Value for 77/23 cyclotol.

b. Value for ρ_o = 1.8 g/cm^3.

d. Pressed at 65°C.

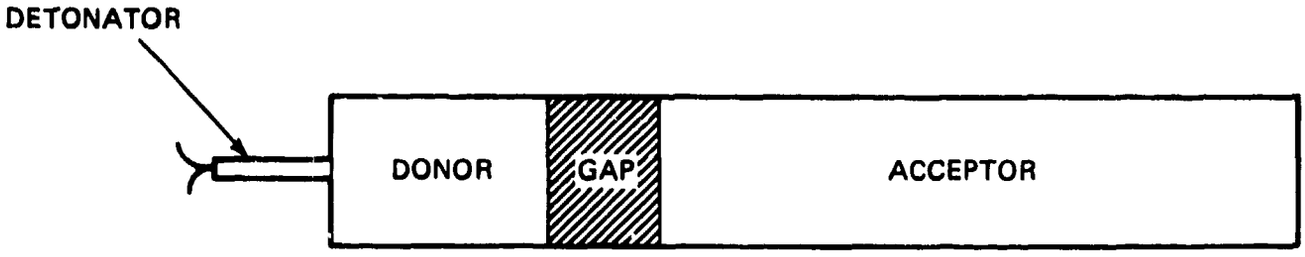

FIGURE 1 SIMPLE GAP TEST

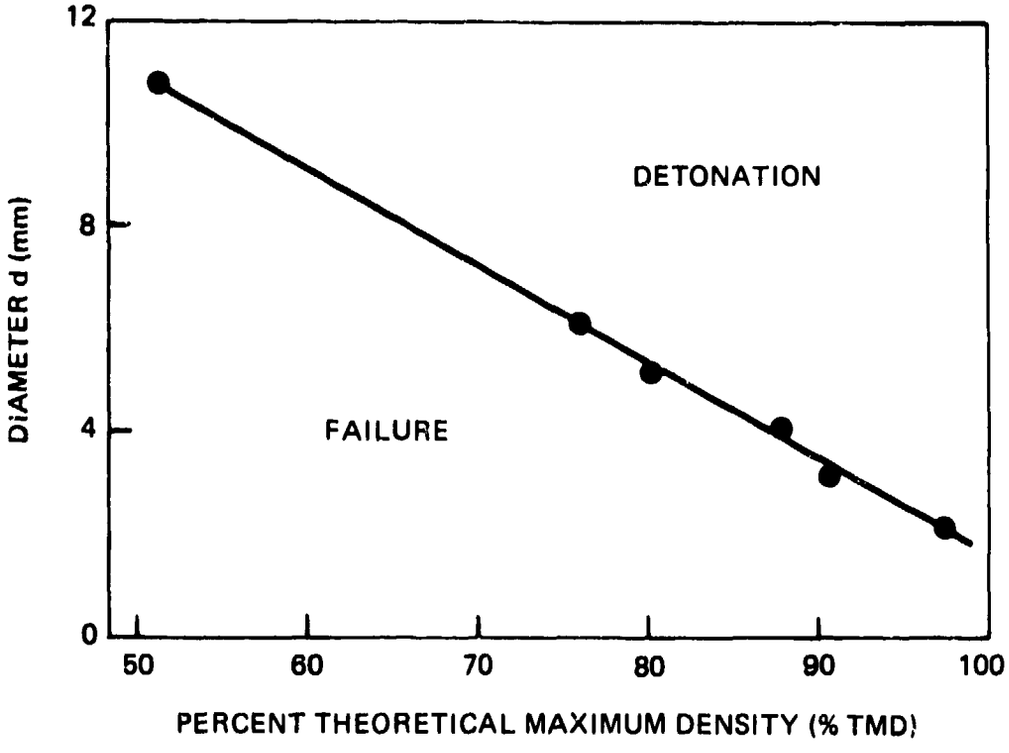

FIGURE 2 DETONABILITY LIMITS IN THE CHARGE DIAMETER-POROSITY PLANE, GROUP 1. EXAMPLE SHOWN IS TNT (GRAIN SIZE 0.07 TO 0.2 mm) DATA (REF. 26)

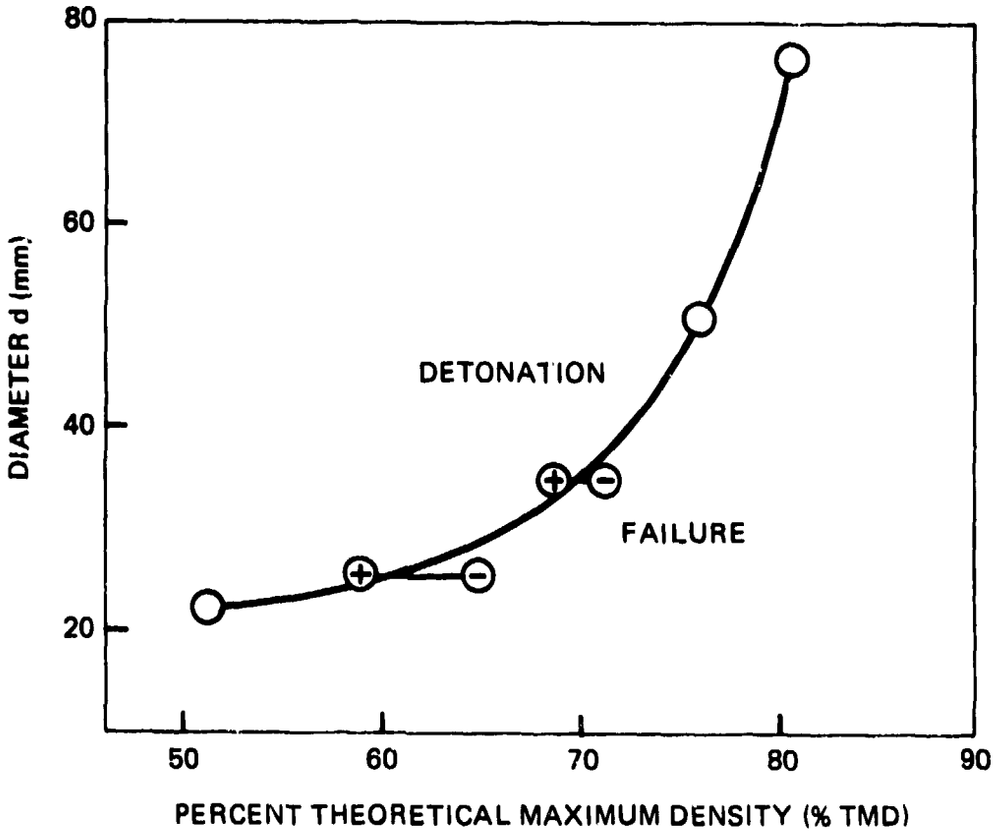

FIGURE 3 DETONABILITY LIMITS IN THE CHARGE DIAMETER POROSITY PLANE, GROUP 2. EXAMPLE SHOWN IS AP (AVERAGE PARTICLE SIZE 10 μ) DATA (REF. 3). WHERE VALUE HAS BEEN BRACKETTED, (+) INDICATES DETONATION, (–), FAILURE

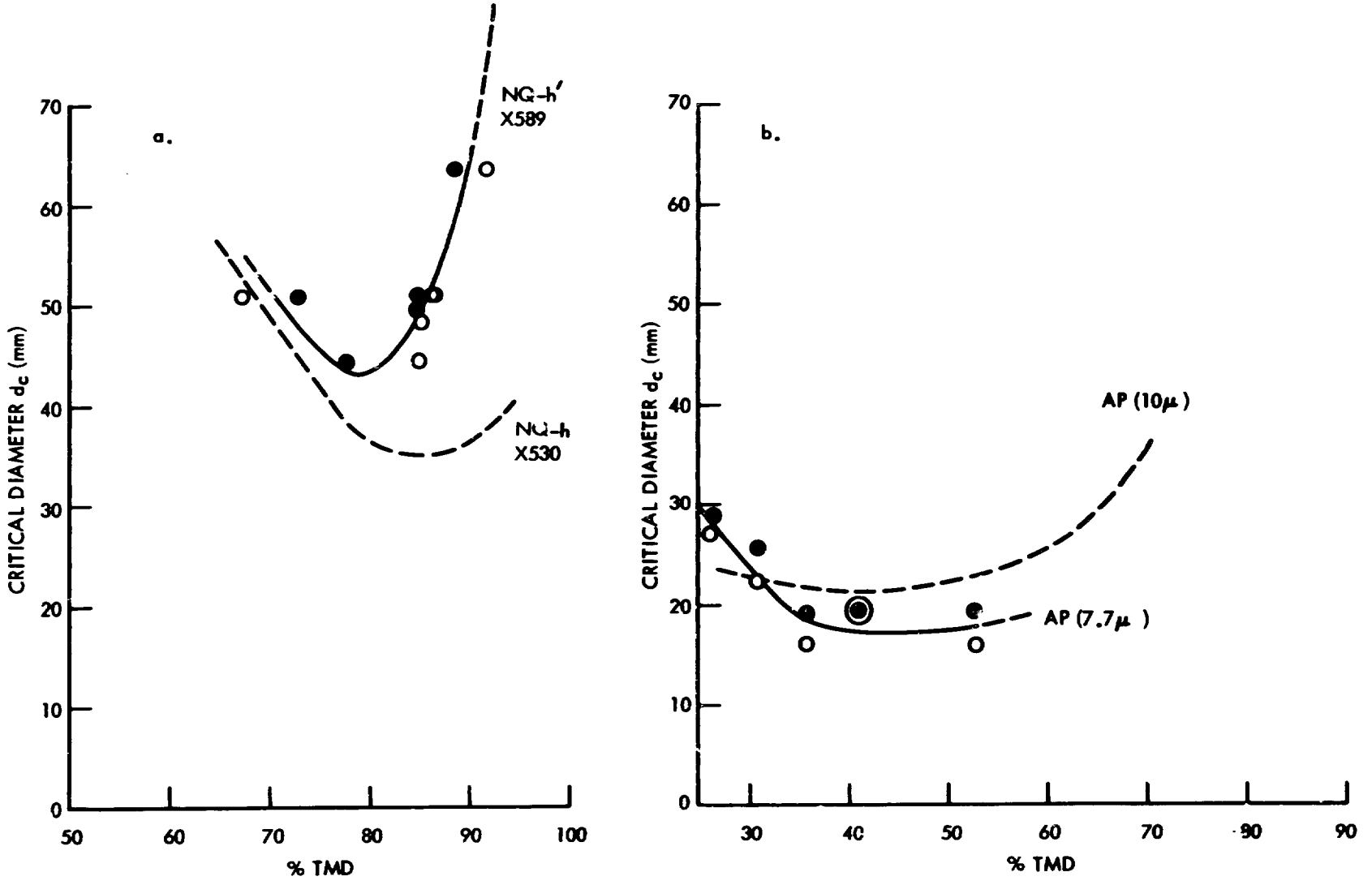

FIGURE 4 MINIMA IN DETONABILITY CURVES. (● DETONATION; O FAILURE). (REF. 28)

The compaction effect on d_c results in rather different D(d) vs % TMD patterns for the two HE groups as shown in Fig. 5. These patterns as well as the detonability curves (d_c vs % TMD) can be used for classification. Although the extrapolated portions of the D vs % TMD curves of Fig. 5a (Group 1) are drawn to show a marked curvature as they approach the failure threshold, such curvature may be difficult to detect experimentally for the rapidly reacting charges of Group 1. Thus TNT appears to have linear curves even to the failure limit except for the smallest diameter charge tested[29]; its detonability plot showed definite curvature.

Figs. 5 a & b illustrate very clearly that Group 1 materials approach ideal behavicr (D_i and small reaction zones) at high % TMD whereas Group 2 HE become more ideal at low % TMD. The different behaviors are attributed to the dominance of homogeneous reaction in Group 1 materials and of heterogeneous reaction in Group 2 materials as discussed in Ref. 27.

Relatively few detonability curves are available, and not a great many investigations of D(d) have been carried out. From the available data, members of Group 1 are:

TNT

All the more powerful common organic explosives*

Mixtures of the above with each other and inerts

NQ**

DNT***

---

[29]Stesik, L. N. and Akimova, L. N., "An Indirect Method of Estimating Reaction Zone Width of a Detonation Wave," Russ. J. Phys. Chem., Vol. 33, No. 8, 1959, pp 148-151.

*So classified because no anomalies in D measurements have been reported. If one should occur, the specific HE should be investigated in detail.

**Group 2 behavior at high densities (Figs. 4 and 8).

***Group 2 behavior at high densities (Fig. 8). Ref. 27 quoted a Russian statement that "weak individual explosives e.g. dinitro-compounds of aromatic hydrocarbons" exhibited Group 2 behavior. Subsequent study showed this false for DNT[2] pressed from material of δ=10μ.

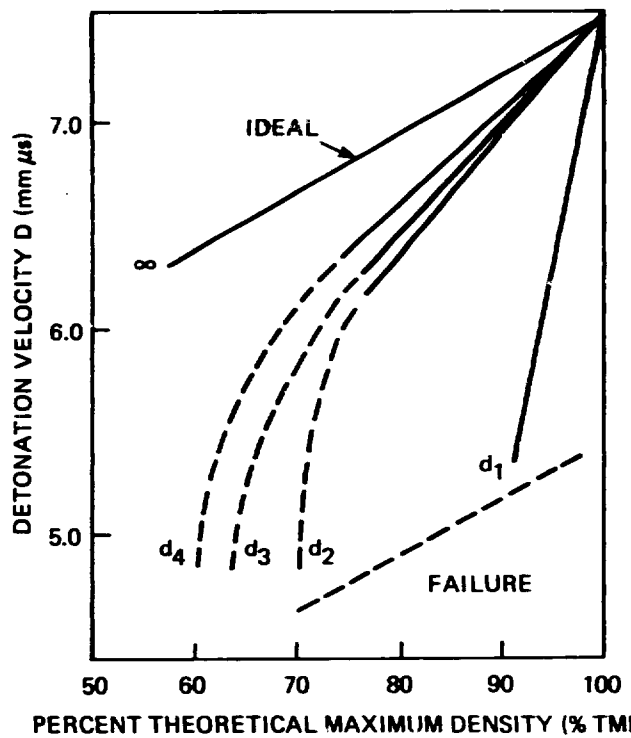

FIGURE 5a PATTERN OF DETONATION VELOCITY VS POROSITY CURVES AT VARIOUS CHARGE DIAMETERS, GROUP 1. EXAMPLE SHOWN IS HBX-1 (RDX/TNT/A1/WAX, 40/38/17/5) DATA (REF. 30). THE CHARGE DIAMETERS d_1 TO d_4 ARE 6.4, 12.7, 25.4, AND 50.8 mm, RESPECTIVELY; SOLID LINES ARE SMOOTHED VALUES FROM THE EXPERIMENTAL DATA WHICH HAVE BEEN EXTRAPOLATED, AS SHOWN. THE VALUE OF THE VOIDLESS DENSITY FOR THIS EXPLOSIVE IS 1.76 g/cc. THE LIMIT LINE FOR FAILURE HAS BEEN ESTIMATED.

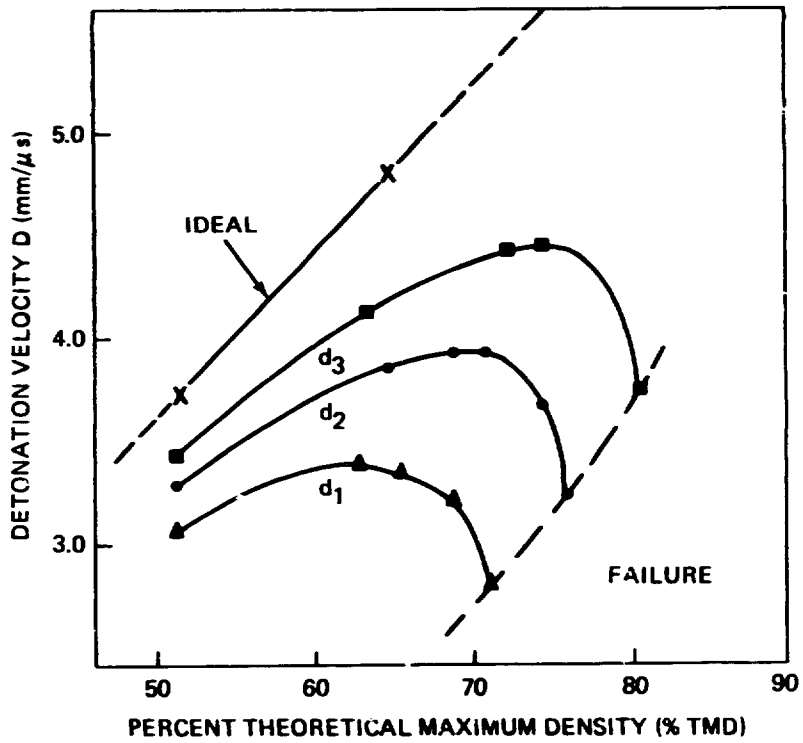

FIGURE 5b PATTERN OF DETONATION VELOCITY VS POROSITY CURVES AT VARIOUS CHARGE DIAMETERS, GROUP 2. EXAMPLE SHOWN IS AP (AVERAGE PARTICLE SIZE 10μ) DATA (REF. 3). THE CHARGE DIAMETERS d_1 TO d_3 ARE 34.9, 50.8, AND 76.2 mm, RESPECTIVELY.

Group 2 members are

AP

AN

Their mixtures with fuel

HN[31]

Ammonium Azide[32]

Hydrazonium Azide[33]

Probably Lead Azide in view of above and fact that it dead presses.

Particle Size (δ) Effect (Critical Particle Size)

The particle size effect on d_c is the same for both groups of explosives: the smaller δ, the smaller d_c. Hence decreasing δ increases the ability of the charge to propagate detonation. Fig. 6 illustrates this for TNT; Fig. 7, for AP. Fig. 8 is also included to show Group 1 and Group 2 plots on the same scale. The failure curve of 10 - 80μ AP in Fig. 7 comes from reference 34. The AP used in that work was obtained from a sieve cut; it had a microscopically observed particle size range of 10 - 80μ, but the particle size distribution and median were not determined. The weight median particle size would of course be smaller than the mean of the projected area diameter of microscopic observations. Hence it is not surprising that this curve lies between those for the weight median particle sizes of 10 and 25μ. More recent work[35] gives a detonability curve for 5μ AP which lies below all the others in Fig. 7.

---

[31]Price, D., Liddiard, T. P., Jr., and Drosd, R. D., "The Detonation Behavior of Hydrazine Mononitrate," NOL TR 66-31, Apr 1966.

[32]Yakovleva, G. S., Kurbangalina, R. Kh., and Stesik, L. N., "Detonation Properties of Ammonium Azide," Combust., Expl., and Sh. Waves, Vol. 13, No. 3, 1977, pp 405-7.

[33]Yakovleva, G. S., Kurbangalina, R. Kh., and Stesik, L. N., "Rate of Detonation of Hydrazonium Azide, ibid, Vol. 10, No. 2, 1974, pp 270-4.

[34]Gor'kov, V. A. and Kurbangalina, R. Kh., "Some Data Concerning the Detonation Ability of Ammonium Perchlorate," Combust., Explosions, and Shock Waves, Vol. 2, No. 2, 1966, p. 12.

[35]Akimova, L. N. and Stesik, L. N., "Detonation Capacity of Perchlorate Explosives," Combust. Expl. and Shock Waves, Vol. 12, No. 2, 1976, pp 247-251.

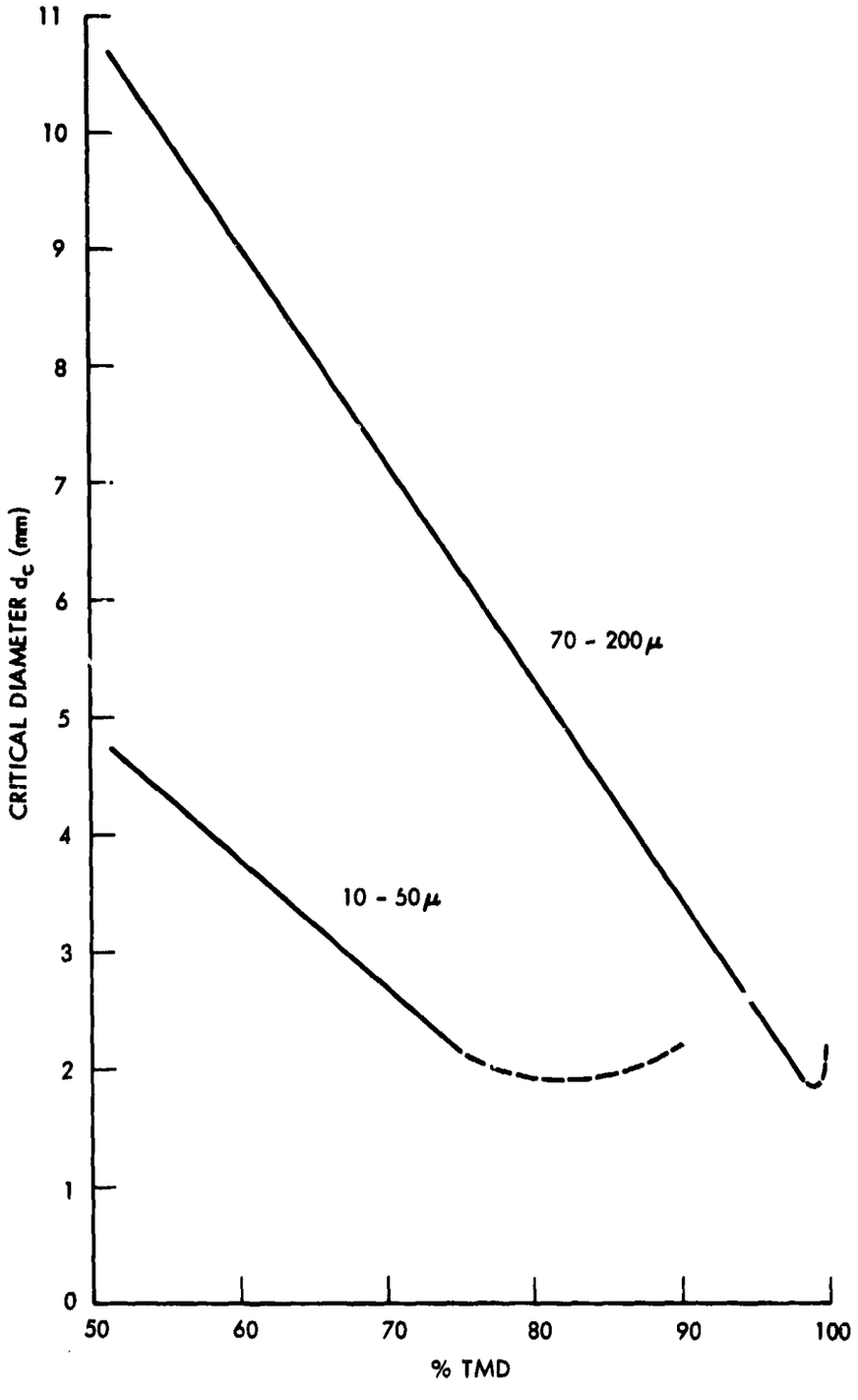

FIGURE 6 DETONATION FAILURE LIMIT CURVES FOR TNT. (REF. 26 & 28)

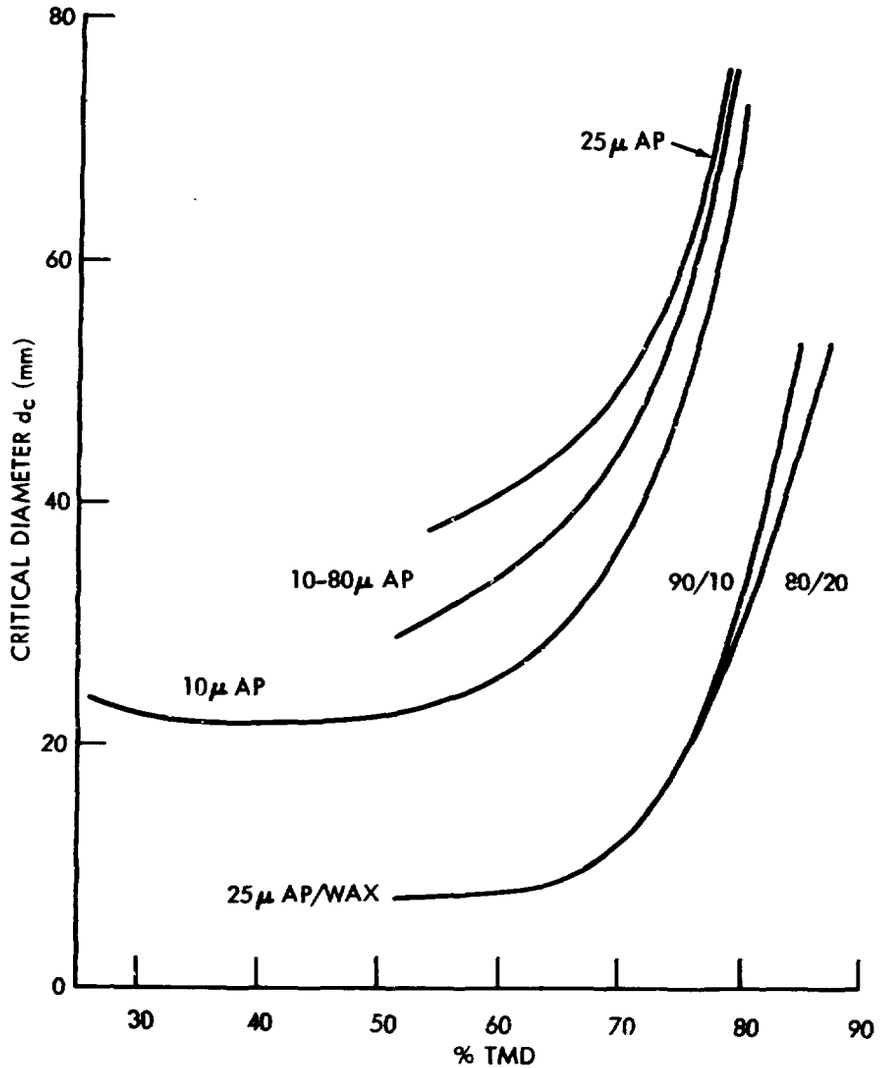

FIGURE 7 DETONABILITY CURVES (GROUP 2). (REF. 28)

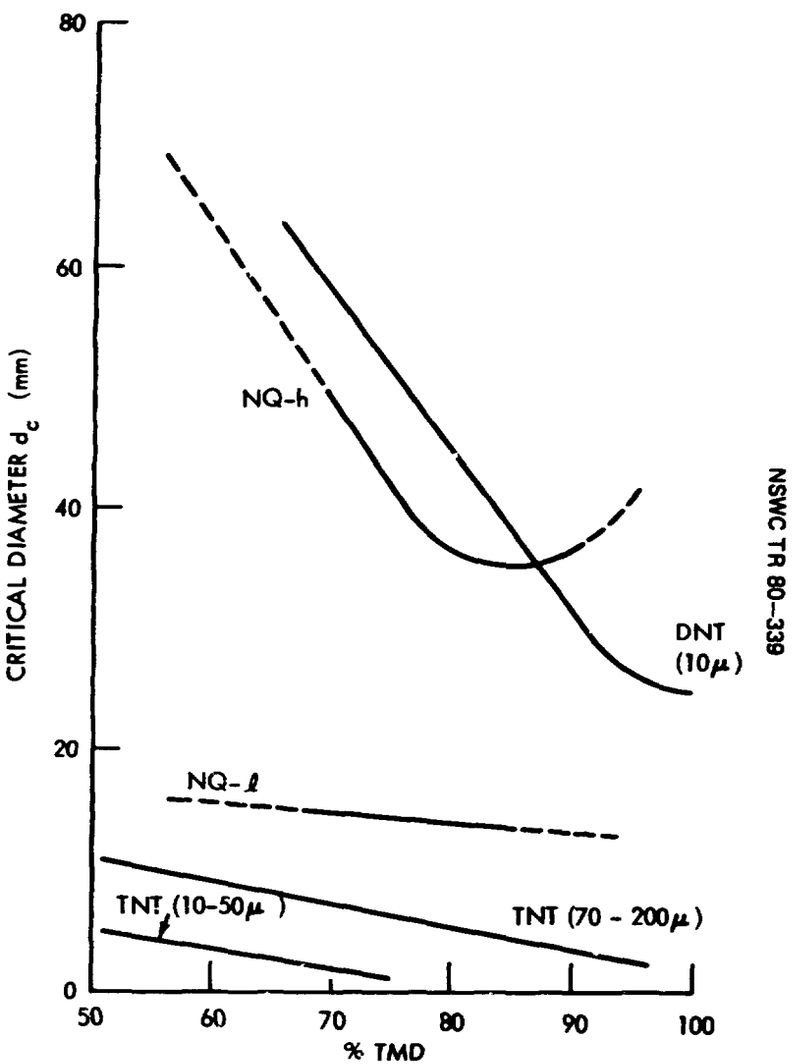

FIGURE 8 DETONABILITY CURVES (GROUP 1). (REF. 28)

The only available data I have encountered for d_c vs δ at a fixed ρ_o (or % TMD) are those of Gor'kov and Kurbangalina[34]. Fig. 9 shows their data for 56.4% TMD AP (ρ_o = 1.1 g/cm^3). Our data for 10 and 25μ AP fall very close to the same curve. As drawn, the curves appear to level off with $d_c \sim 110$ mm at $\delta \geq 500\mu$. This value of 500μ may be inexact; it is possible that there is a low gradient yet continuing particle size effect on very coarse AP. The existence of curves such as Figs. 6-9 implies that for a given initial temperature and density, there is a critical δ above which steady state detonation cannot propagate.

The examples of AP charges were at low % TMD. For charges of granular TNT or other HE easily detonable at high % TMD, Fig. 6 shows that the initial particle size effect is almost negligible at high % TMD. This would be expected since pressing to voidless density tends to eliminate differences in initial δ.

Melt-Casting Effect

Cybulski et al.[36] gave an excellent example of the effect of different casting techniques (and consequent different grain-sized products) on the critical diameter of TNT. Their results were:

Casting Method	d_c, cm
Poured clear	$3.17 < d_c$
Creamed*	$2.20 < d_c < 2.54$
Creamed* plus 10% fines	$1.26 < d_c < 1.66$

Examples given in Ref. 1 showed that the more rapid the cooling rate of the melt, the smaller the grain size and the lower the d_c value.

Temperature Effects (Critical Temperature)

Temperature would be expected to affect the reaction rate and hence the critical diameter. Such an expected temperature gradient is shown in Fig. 10 for granular TNT[37]. It is for a charge of ρ_o = 1.0 g/cm^3 [and presumably fixed δ] over a temperature range of -193° to 75° C, and the limit curve

[36] Cybulski, W. B Payman, W., and Woodhead, D. W., "Explosion Waves and Shock Waves VI.. The Velocity of Detonation in Cast TNT," Proc. Roy. Soc. (London), Vol. 197A, 1949, pp 51-72.

[37] Belyaev, A. F. and Kurbangalina, R. Kh., "Effect of Initial Temperature on Critical Diameter of Nitroglycerin and Trinitrotoluene," Russian J. Phys. Chem., Vol. 34, No. 3, 1960, pp 285-9.

*Term as used at NSWC i.e., melt stirred until it becomes milky because of formation of small crystals; at this point it is poured into the mold.

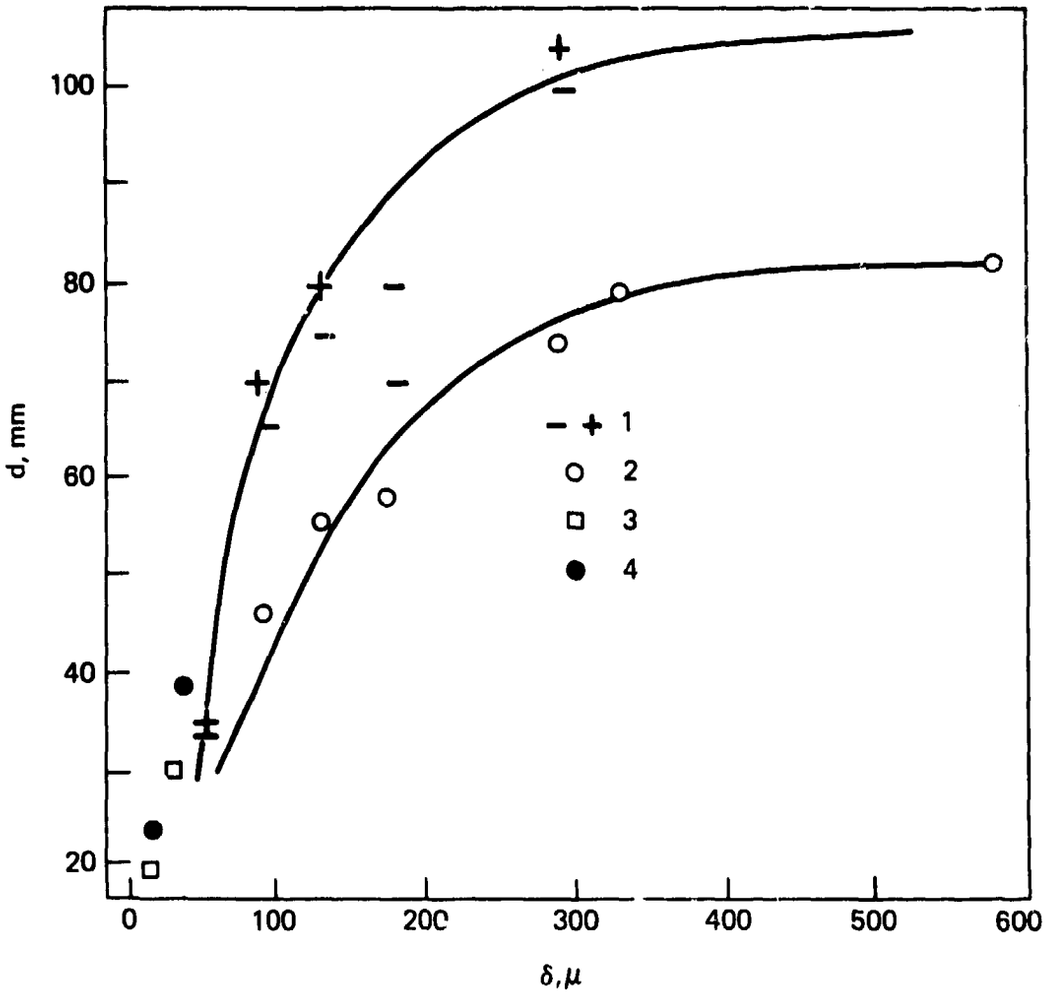

1. DATA FOR CYLINDRICAL CHARGE
2. DATA FOR A CONE
3. DATA OF ANDERSON, et al.
4. NSWC DATA

FIGURE 9 DEPENDENCE OF CRITICAL DIAMETER OF AP ON PARTICULAR SIZE (DENSITY OF CHARGE IS 1.1 g/cm^3, 56.4% TMD). (REF. 34)

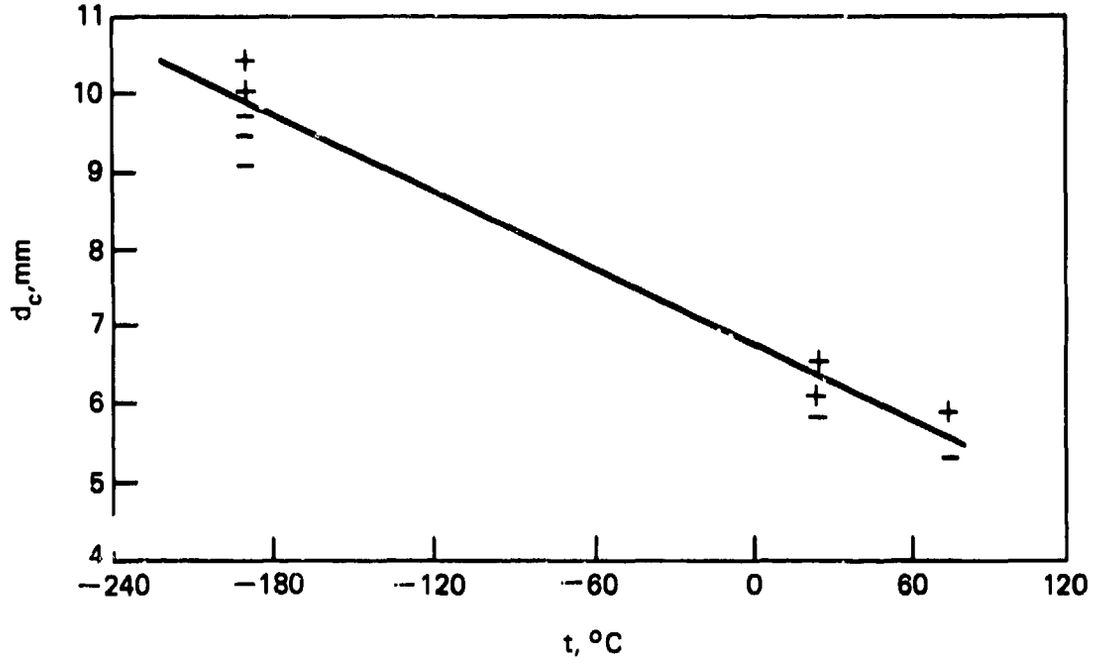

FIGURE 10 CRITICAL DIAMETER OF POWDERED TNT AS A FUNCTION OF INITIAL TEMPERATURE. + STEADY DETONATION; − DETONATION FAILURE. (REF. 37)

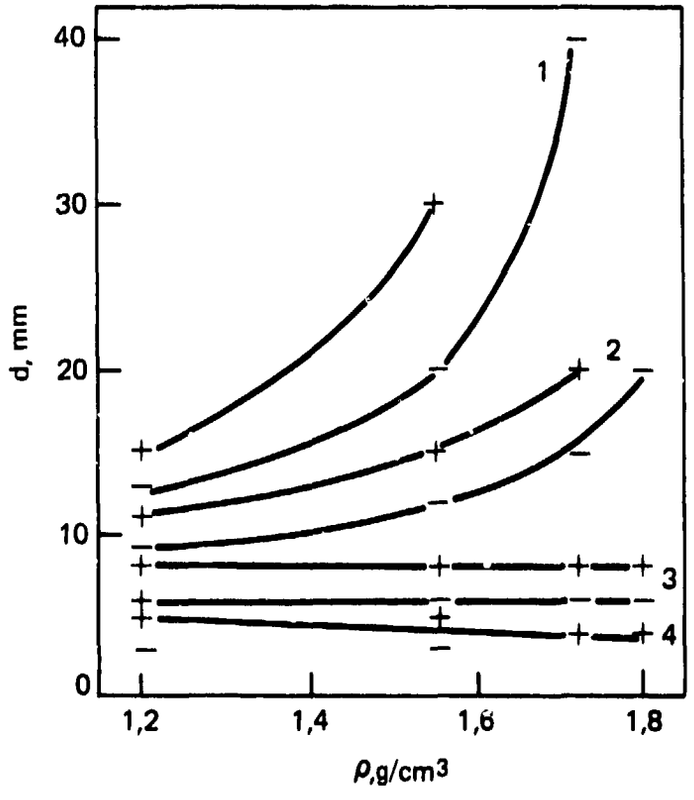

FIGURE 11 DENSITY DEPENDENCE OF d_c FOR AP MIXED WITH OCTOGEN: 1) 95:5; 2) 90:10; 3) 85:15; 4) 75:25. (REF. 35)

divides the plane into super- and sub-critical regions. Thus for a fixed initial density and particle size, there exists a critical temperature (t_c) below which detonation cannot occur.

Although t_c has not been featured in the literature to the extent of d_c, it is a very important critical parameter and most evident in the explosive behavior of propellants and propellant components. Thus AN prills at pour density are subcritical under heavy confinement (ID of 38.1 mm) until their temperature is increased to 140°C or higher[38]. AP also shows a marked effect of temperature with a gradient of about 0.1 mm/°C[34] as compared to the TNT gradient of about 0.02 mm/°C (Fig. 10). Several double base propellants, tested in the confinement of the NOL large scale gap test, failed to detonate at -60°C and -32°C but did detonate at 25°C and 66°C[38].

In addition to the usual temperature effect on d_c, described above, there exists the possibility of a temperature effect on the structure of cast materials; this physical change can then cause a change in d_c. Cast TNT, when rapidly cooled to 77.4°K and allowed to return to its initial temperature of 290°K by slow heating, showed no visible change in its microstructure. Nevertheless, d_c had been decreased from 15 to 7 mm (fine crystal casting) and from 27.5 to 9 mm (coarse crystal casting)*; the initial ρ_o was reduced by 0.01 g/cm^3 from 1.62 and 1.60 g/cm^3, respectively[10]. Although two such temperature cycles equallized the d_c values of the two castings at 6.5 mm, further cycling had no additional effect. In other words, after the temperature cycling, the cast material had a d_c value still about 2.5 times that of pressed TNT at the same density.

Chemical Composition Effects

In the earlier Russian literature, it was reported that a mixture of a Group 1 HE with a Group 2 HE (50/50 TNT/AN) exhibited a maximum in its d_c vs % TMD curve. Subsequent Russian work[35] makes this seem doubtful. Fig. 11 shows detonability curves for a series of Group 1/Group 2 mixtures - in this case, HMX/AP. Each composition gave a smooth, monotonic detonability (d vs ρ_o) curve

[38] Price, D., Jaffe, I., and Roberson, G. E., "Shock Sensitivity of Solid Explosives and Propellants," Ind. Chim. Belge, 1967, No. 32 (Spec. No.), pp 506-510.

*The d_c value measured at 77.4°K was 9 mm in both cases.

with Group 2 behavior predominating at 90% or more AP, 10% or less HMX; Group 1 behavior, at 85% or less AP, 15% or more HMX. We found a similar shift in the detonability curves from two mixtures: I. 62.5/18.75/18.75 AP/Al/Wax and II. 50/15/15/20 AP/Al/Wax/HMX or 80/20 I/HMX. Fig. 12 shows the shift from Group 2 behavior to that very close to Group 1 caused by the addition of 20% HMX. Whereas 15% HMX sufficed to convert an AP/HMX mixture to Group 1 behavior (Fig. 11), about 32% TNT is required for such a conversion[35]. However, the change from one behavior to the other is a continuous, smooth variation following the variation in composition.

If the two component mixture is made up of members of the same group, the mixture will also exhibit a detonability curve typical of that group. The magnitude of its d_c will depend, of course, on its composition. Fig. 13 shows a d_c vs composition curve for cyclotols (RDX/TNT), with linear variation of d_c between the value for RDX at ρ_o = 1.0 g/cm^3 to TNT at ρ_o = 1.0 g/cm^3.

Figure 12 showed that addition of Al to AP depressed the curve (i.e. decreased d_c) but did not change its form. This may also be the case for porous TNT charges[40]. Dimza's data[40] were obtained at a constant volume fraction of HE and no value for the unadulterated HE was given; hence, it is impossible to separate the effect of the additive from the effect of the change in porosity it caused. It should be noted here, however, that addition of Al to cast TNT definitely decreases d_c from 2.7 cm to 0.7 cm at 20% Al[21].

Addition of water to AP or TNT increases d_c; the effect is very much greater for AP[34], possibly because of its solubility. Water behaves in both cases as an inert diluent. Addition of wax to TNT, RDX, or HMX increases d_c[40] {In this case, Dimza's data show a monotonic <u>increase</u> or no change with simultaneous increase in diluent and decrease in porosity. Since the latter change decreases d_c of Group 1 HE, it is evident that the wax must have acted as an inert diluent.} On the other hand, addition of wax to AP <u>decreases</u> d_c; see Fig. 7. This is typical of any AP/fuel mixture[34,35]. Both this fact and the fact that the decrease is much greater if the fuel is finely divided[35]

[40]Dimza, G. V., "Critical Detonation Diameter for an Explosive Containing an Inert-Additive," <u>Comb., Expl. and Shock Waves</u>, Vol. 12, No. 2, 1976, pp 244-47.

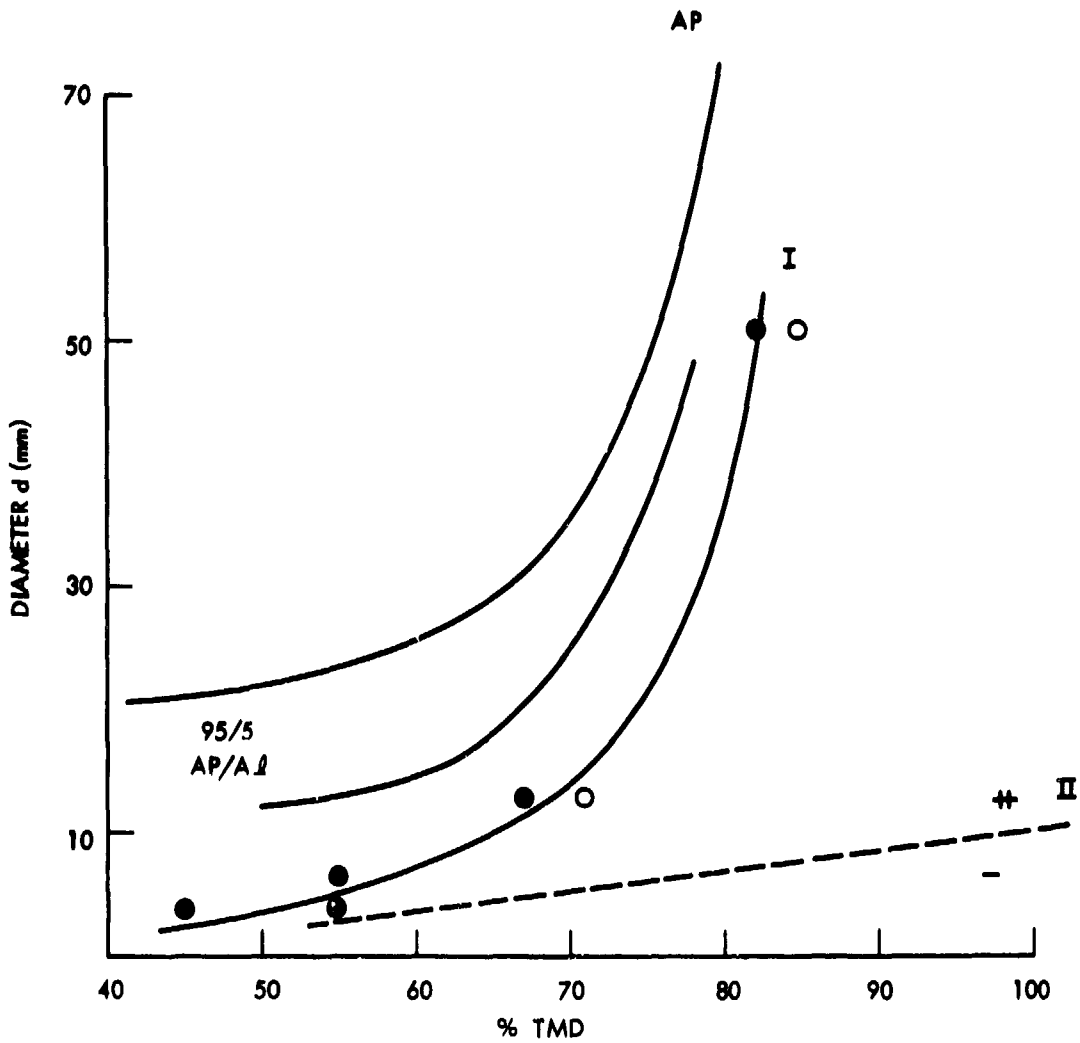

FIGURE 12 CRITICAL DIAMETER VS. PERCENT TMD FOR COMPOSITE MODELS (SOLID CIRCLE OR + FOR DETONATION; OPEN CIRCLE OR– FOR FAILURE). (REF. 28 & 39)

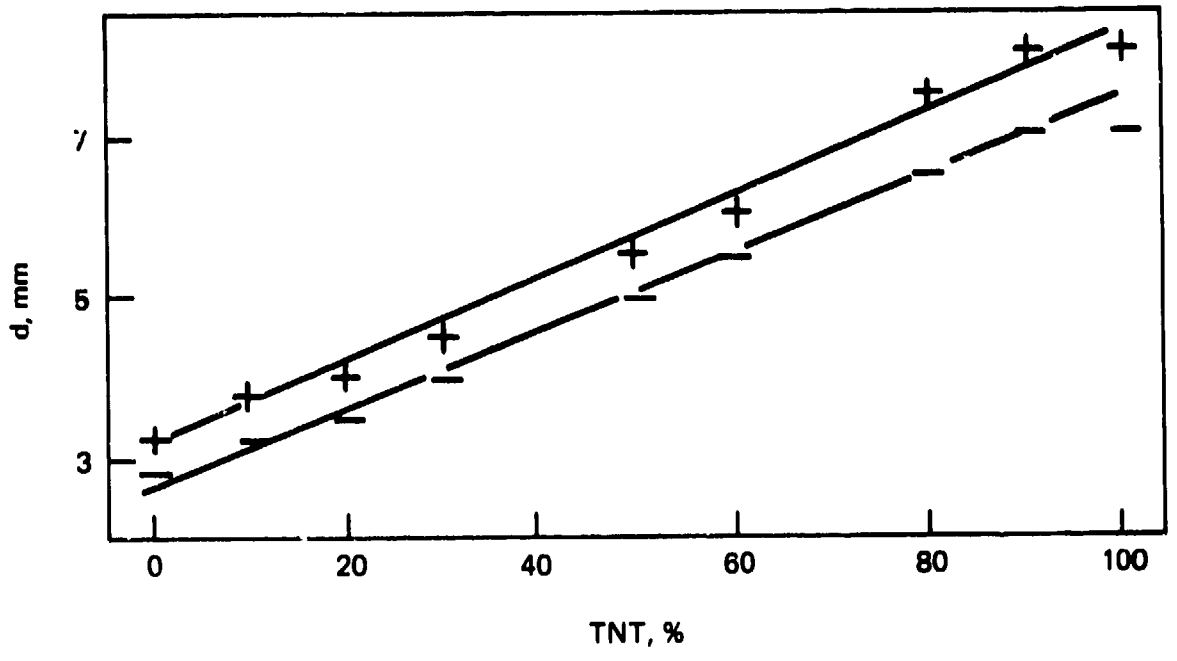

FIGURE 12. COMPOSITION DEPENDENCE OF d_c FOR CYCLOTOLS AT ρ = 1 g/cm3. (REF. 35)

are indicative of an oxidant-reductant reaction contributing to the detonation behavior. A further indication of this is the increase in D observed with the addition of wax to AP[39].

Finally, it should be noted that the addition of inert materials to voidless explosives can affect d_c. (Al in cast TNT may be an example of this.) Apin and Stesik[41] added relatively dense powdered diluents ($CaCO_3$, MgO, Bi_2O_3, PbO, HgO, and W) to plastisol type propellants. They found that such diluents reduced d_c according to the formula:

$$d_c = \frac{A}{(n + n_o)^{1/3}} + B \qquad (9)$$

where A & B are functions of the diluent,

n = concentration of additive particles,

n_o = concentration of reaction foci in matrix before addition of inert.

The first term of Equation 9 is the average distance between foci. It was assumed that the inert particles of $\rho > \rho_{matrix}$ afforded a focus where shock reflection and intensification could produce a hot spot.

Very few data have been available for the effect of inert diluents in porous explosives; recently such data have been compiled and supplemented[42]. Inert diluents in HE, at concentrations of 5% or greater and at the pour density of the mixture, either show no effect on d_c (RDX/paraffin up to ca. 35% paraffin) or increase it (TNT/talc, paraffin, or NaCl and RDX/NaCl). Moreover, curves of d_c vs δ (initial particle size of diluent) showed a minimum. In other words, there was a δ which caused the smallest increase in d_c at a fixed concentration of inert.

---

[39] Price, D., and Clairmont, Jr., A. R., "Explosive Behavior of Simplified Propellant Models," Combust. Flame, Vol. 29, 1977, pp 87-93.

[41] Apin, A. Ya. and Stesik, L. N., "The Chemical Reaction Mechanism in the Detonation of Explosives, PMTF, No. 2, 1965, pp 142-145.

[42] Shvedov, K.K., Aniskin, A. I., Il'in, A. N., and Dremin, A. N., "Detonation of Highly Diluted Porous Explosives I. Effect of Inert Additives on Detonation Parameters," Comb., Expl. and Shock Waves, Vol. 16, No. 3, 1980, pp 324-331.

Confinement Effect

It has been well known for many years that confining a charge will decrease d_c*, i.e. the charge diameter within the sheath which will support a detonation. Very few quantitative measurements of this effect have been made, and there is no adequate theoretical treatment with which predictions can be made. Apparently the confinement effect is most striking for materials of large d_c. Thus d_c of AP in thin cellophane is 4-5 times greater than that in glass which is in turn, 4-5 times greater than that of AP in copper foil[34]. Similarly, ammonium nitrate (AN) at ρ_o = 1.06 g/cm^3 has $d_c \geq 100$ mm, ≥ 80 mm, and < 3 mm in cellophane glass, and steel, respectively[43]. A steel wall thickness of 3 mm was adequate to assure detonation in a 4 mm ID steel tube filled with AN at ρ_o = 0.8 g/cm^3 [43].

*The confinement delays the expansion of the gaseous detonation products and thus increases the time available for reaction at high temperature and pressure before a rarefaction reaches the reaction zone. In this manner, the charge behaves like a much larger bare charge. Hence confinement has increased its "effective diameter."

[43]Kurbangalina, R. Kh. and Patronova, L. I., "Effect of a Steel Sheath on the Critical Detonation Diameter of Condensed Explosives," Comb., Expl., and Shock Waves, Vol. 12, No. 4, 1976, pp 587-90.

CRITICAL INITIATING PRESSURE

Background

In the previous section, the parameters critical for propagation of detonation were considered. In this section we will consider the parameter, critical initiating pressure (P_{ci}) which helps to define the threshold for a shock-to-detonation transition (SDT) and is an inverse measure of the shock sensitivity of an explosive.

The critical initiating pressure is defined as the minimum pressure (P_{ci}) required to initiated detonation of the explosive in 50% of the trials. It defines a threshold for the initiation of detonation under transient conditions. The value of P_{ci} measured in any given test is determined not only by the chemical composition of the test material and its physical state but also, in large part, by the physical dimensions of the test. These dimensions control the times at which rear and lateral rarefactions can arrive at the shock front and relieve the pressure. Thus, each test devised to measure P_{ci} is apt to use a different pressure pulse (pressure-time profile) to excite reaction of the explosive. Different profiles can be obtained by varying the composition and shape of donor explosives in the gap, booster, and wedge tests and by varying projectile material, shape, and velocity in the projectile impact and wedge experiments. They are also obtained by varying the diameter of the acceptor explosive. The explosive response differs as the stimulus differs, and, hence, gives different P_{ci} values in different tests. Any single adequately designed test will give a relative sensitivity rating to a group of different HE charges.

Some time ago it was shown theoretically[44] that a limiting pressure-time (P-t) curve exists for a 50% chance of build-up to detonation in homogeneous

[44] Hubbard, H. W. and Johnson, M. H., "Initiation of Detonations," J. Appl. Phys. Vol. 30, No. 5, 1959, pp 765-69

explosives; the limiting curve divides the impulse plane into a detonation region and a failure region. Brown and Whitbread[45] demonstrated by impact of cylindrical projectiles on two physically heterogeneous explosives that the P_{ci} determined must have a minimum duration for detonation to occur. They also showed qualitatively that, at $P > P_{ci}$ and a duration shorter than that required at the critical pressure level, detonation could also be initiated. Since then there has been rather general agreement that initiation of detonation must be the result of the pressure-time history of the initiating shock, and that a critical limit curve such as Figure 14 must exist in the P-t plane for each explosive.

In many cases of explosive loading (e.g., a gap test), maximum shock pressure can be determined much more readily than the pressure-time profile. Hence, many of the shock sensitivity measurements have been restricted to pressure measurements only. However, it is generally known that the P_{ci} will depend on its duration. Consequently, for each test in which the pressure-time history of the shock loading is unknown, the experimental details are carefully specified (e.g., dimensions and character of the donor explosive in the gap test.)

Solid heterogeneous explosives (cast and pressed) exhibit the following shock sensitivity behavior[46,47]: a critical initiating pressure (P_{ci}) for detonation, breakout of detonation downstream from the shocked boundary, and a consistent decrease of both the run length and delay time to steady-state detonation with increased amplitude of the applied shock. The run length is the distance from the plane of shock entry into the explosive to the plane in which steady-state detonation is first established. The delay time is the total time from the moment of shock entry to the time at which steady-state detonation begins. Figure 15 illustrates this behavior; in particular, it

[45] Brown, S. M. and Whitbread, E. G., "The Initiation of Detonation by Shock Waves of Known Duration and Intensity,", Les Ondes de Detonation, Edition du Centre National de la Recherche Scientifique, Paris, 1962; pp. 69-80.

[46] Jacobs, S. J., Liddiard, T. P., and Drimmer, B. E., "The Shock-to-Detonation Transition in Solid Explosives," Ninth Symposium (International) on Combustion, Academic Press, N.Y.C., 1963; pp 517-529.

[47] Price, D. and Petrone, F. J., "Detonation Initiated by High-Pressure Gas Loading of a Solid Explosive," J. Appl. Phys., Vol. 35, No. 3, 1964, pp 710-714.

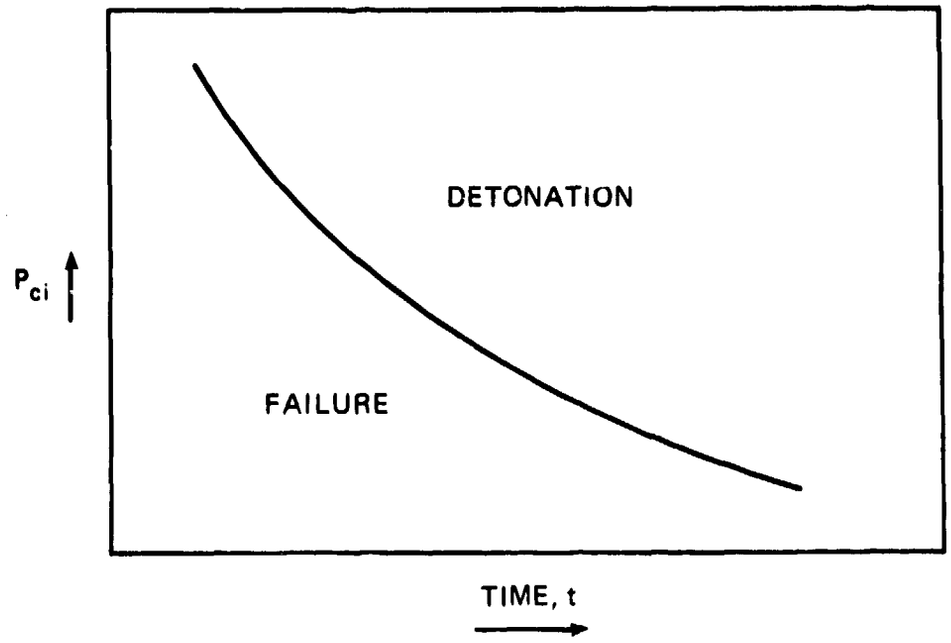

FIGURE 14 VARIATION OF INITIATING PRESSURE WITH ITS DURATION

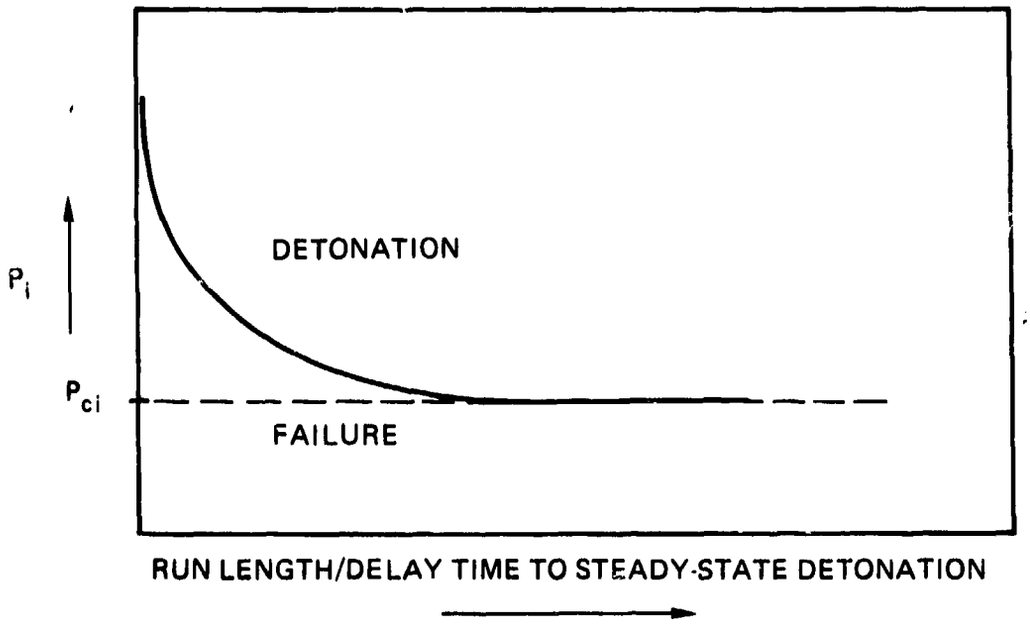

FIGURE 15 VARIATION OF RUN LENGTH/DELAY TIME WITH AMPLITUDE OF INITIATING SHOCK

shows how the initiating pressure P_i (for a specific test charge) decreases to the critical initiating pressure P_{ci} as the run length increases to a large value. The approach to P_{ci} is asymptotic. If the charge is cylindrical and at its critical diameter, the value of P_{ci} should be approximately the C-J pressure for that explosive at $d = d_c$, the pressure needed just to sustain steady-state detonation.

The P_{ci}-diameter relationship should follow a curve such as Fig. 16 where the upper point on the threshold curve is at $(P_j)_c$ for $d = d_c$ (and consequently at a time duration of the detonation reaction time τ_c at $d = d_c$). The larger the diameter, the longer the path and travel time of the lateral rarefaction waves from the charge periphery to the charge axis; it is the arrival of these release waves that quenches the reaction. Therefore the larger d, the longer P_j and T_j are maintained. Hence the reaction zone length and reaction time decrease with increasing charge diameter to their ideal values. As d increases above d_c, P_{ci} should drop sharply and approach asymptotically its infinite diameter value where τ also assumes its ideal value. (A similar sharp change in P_{ci} would be expected in approaching the critical values of other parameters, e.g. t_c, δ_c.) Fig. 16 indicates that the test value of P_{ci} for any given explosive will depend on d/d_c, as it is known to do, and Ref. 48 gives an experimental curve P_{ci} vs d for NB-40* powder at 1.58 g/cc for $d > d_c$. Inasmuch as the critical diameter value is a function of temperature, initial particle size, density, composition, and confinement, and P_{ci} is a function of d/d_c, it follows that P_{ci} is also a function of t, δ, ρ_o, composition, and confinement. However, the effect of these variables on P_{ci} is not alone through their effect on d_c because the same change in δ, ρ_o and composition can change P_{ci} and d_c in opposite directions as we will demonstrate later.

P_{ci} can be measured by gap, booster, projectile impact and wedge tests provided the test is calibrated and Hugoniot data for the non-reacting explosive are available. Only the first and last of these tests will be considered in detail. We believe all the test results are related and will later illustrate relations between gap tests and between gap and wedge tests.

---

[48] Afanasenkov, A. N. and Voskoboinikov, I. M., "Shock-Ignition Sensitivity of Ballistite," Comb. Expl. Shock Waves, Vol. 9, No. 2, 1973, pp 331-332.

*A NC/NG double-base powder containing 40% NG.

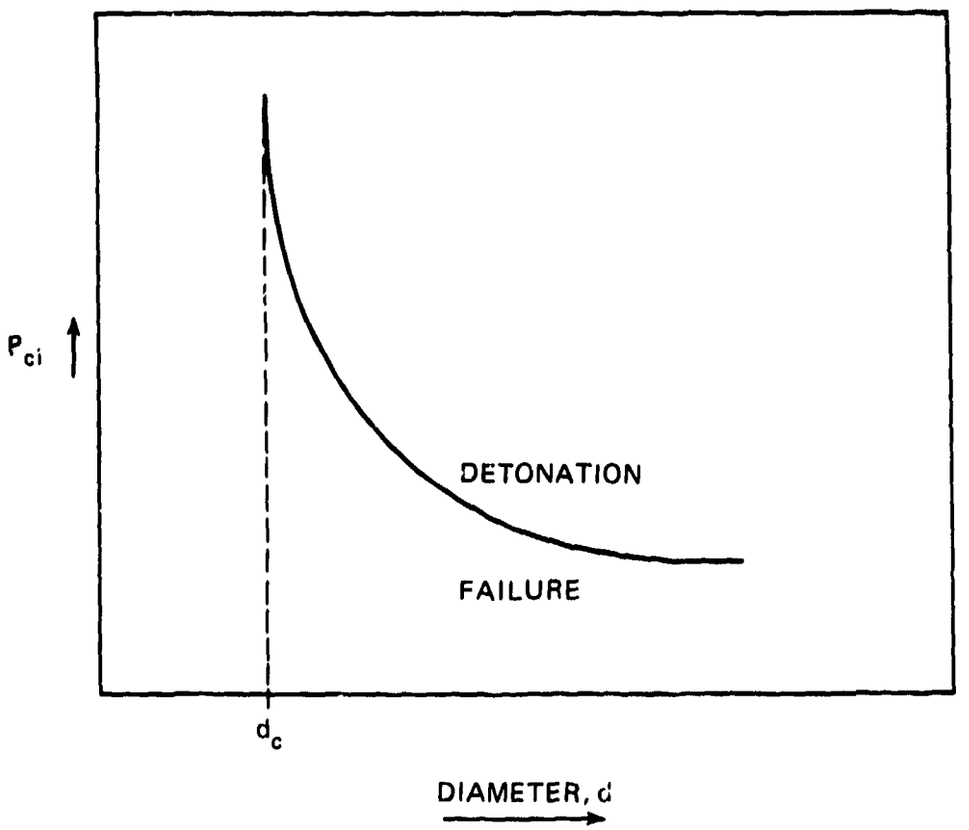

FIGURE 16 VARIATION OF P_{ci} WITH CHARGE DIAMETER

NOL Large Scale Gap Test

The NOL large scale gap test (LSGT) was used for much of the data quoted later, and will therefore be described in some detail. Figure 17 shows that this LSGT is a conventional gap test with a 5 cm dia x 5 cm long, 1.56 g/cc 50/50 pentolite donor and an attenuator gap of polymethyl methacrylate (PMMA) or its equivalent. The acceptor explosive can be tested unconfined or in the standard moderate confinement of a steel sleeve (3.65 cm ID, 4.76 cm OD). A mild steel witness plate is used in both cases, and the gap length is varied until the 50% value is found, that is, the attenuation at which a hole is punched in the witness plate in 50% of the trials. The system donor/gap has been calibrated [Fig. 18[49]]to give shock pressure as a function of gap length. This 50% pressure (P_g) at the end of the gap can be converted to the initiating pressure (P_{ci}) transmitted to the explosive by the use of the Hugoniot of the gap material[49] and that of the explosive, e.g., cast TNT[4].

The Hugoniot adiabat or equation of state of the attenuator PMMA (ρ_o = 1.18 g/cm^3) is required for the calibration of the test. Usually this is known in the form of

$$U = a_o + su \tag{10}$$

where U, u are shock and particle velocity, respectively, and a_o and s are constants specific to the material. Actually PMMA is visco-elastic and its exact Hugoniot is more complicated than the linear relation of Eq. 10 (See Ref. 49). However Eq. 10 is a good approximation and quite adequate for this illustration. In combination with the hydrodynamic relationship derived from the conservation of momentum,

$$P = \rho_o Uu \tag{11}$$

the non-linear relationship between pressure P and u in the shocked PMMA can be obtained. This is the customary and convenient relationship with which to work because boundary conditions for reflection and transmission of shock waves at the interface between two different materials require that pressure P and particle velocity u must be equalized across the boundary.

[49] Erkman, J. O., Edwards, D. J., Clairmont, A. R., Jr., and Price, D., "Calibration of the NOL Large Scale Gap Test; Hugoniot Data for Polymethyl Methacrylate," NOLTR 73-15, Apr 1973.

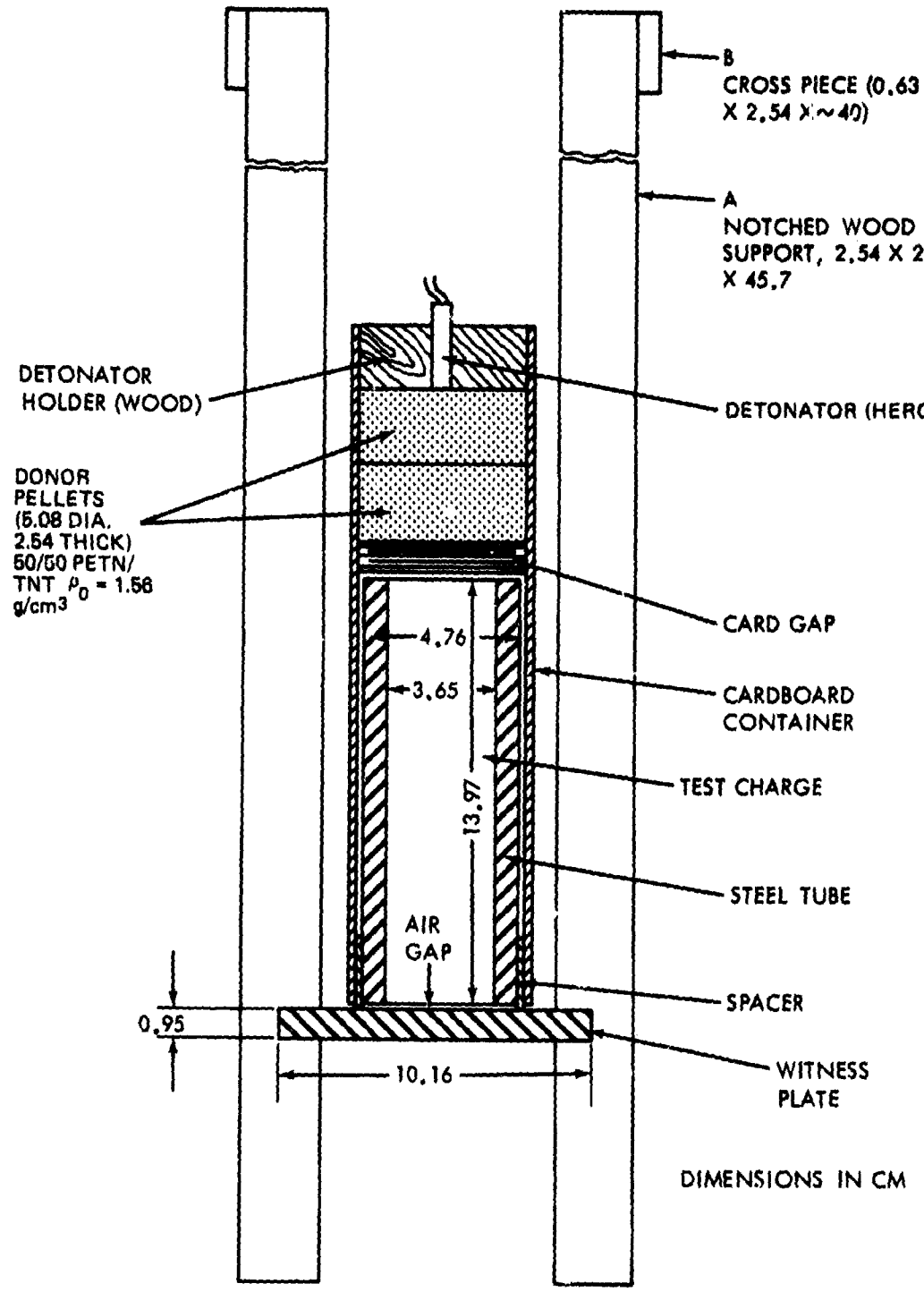

FIGURE 17 CROSS SECTION OF GAP TEST ASSEMBLY

Measurement of shock velocity vs gap thickness L_g or of particle velocity vs L_g in the shocked PMMA together with the P-u Hugoniot provides the P_g-L_g calibration of Fig. 18. Both U and u measurements were made on the longitudinal axis and compared to a computation of the hydrodynamic flow in the donor/PMMA system to obtain the calibration[49].

P_g is generally used to compare different HE because non-reactive Hugoniot data are not available for all explosives. Where such data are available the measured P_g can be converted to P_{ci}, the critical initiating pressure in the explosive. For example the cast TNT Hugoniot[4] and that for PMMA are shown in Fig. 19. P_g at the 50% point was 44 kbar in PMMA (ρ_o = 1.18 g/cm^3). At point X (L_g) the P,u values are 44 kbar and 0.92 mm/μs, respectively. At the interface with the denser TNT (1.61 g/cm^3), a reflected shock (dashed line) is sent back into the PMMA to raise its pressure to 52 kbar which is also the pressure of the shock transmitted to the TNT (point b). Fig. 20 shows a comparison of P_g with P_{ci} for six cast and three pressed HE all near voidless density[50]. There is no reversal in the sensitivity ordering although the P_{ci} are 16-30% greater than the corresponding P_g. Hence the P_g rating shrinks but does not distort the true sensitivity scale based on P_{ci}.

The standard donor of the LSGT is approximately point initiated; hence, the detonation front in the donor is spherical and the hydrodynamic flow in the gap and in the acceptor is divergent. The transmitted pressure falls off rapidly as Fig. 18 shows. From optical observations of the tetryl*/PMMA system, the shock pressure decreases to half its initial amplitude in about one μsec[51]. Walker and Wasley[52] estimated that such a pulse was equivalent to a square pulse of an amplitude of 0.9 P_i and 1.6 μsec duration. Although a one-dimensional hydrodynamic flow computation on the tetryl/PMMA system produced a half-width

[50] Price, D., "Large Scale Gap Test: Interpretation of Results for Propellants," NAVWEP 7401, Mar 1961.

[51] Jaffe, I., Toscano, J., and Price, D., "Behavior of Plexiglass under Shock Loading by a Tetryl Donor," NOLTR 64-66, 2 Jul 1964.

[52] Walker, F. E., and Wasley, R. J., "Critical Energy for Shock Initiation of Heterogeneous Explosives," Explosivstoffe, Vol. 17, No. 1, 1969, p. 9.

*Pressed tetryl pellets at 1.51 g/cm^3 were originally used as the LSGT donor in place of the present standard pentolite.

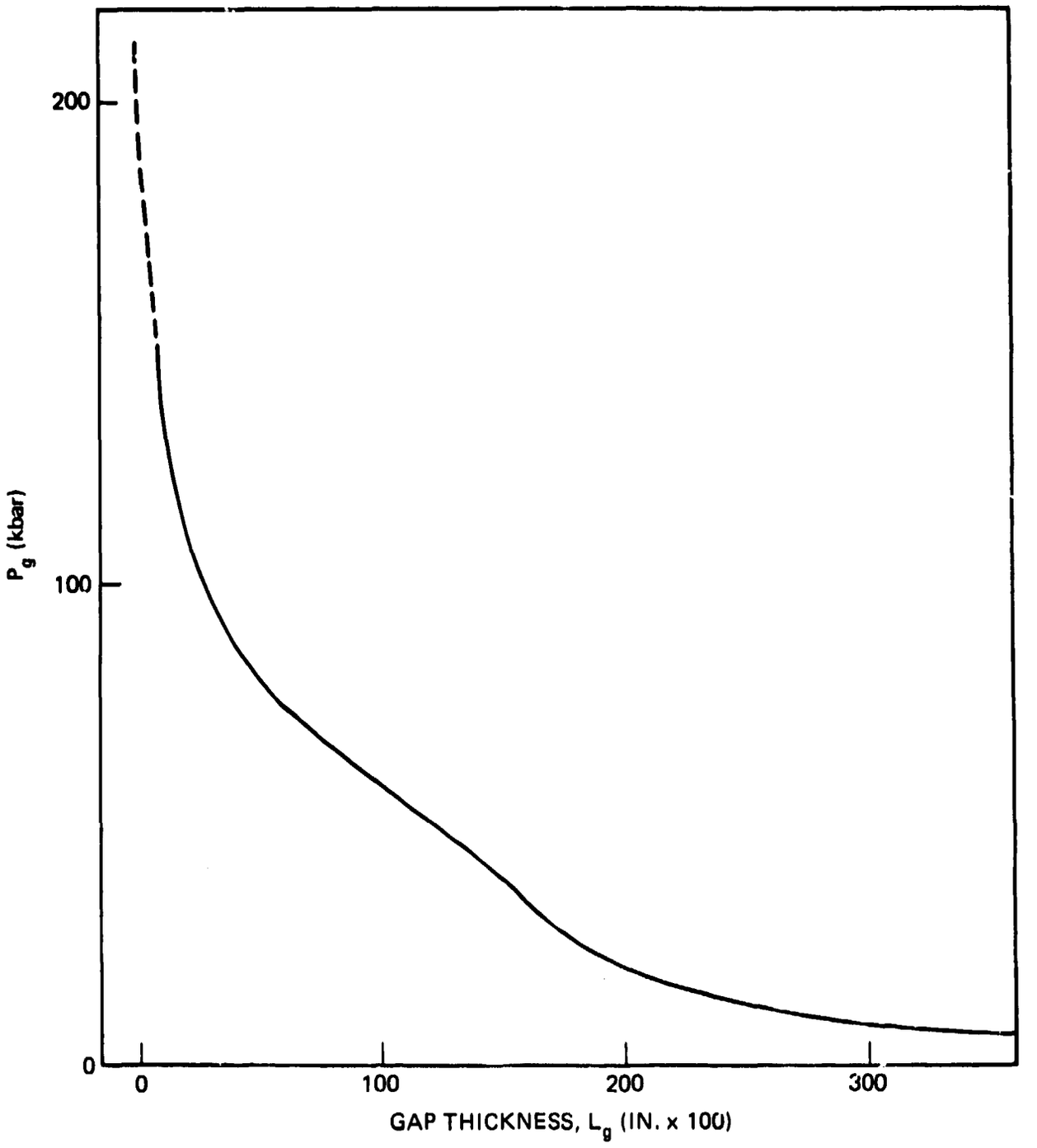

FIGURE 18 CALIBRATION CURVE FOR NOL LSGT WITH PENTOLITE DONOR

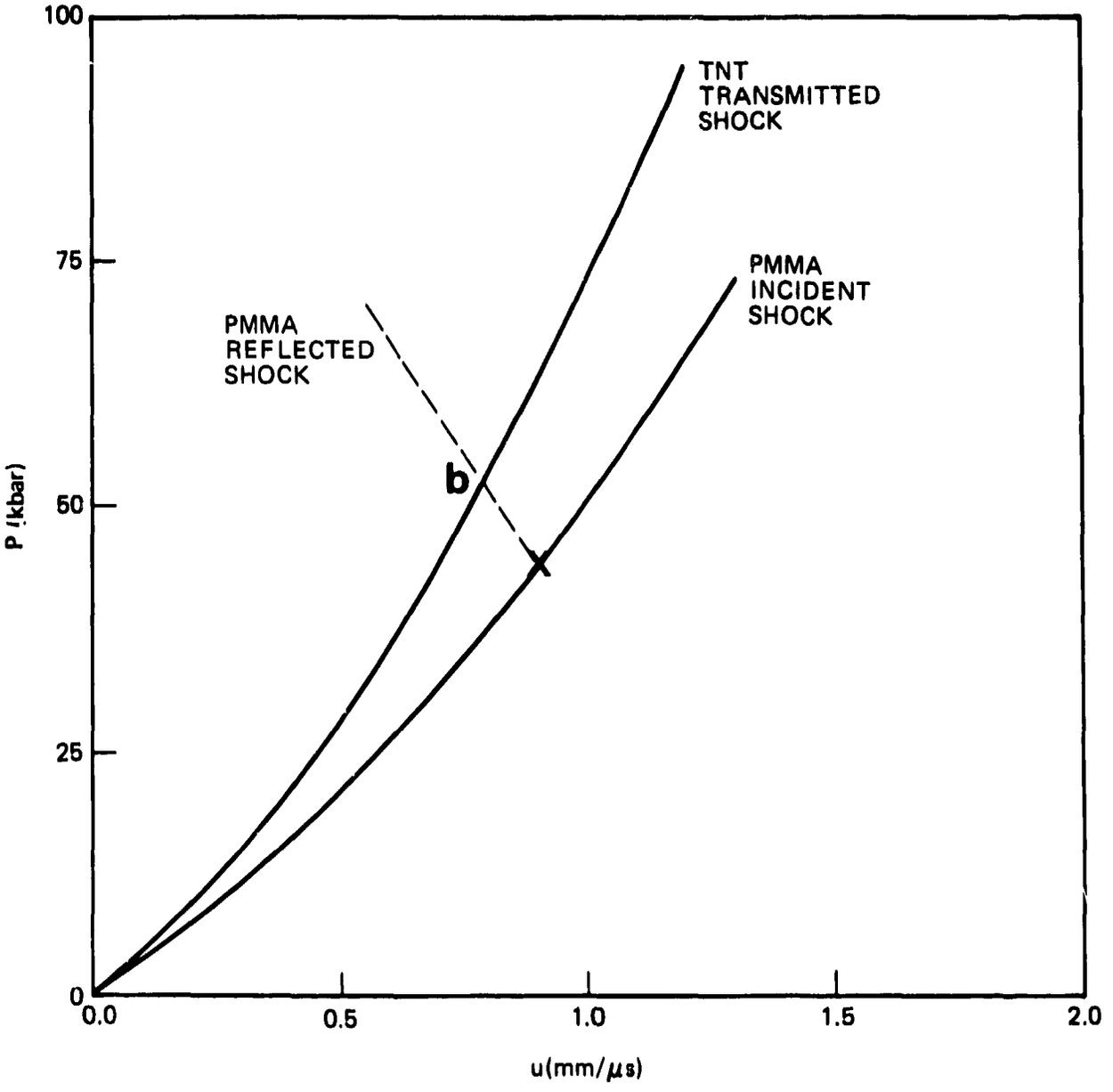

FIGURE 19 DETERMINATION OF P_{ci} FROM P_g IN CAST TNT

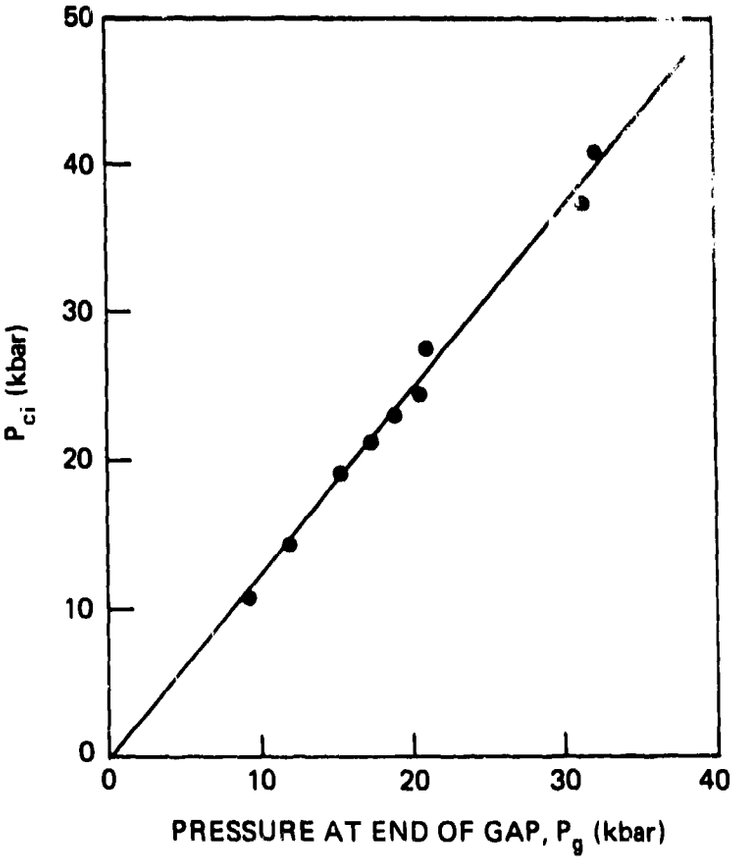

FIGURE 20 COMPARISON OF SHOCK LOADING AT 50% POINT WITH CRITICAL INITIATING PRESSURE IN CHARGE. (REF. 50)

of 4 μs[51], analogous two-dimensional computations[53] indicated a value of about 2 μs, in fair agreement with the original estimate from experimental work.

Like all such tests, the LSGT exhibits a diameter effect. Inasmuch as doubling the length of the standard booster increases L_g but does not affect the measured pressure P_g[54], rear rarefactions affect the duration of the pressure pulse produced by the standard donor, but, from the standpoint of initiation, the pulse is already of infinite duration. It is therefore the lateral rather than the rear rarefaction that has the more important effect in reducing the pressure amplitude. Because confinement of the charge delays the arrival of lateral rarefactions at the charge axis, we find, for the same measured P_{ci}, that the diameter of the equivalent unconfined charge is approximately twice the core diameter of the confined charge, i.e., 76 mm.

As in the case of d_c, both P_g and P_{ci} in the gap test are end effects of multidimensional hydrodynamic flow, and cannot be adequately studied within the framework of simple 1-D planar theory. However, there are 2-D codes available to make numerical computations illustrating the flow that will occur in the LSGT. Computations that have been carried out on the donor/PMMA system in conjunction with particle velocity measurements indicate that the lateral rarefaction reaches the axis of the PMMA cylinder (gap) after the shock has travelled 35 mm (about 2/3 the cylinder diameter)[49]. [The arrival of the release wave is responsible for the hump which appears in the calibration curve of Fig. 18. Indeed with more accurate determination of P, we might see, instead of a hump, a cusp at the join of two different curves; this was the pattern found in the u-x curves.] The detailed numerical study of the flow caused by the shock transmitted to the acceptor will be considered after an experimental study of both confined and unconfined shocked acceptors has been described.

---

[53] Kamegai, M. and Erkman, J. O., "Numerical Analysis of a Diverging Shock Wave in Cylinders of Plexiglas," Fifth Symposium (International) on Detonation, ONR ACR-184, U.S. Gov't Print. Office, Washington, DC, 1972; pp 477-485.

[54] Jaffe, I. and Clairmont, A. R., Jr., "The Effect of Configuration and Confinement on Booster Characteristics," NOLTR 65-33, 13 Apr 1965.

Cast DINA (diethanol dinitrate) was the acceptor studied for its response to shock[55]. The standard LSGT configuration was used except that charge diameters were 38.1 mm (standard for unconfined charges, but 1.6 mm larger than the standard for confined charges) and 152.4 mm instead of 139.7 mm long. The acceptors were instrumented with continuous resistance wire circuits which measured the position of the detonation front as a function of time. Scopes were triggered by a pin between donor pellets; in addition, x-t data from the LSGT calibration were available. The data were reduced to obtain run length x_s and delay time as a function of initiating pressure P_i. Fig. 21 summarized the data x_s vs P_i for the confined and unconfined charges, and shows the approach to P_{ci} for this experiment in each case (P_{ci} value is shown by vertical lines at the asymptotic values). As this figure shows, the curve for the confined acceptor conforms exactly to that expected (Fig. 15). The curve for the unconfined acceptor is initially (at high pressure and small lengths traveled by the shock) coincident with the curve for the confined charge. This merely means that confinement has no effect until the entering curved shock front strikes and interacts with the confining walls. However, the two curves diverge rapidly after that, and a cusp appears in the upper one. After considering possible causes for this behavior and noting a similar cusp in another worker's unconfined gap testing of Comp B, we concluded that it is an effect caused by the lateral rarefaction waves and perhaps, in small part, by the curvature of the entering shock front.*

On the other hand, the x_s vs P_i curve for the confined (standard) LSGT shows no cusp and also shows a linear plot x_s^{-1} vs P_i as does the wedge test which will be described later. It appears that the measurements were completed before the arrival of lateral rarefactions. Hence P_{ci} measured in the standard

[55]Price, D., Toscano, J. P., and Jaffe, I., "Development of the Continuous Wire Method. Progress Report III, Measurements in Cast DINA," 20 Apr 1967.

*It is known that the shape of the entering shock wave (planar or non-planar) affects the flow and presumeably the value of P_{ci} measured. In fact, a recent projectile impact study on cast Comp B3[56] showed that local critical energies for initiation varied with the area impacted and were generally much higher than that measured (and found constant) in 1-D experiments. That suggested a concept of critical shocked area to be added to the critical parameters of pressure and time.

[56]Moulard, H., "Critical Conditions for Shock Initiation of Detonation by Small Projectile Impact," Preprints of the Seventh Symposium (International) on Detonation, Vol. 1, 1981, pp 182-189.

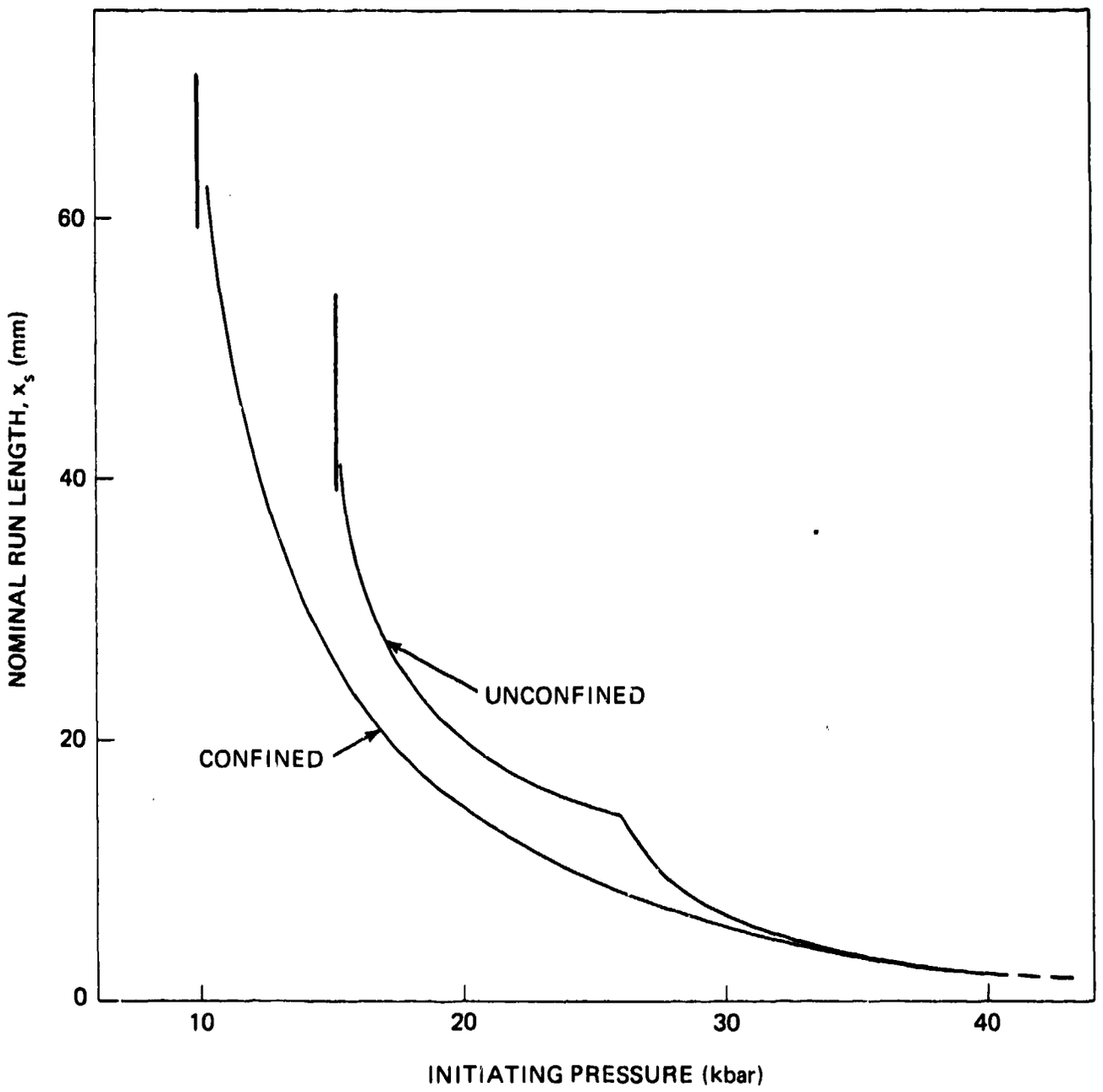

FIGURE 21 COMPARISON OF x_s VS. P_i FOR CONFINED AND UNCONFINED CHARGES. (REF. 55)

confined LSGT would be expected to approach the values obtained under 1-D planar conditions; there would be no similar expectation for those obtained with unconfined acceptors.

Very recently hydrodynamic calculations have been made of the flow in the shocked acceptor of the LSGT[57]. To best understand the results, information from other work on this test must be considered at the same time. As Fig. 17 shows, the detonator provides essentially a point initiation of the cylindrical pentolite donor. The detonation front expands spherically as it travels down the cylinder. Piacesi[58] carried out a hydrocalculation (2D Cyclone code) of such a divergent flow in a 50/50 pentolite cylinder of 50.8 mm dia; his calculations were carried out to an ℓ/d of 1.7 (the point at which the lateral rarefactions eliminate the rear rarefactions), i.e. well beyond the ℓ/d of 1.0 of the standard donor. Those calculations give us only a semi-quantitative picture of the flow in the standard donor because the donor density chosen was 1.65 g/cm^3 instead of the standard 1.56 g/cm^3 of the LSGT donor. In particular, the calculation showed that the detonation front in the cylinder is that of the spherical Taylor expansion wave down to the sonic point. As illustrated in Fig. 22, the pressure gradient at the detonation front is very large. Hence it is most unlikely that the ideal P_j can be measured or that a corresponding transmitted shock into the PMMA can be attained. This fact was ignored in deriving the calibration curve of Fig. 18 because the curve was forced to terminate (zero gap) at the pressure that would have been transmitted by the one dimensional P_j.

The spherical expansion of the detonation front in the donor resulted in a radius of curvature (R_c) equal to the distance traveled by the front. The shock transmitted to the PMMA gap shows uninterrupted continuation of the spherical expansion until lateral rarefactions affect it at about $L_g \sim 25$ mm. There is a jump in the pressure at the interface; the pressure transmitted into the gap is, of course, lower than the donor loading pressure. As the shock

[57] Bowman, A. L., Kershner, J. D., and Mader, C. L., "A Numerical Model of the Gap Test," LA-8408, Oct 1980.

[58] Piacesi, Jr., D., "Numerical Hydrodynamic Calculations of the Flow of the Detonation Products from a Point-Initiated Explosive Cylinder," NOLTR 66-150, Jan 1967.

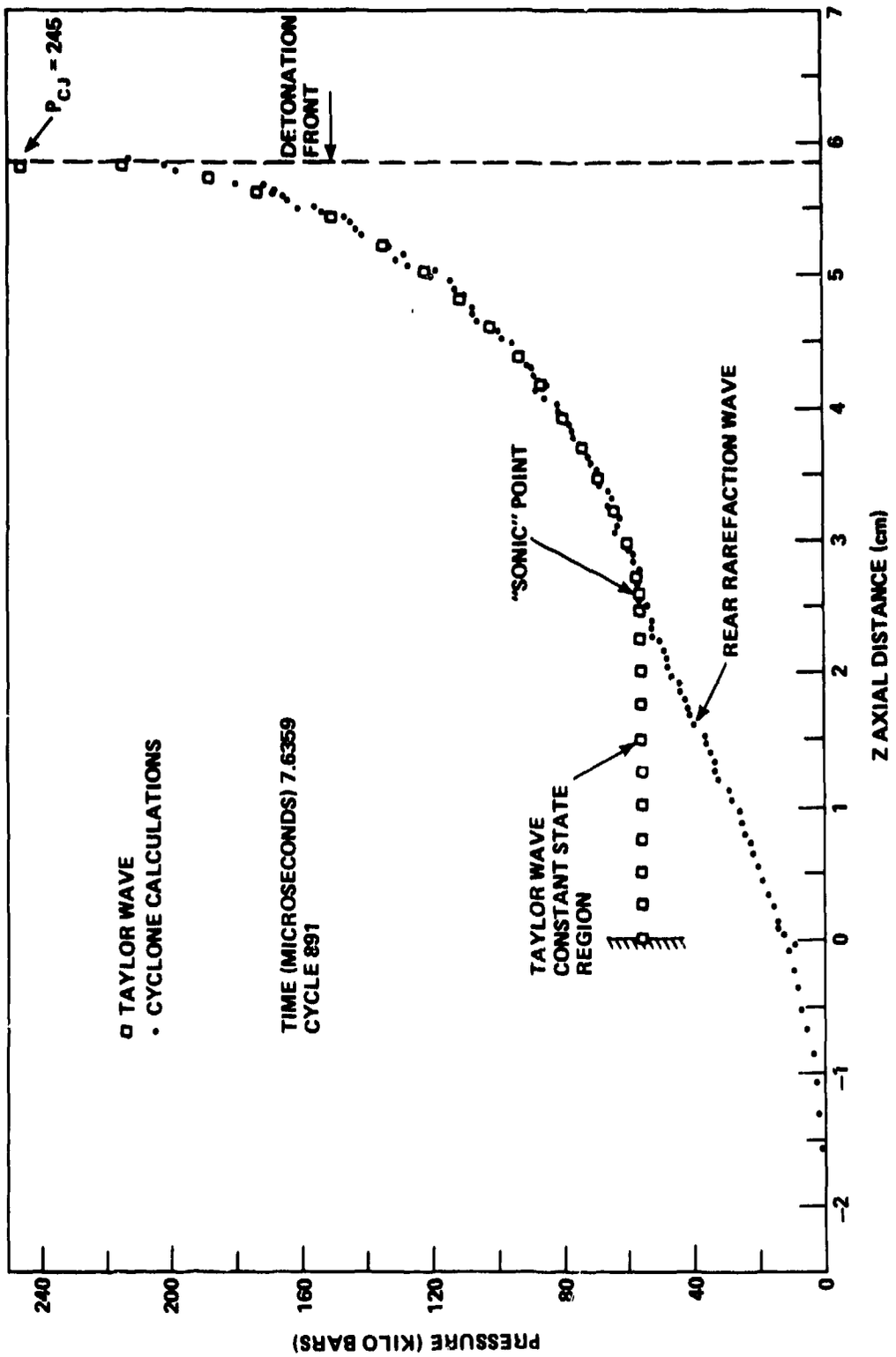

FIGURE 22 COMPARISON OF THE PRESSURE ALONG THE CENTRAL AXIS OF A POINT INITIATED CYLINDER (CYCLONE CALCULATIONS) AND THE RADIAL PRESSURE DISTRIBUTION IN A SPHERICAL TAYLOR WAVE. (THE CYCLONE VALUES ARE TAKEN AT t = 7.6359 MICROSECONDS AFTER INITIATION. POINT OF INITIATION IS AT Z = 0. (REF 58))

travels from the PMMA to the acceptor, there is another pressure jump with the amplitude changed again according to the impedance of the acceptor.

Ref. 57 carried out calculations with the 2DE (two dimensional reactive) code in which the Forest Fire burn rate was used for all explosives except pentolite. For that HE, the C-J volume burn model was used. With this model, the divergent detonation wave reached a steady pressure of 145 kbar rather than a C-J pressure of 228 kbar (P_j of 215 kbar was used for Fig. 18), and the error of using P_j instead of a lesser pressure in the donor loading was pointed out. As a result, the computed calibration curve of Ref. 57 was much lower at L_g < 10 mm (in the "nominal" range of Fig. 18) and somewhat higher at L_g > 10 mm than the LSGT curve of Fig. 18. Fig. 23 illustrates the comparison.

It should be remarked at this point that the Taylor wave and Cyclone code calculations of Fig. 22 suggest a much steeper pressure gradient than the approximately constant 103-90 kbar of Fig. 23 at L_g < 10 mm. Moreover, experimental data for both shock velocity vs distance and particle velocity vs distance curves in donor shocked PMMA indicate steeper slopes[49]. In particular, the u-x curve obtained by the electromagnetic velocity (EMV) gage measurements on tetryl loaded PMMA included 10 experiments at x ≤ 10 mm. That curve is shown in Fig. 24 and illustrates the steep initial slope. (The initial point was for plane wave boosting of the tetryl donor, but previous EMV measurements in a 50.8 mm dia x 50.8 mm long tetryl cylinder had resulted in the same values for both plane wave and detonator point initiation[59].

In view of the above, it seems likely that both curves of Fig. 23 are in error for x ≤ 10 mm: the calibration curve of Fig. 18 too high and the computed curve of Ref. 57 too low in that range. Moreover, the EMV data at x ≤ 10 mm for pentolite loading of the PMMA can be used to compute the shock amplitude by combining Eq. 10.

$$U = 2.561 + 1.595\ u$$

with Eq. 11 to obtain

$$P = 1.185\ (2.561 + 1.595\ u)\ u$$

[59] Edwards, D. J., Erkman, J. O., and Price, D., "The Measurement of Particle Velocity in Pressed Tetryl," NOLTR 72-83, Aug 1972.

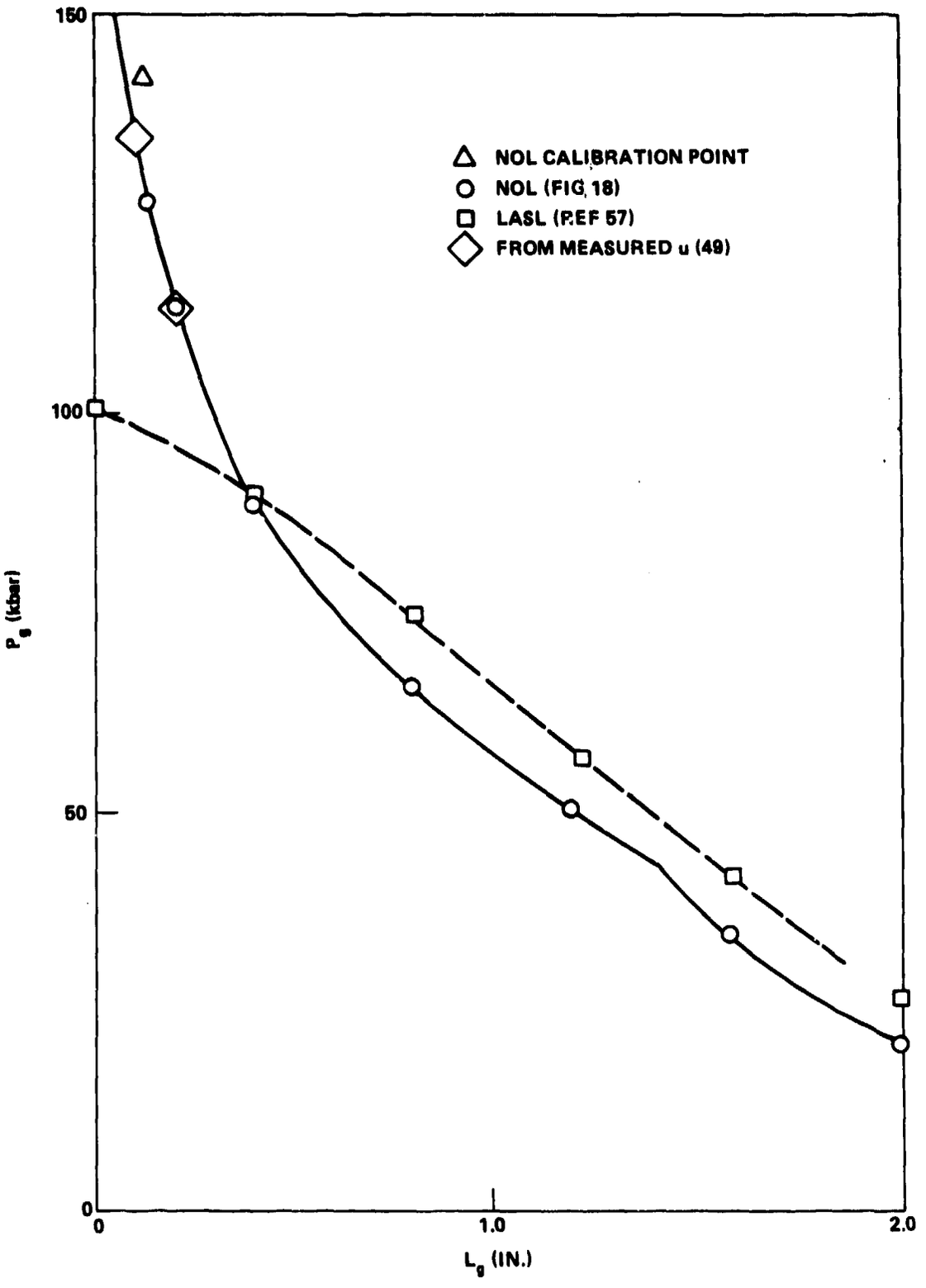

FIGURE 23 COMPARISON OF CALIBRATION CURVES FOR STANDARD NOL LSGT

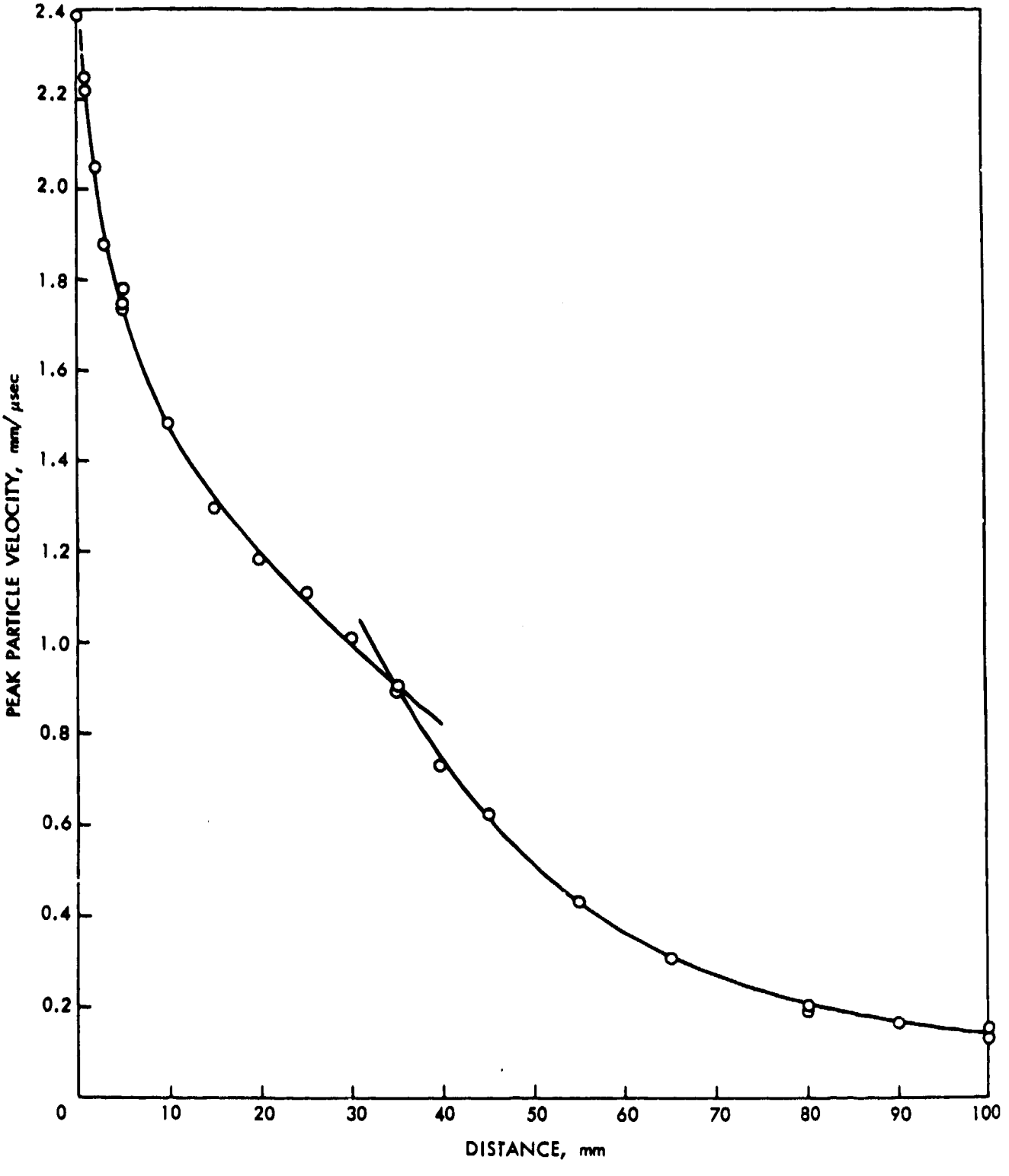

FIGURE 24 RESULTS OF FITTING PEAK PARTICLE VELOCITIES VS DISTANCE (TETRYL DONOR) REF 49

where P and u have the respective units of GPa and mm/μs. Then if the data are forced to terminate on the experimental point at x = 0, the calibration curve of Fig. 18 is corrected to the curve derived from u-x data shown in Fig. 25. Both from shock front curvature in the PMMA and inertial effects of the Al foil gage, errors in particle velocity measurements would be expected to result in values below rather than above the true values. Hence, they suggest that the Reference 57 curve is too low for the range $x \leq 10$ mm. Moreover, the EMV measurements result in P values that fall on the old calibration curve for $x \geq 5$ mm, below it at $x < 5$ mm.

As the Fig. 25 curves show, the Ref. 57 computation and the experimental calibration curve agree within the maximum estimated experimental error at $x \geq 6$ mm. Moreover, whether the CJ volume burn of the pentolite donor represents the exact loading of the PMMA or not, the computations with that loading provide much information about the shock in the acceptor of the LSGT. In our standard test with steel confinement, it shows in the acceptor an entering curved shock front which rapidly flattens out because of reinforcement by the shock interaction at the steel walls. It also shows the reaction starting at the walls and not at the charge center on the longitudinal axis; this may be the case or may be an artifact of the sensitivity of the Forest Fire code. The results for the unconfined acceptor are those expected: increasing curvature of the shock front with increasing penetration of the charge, and reaction starting on axis. Hence with the pentolite loading of Ref. 57, the computations reinforce the experimental results on DINA: the standard LSGT (steel confinement) approximates the 1-D condition in the acceptor; the use of unconfined acceptors does not.

Ref. 28 was devoted to the LSGT and summarized much information about it. Some of that information was repeated (and sometimes updated) above. The remainder will be summarized very briefly. Increasing temperature decreases P_g; the effect is extreme if the temperature is just above t_c. The porosity effect is the same for both Group 1 and 2 HE: P_g increases with decreasing porosity; the increase is particularly sharp as d_c (and dead-pressing) is approached for Group 2 materials. See Fig. 26 and 27. The particle size effect differs for granular and voidless (cast or plastic bonded) charges. The former show P_g increasing as δ decreases; the latter show the reverse

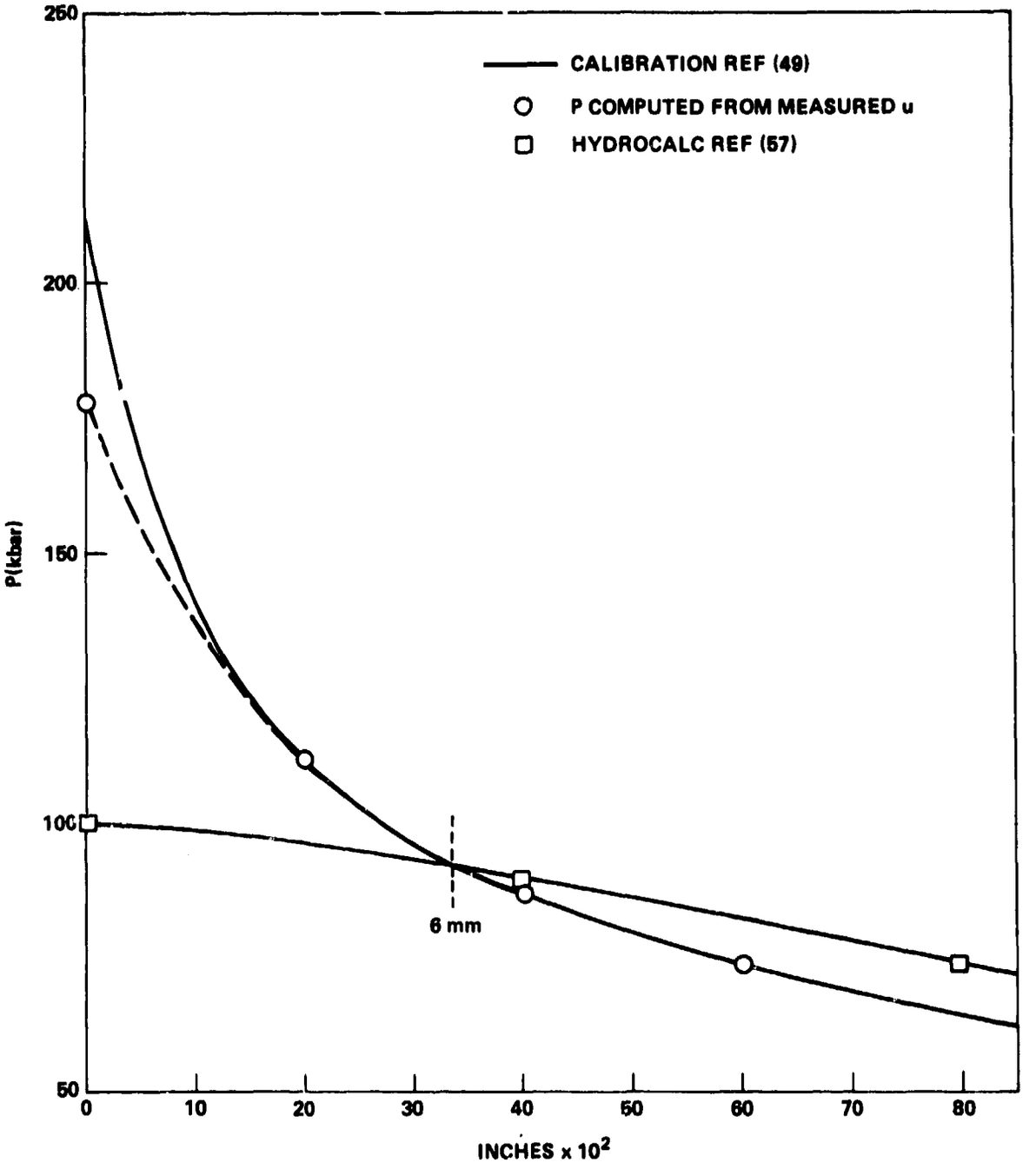

FIGURE 25 P VS x CALIBRATIONS FOR SMALL GAP VALUES

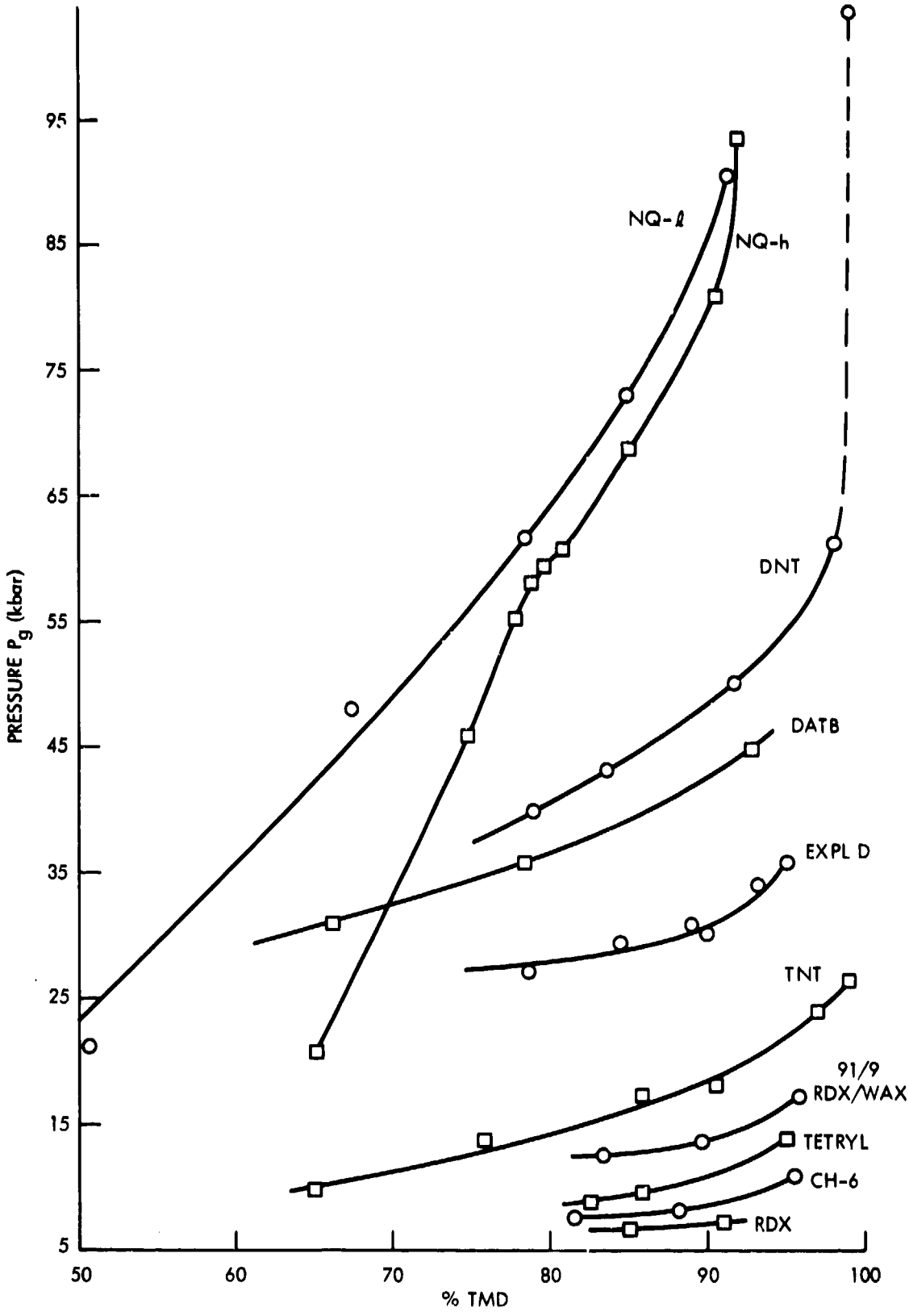

FIGURE 26 LSGT RESULTS FOR PRESSED CHARGES OF ORGANIC HE(Gr. 1).(REF. 28)

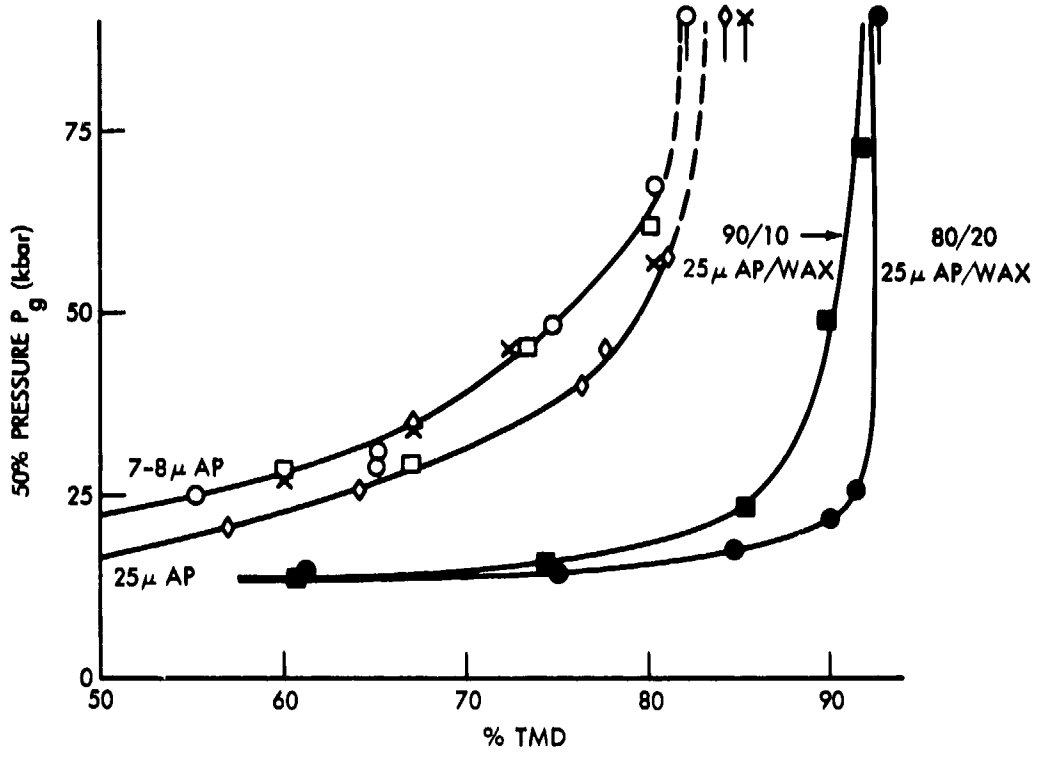

FIGURE 27 LSGT RESULTS FOR PRESSED CHARGES OF AP AND AP/FUEL MIXTURES. (GROUP 2). (REF. 28). (○ AP 141,7μ ; □ AP 145,8μ ; × AP 145/Aℓ (7μ), 95/5; △ AP 145/Aℓ (7μ), 90/10).

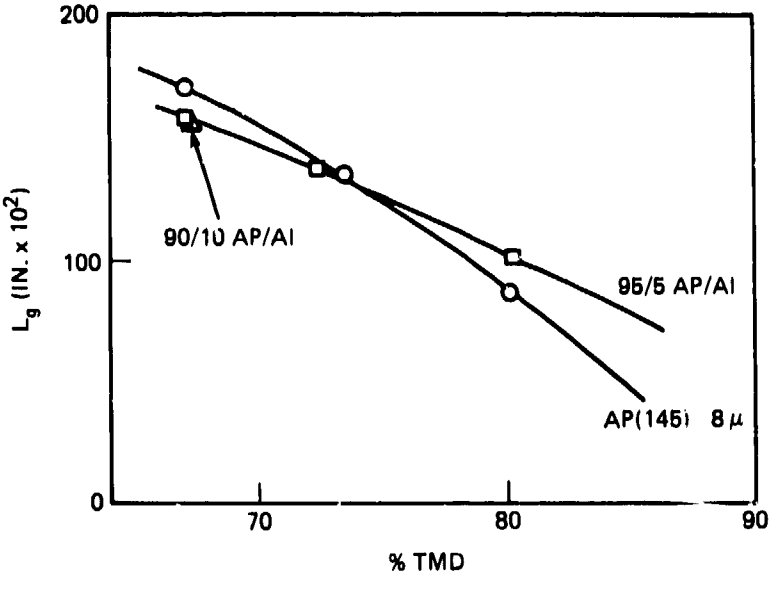

FIGURE 28 EFFECT OF ALUMINUM ON SHOCK SENSITIVITY OF AP

trend. Addition of wax to Group 1 explosives increases P_g; to AP, decreases it (Fig. 27). Addition of Al to cast or pressed TNT (at 95% TMD) increases P_g; Al added to pressed AP appears to have the same effect (increased P_g) at % TMD $\leq$ 72, but the opposite one at 80% TMD or greater. (See Fig. 28).

Although we have concentrated on P_g, we have mentioned the effect of duration several times. It remains to consider a critical energy concept and how the LSGT values conform to it. The existence of a critical initiation energy has been proposed many times in the past. The first quantitative proposal was made by Walker and Wasley[52]. They showed that for several essentially voidless HE, under 1-D experimental conditions, there is a constant energy/unit area

$$E = \frac{P^2\tau}{\rho_0 U} = Pu\tau \qquad (12)$$

required for initiation. Eq. 12 applies for a square pressure pulse of amplitude P, duration τ, and velocity U in the unreacted explosive; u and ρ_0 are the particle velocity and density, respectively. Subsequently, de Longueville et al.[60] showed that the concept held not at all for the liquids, TNT and NM, very poorly for granular RDX (ρ_0 = 1.55 g/cm^3), only approximately for plastic bonded HMX and RDX, and quite well for PBX 9404 and cast Comp B3. See Fig. 29. Despite its inapplicability to liquid and porous HE and to occasional voidless solid HEs*, the energy criterion has served as a useful engineering guide. By applying it to essentially voidless pressed TNT[1], it was possible to obtain a quantitative version of the pressure-time threshold for initiation outlined in Fig. 14. Fig. 30 shows the result

---

[60] de Longueville, Y., Fauquignon, C., and Moulard, H., "Initiation of Several Condensed Explosives by a Given Duration Shock Wave," Sixth Symposium (International) on Detonation, ONR ACR-221, U.S. Gov. Print. Office, Washington, DC, 1978; pp 105-114.

*Plastic bonded TATB behaves like the liquids with regard to shock initiation of detonation[61].

[61] Jackson, R. K., Green, L. G., Bartlett, R. H., Hofer, W. W., Kramer, P. E., Lee, R. S., Nidick, E. J., Jr., Shaw, L. L., and Weingart, R. C., "Initiation and Detonation Characteristics of TATB," ibid. pp 755-765.

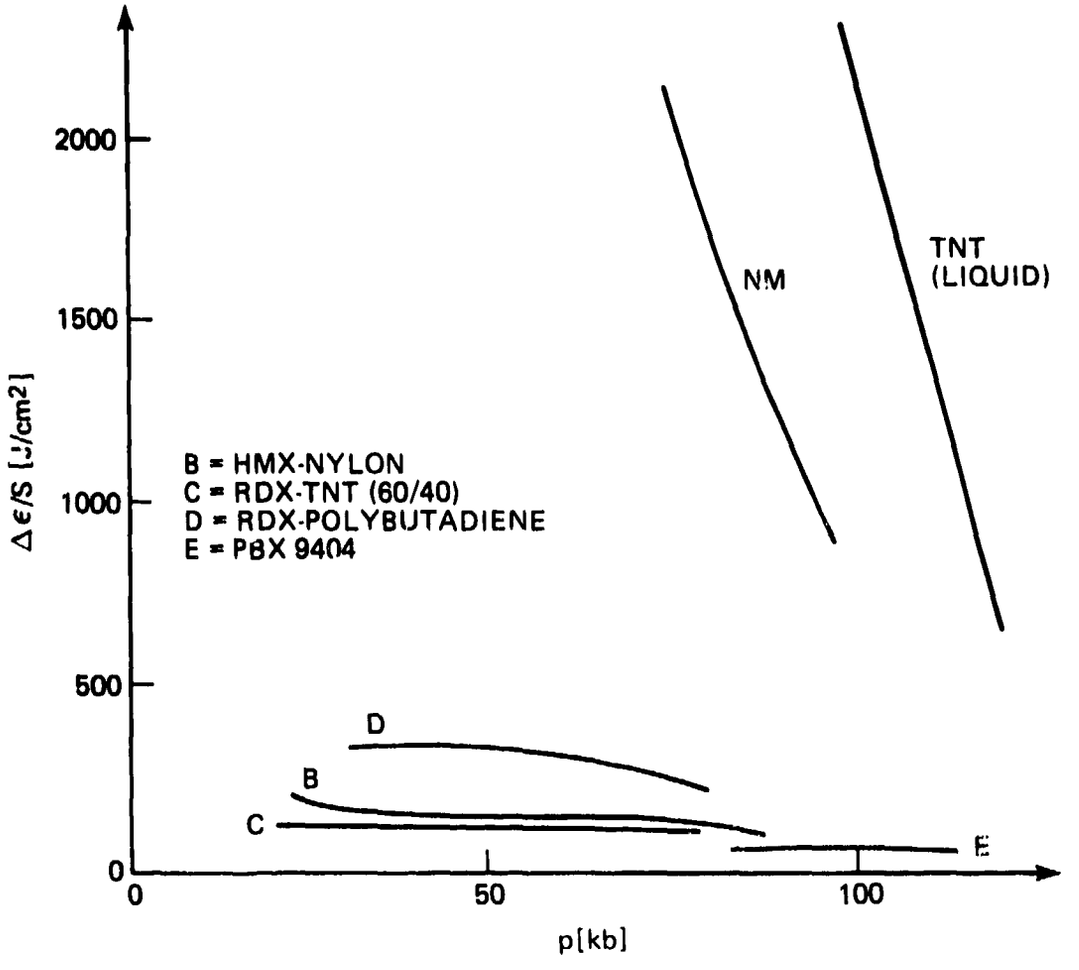

FIGURE 29 ENERGY THRESHOLD VS SHOCK PRESSURE (REF. 60)

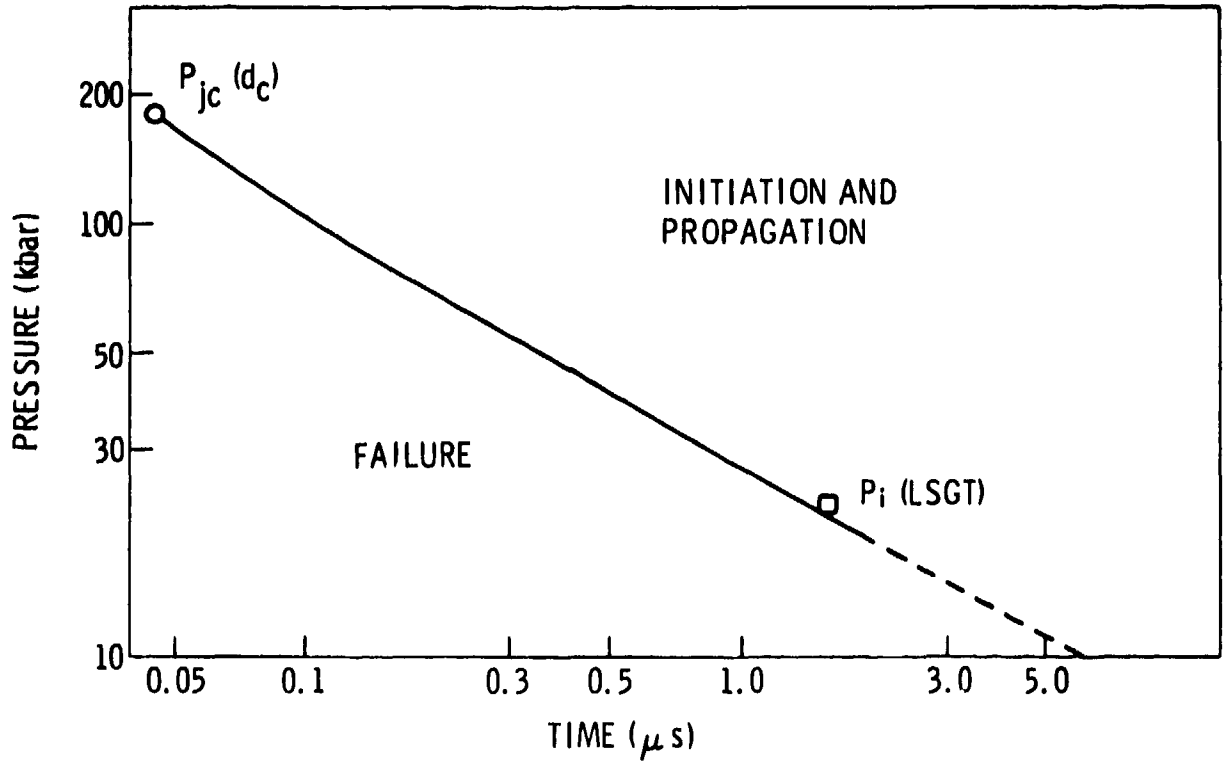

FIGURE 30 CRITICAL CURVE THROUGH THRESHOLD VALUES FOR PRESSED TNT (ρ_0 = 1.62, E = 32 cal/cm^2). (REF. 1)

for pressed TNT. (The same procedure indicated that cast TNT had a critical energy about four times as large.) As Fig. 30 shows, the limit curve was drawn from the critical pressure (taken as the C-J pressure lasting for the reaction time) at $d = d_c$, and the value measured in the LSGT falls on the curve near its lower end. Presumeably, threshold values for other initiation tests of this TNT (e.g., gap, wedges, projectile, and booster tests) will also fall on this limit curve. In other words, all initiation tests values for a given HE should be related.

The Wedge Test

The wedge test was designed as a plane-wave system so arranged as to permit continuous optical monitoring of the wave front within the shocked explosive[46]. A typical experimental setup is shown in Fig. 31. This is a sophisticated experiment and correspondingly yields much information from the streak camera record synchronized with the event. The emergence of the planar shock from the barrier (a material of known Hugoniot), its tilt (if any), and the position of intersection of the shock waves and the inclined mylar covered face of the wedge are recorded as a function of time. The initial pressure of the shock wave entering the explosive may be varied by selecting different explosives and thicknesses of the explosive pad and different attenuators and thicknesses of the barrier. The reduced data give $P(x,t)$, $U(x,t)$, run distance, and delay time.

Although most gap tests use a cylindrical charge and d_c is defined for a cylindrical charge, there is no restriction on the charge geometry used in measuring P_{ci}. The choice of the wedge shape (to obtain continuous measurements) and of the wedge angle, to assure that release waves cannot arrive before the shock wave, result in data reproducing that expected in the interior of larger charges. The records of run length vs initial pressure are very similar to that of Fig. 21 for the standard LSGT. Jacobs et al.[46] concluded that their results agree reasonably well with shock initiation work on cylinders of cross-sectional area comparable to the face area of the test wedge provided only axial measurements are made on the cylinders and the initial shocks have comparable pressure-time profiles. Fig. 21 indicates that there is more apt to be agreement between wedge and the standard LSGT (i.e., confined charge) than in the unconfined case.

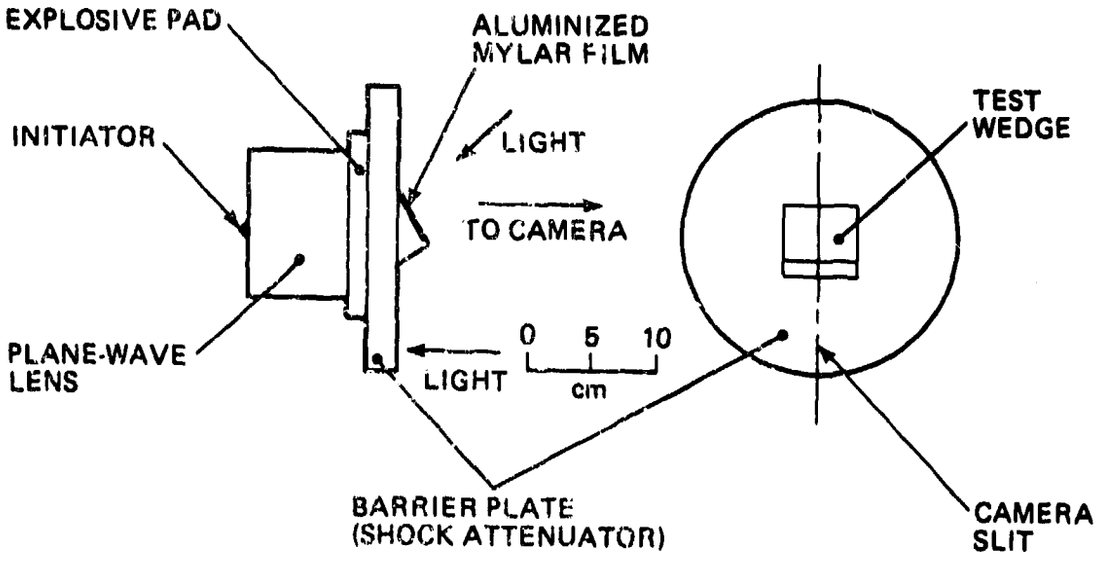

(TYPICAL WEDGE: 32 x 32 x 14 mm, 25° WEDGE WITH APEX ANGLE 90°.)

FIGURE 31 WEDGE-TEST ARRANGEMENT. (REF. 46)

A comparison of wedge test results with the NOL LSGT was first presented in the appendix of Ref. 50. Subsequently corrected data for the wedge tests were used for the comparison in Ref. 28 together with better Hugoniot data available at that time. The parameters considered in reference 50 were:

- x_s Run length, distance from the shocked surface to the plane in which steady-state detonation is first established.
- τ_s Delay time, total time from entry of shock into the explosive until the time at which steady-state detonation begins.
- Δ Excess delay time, amount by which τ_s exceeds the time required for the detonation to travel distance x_s. $\Delta = \tau_s - x_s/D$.
- P_g Pressure (50% point) in PMMA at gap/acceptor interface.
- P_i Shock pressure.
- P_{ci} Threshold pressure in explosive required to initiate detonation in LSGT.

It was tentatively concluded that Δ^{-1} vs P, τ_s^{-1} vs P, and x_s^{-1} vs P were all linear, and that, in the last case, the point (P_{ci}, 0.02 mm^{-1}) fell on the curve. Moreover, it was pointed out that log x_s vs log P was also linear and, in some cases, extrapolated to reasonable values of P for $x_s \sim$ reaction zone length whereas the x_s^{-1} vs P curves did not.

Because the average set of data[50] consisted of only three points, the suggested relationships were considered tentative. However, Jacobs et al[46] working independently showed linearity of x_s^{-1} vs P for some nine points of data for cast Comp B-3. Somewhat later Ramsay and Popolato[62] published linear log x_s vs log P curves for five explosives. Since then both Los Alamos Scientific Laboratory and Lawrence Livermore Laboratory have used this empirical relationship for evaluating shock sensitivities.

Data for confined DINA (LSGT-Fig. 21) gave a linear curve x_s^{-1} vs P whereas data for unconfined DINA showed a sharp change in slope and non-linearity over the low pressure portion of the x_s^{-1} vs P curve.

[62] Ramsay, J. B. and Popolato, A., "Analysis of Shock Wave and Initiation Data for Solid Explosives," Fourth Symp. (Int.) on Detonation, ONR, ACR-126, U.S. Gov. Print. Office, Washington, D.C., 1967, pp 233-238.

Data for the confined DINA were also examined in the other empirical relationships that have been mentioned (log x_s vs log P, log x_s vs log Δ, τ_s^{-1} vs P, Δ^{-1} vs P). All showed some curvature when all eight pairs of data were included. However, if the first two pairs (i.e., at P values of 42.8 and 49.5 kbar) were discarded, the remaining six showed linearity for all the other relationships mentioned. Thus for the confined DINA and presumably any comparable data obtained in the LSGT set-up, the most successful linear relation is that of x_s^{-1} vs P.

This same relation (x_s^{-1} vs P) has been used for reexamination of the wedge test data. The transition data for cast pentolite and DINA are plotted in Figure 32; those for the remaining cast materials, in Figure 33. The data for pentolite and DINA have been plotted separately (1) to emphasize the similarity between the wedge test results and those from the regular LSGT configuration on similar explosives and (2) because these curves cross those of Figure 33 for the other TNT based castings. Both the pentolite and DINA data (x_s^{-1} vs P) seem to terminate at P_{ci}. The apparent crossing of these curves near P_{ci} is probably fictitious. The P_{ci} values of 11.9 (pentolite) and 11.0 kbars (DINA) are not significantly different and could be reversed by small errors in the measurements or the Hugoniots used or both. Moreover, unconfined pentolite showed P_{ci} of 12 - 14 kbar as compared to 15 kbar for unconfined DINA, i.e., the reverse of the relative sensitivities of the confined charges. If the run length for the same shock amplitude is considered a measure of the shock sensitivity, then cast pentolite is more shock sensitive than cast DINA, probably over the entire pressure range. However, both curves of Figure 32 intersect some of the curves of Figure 33. Hence on the run-length criterion, reversals in relative sensitivity will occur between the higher and lower pressure ranges, e.g., for pentolite and Comp B-3 and for DINA and Octol 65/35.

In Figure 33, all five cast explosives show a satisfactory linear extrapolation of x_s^{-1} vs P to P_{ci}, save possibly Comp B. Of course the data for Comp B-3 include only the higher pressure, shorter run length data. Reference 44 gives, in addition, lower pressure, longer run length data that resulted in an extrapolation to 28 kbar instead of the present 22 kbar. This difference is the order of magnitude of errors in P_{ci}

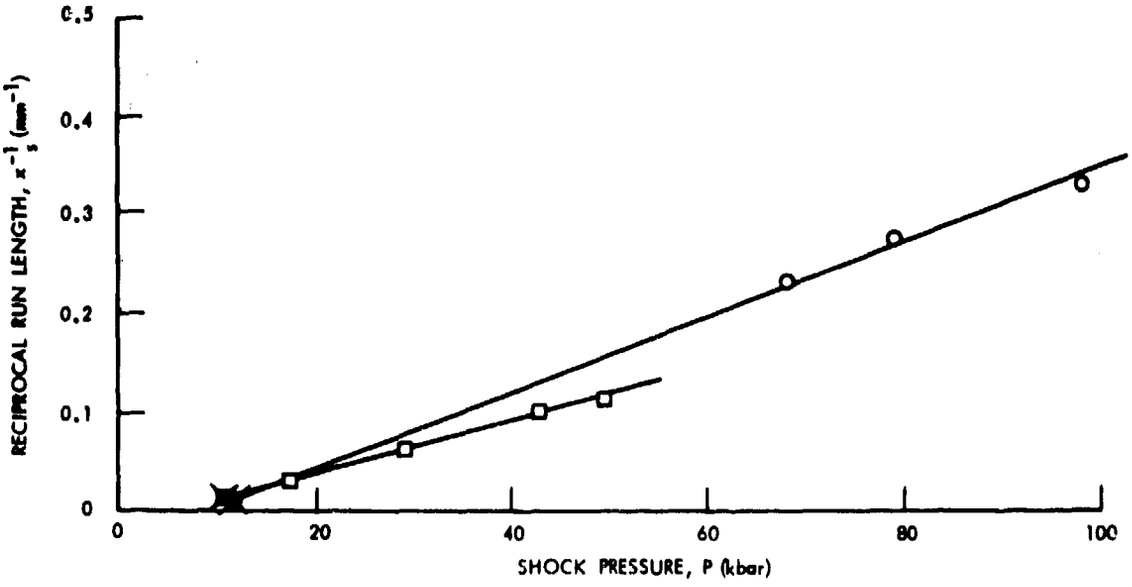

FIGURE 32 SHOCK TO DETONATION TRANSITION FOR CAST PENTONITE AND DINA. (○ PENTONITE, WEDGE DATA; □ DINA, REGULAR LSGT CONFIGURATION; X P_{ci} VALUE). (REF. 28)

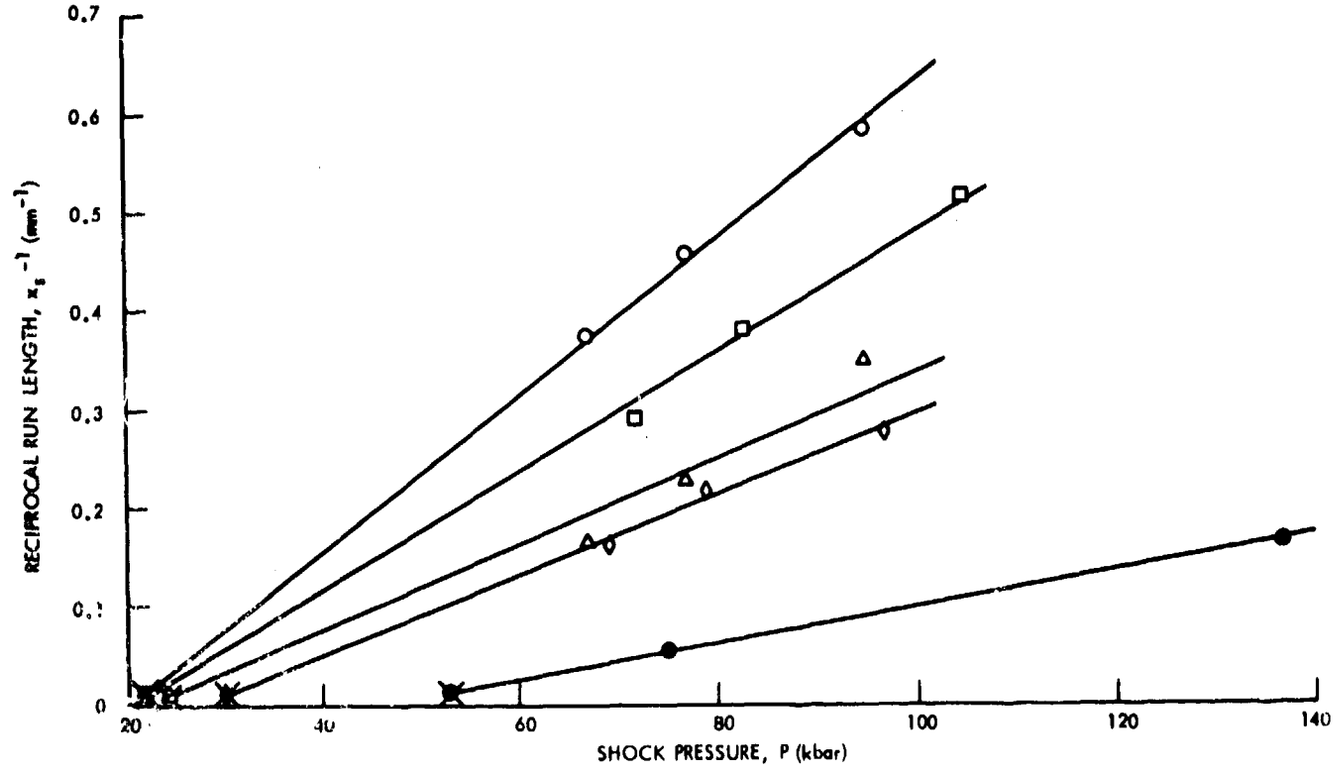

FIGURE 33 SHOCK TO DETONATION TRANSITION FOR OTHER TNT BASED CAST EXPLOSIVES. (○ COMP B-3; □ OCTOL 65/35; △ COMP B; ◇ CYCLOTOL 75/25; ● TNT; X P_{ci} VALUE). (REF. 28)

and possibly of the lower shock pressure measurements. It might also be caused by an unmonitored duration effect in the action of the shock wave; such an effect becomes more important at the lower amplitudes. Whatever the cause(s), the discrepancy cannot be resolved without further experimental work.

By the run-length criterion, the shock sensitivities of Figure 33, in descending order, are Comp B-3 (RDX/TNT, 60/40), Octol 65/35, Comp B (RDX/TNT/Wax, 60/40/1), Cyclotol 75/25, and TNT. This ordering of cast explosives can be reconciled with composition effects if the role of particle size in affecting shock sensitivity is recognized. Seely[63] demonstrated in 1963 that shock sensitivity increased with increasing particle size if air was the continuous medium, but increased with decreasing particle size if the continuous medium was a condensed one. Cast explosives fall in the latter category and should show increasing sensitivity with decreasing particle size. RDX Class F is recommended for preparing Comp B-3; Class A for Comp B; and Class D for cyclotols. The relative weight mean diameters are 58, 130, and 740μ respectively for Classes F, A, and D. It is evident that the difference in the RDX particle size can account for the fact that cast Comp B-3 is more shock sensitive than cast Comp B. The difference between Classes A and D RDX can also account for the cast cyclotol (75% RDX) being less sensitive than the cast Comp B (60% RDX).*

Finally, Figures 32 and 33 reemphasize the inadequacy of an attempt to characterize shock sensitivity by measurement at only the 50% point. The curves x_s^{-1} vs P_i not only demonstrate differences in sensitivity much better than LSGT values alone can do; they also show reversals in behavior that cannot be predicted from the LSGT values unless an instrumented LSGT

[63] Seely, L. B., "A Proposed Mechanism for Shock Initiation of Low Density Granular Explosives," Proc. Fourth Elec. Initiation Symposium, Franklin Institute, Phila. 1963; Paper 27 of Rept. EIS-A-2357.

*When pressed cyclotol 75/25 and pressed Comp B are compared at 96.4% TMD in the LSGT their respective 50% values of P_g are 12 and 18 kbar. By going to highly pressed charges, the initial particle size effect has been reversed and the chemical effect (75 vs 60% RDX) is still present. Hence the relative sensitivity has not only been reversed (compared to ratings of the cast materials), but the difference is significant.

(such as that of Fig. 32) is used. Even Figures 32 and 33 are incomplete descriptions of shock sensitivity. As discussed earlier, a limit curve in the pressure-time plane exists for the shock initiation of detonation in each charge, and a similar limit curve probably exists for the shock initiation of burning and sub-detonation reactions. Liddiard[64] has shown that threshold conditions for initiating such reactions can be defined and measured. Moreover such shock induced reactions are also an important aspect of a material's sensitivity to shock.

Relations Between Results of Various Gap Tests

In accord with the idea that all P_{ci} values measured in different tests should lie on curves such as those of Figs. 14, 16, 30 (for a specific explosive) and should be related to each other, correlations between different gap tests were investigated. It has been shown[28] that the NOL small scale gap test (SSGT) results correlate well with the LSGT results. Surprisingly, it has been shown[28] that LSGT results for confined and unconfined cast HE acceptors also correlate.* Hence a relationship might be expected between any other well standardized shock initiation tests carried out on identical explosive samples. Such comparisons with results of other laboratories have to be made with 50% point gap length (L_g) values because of uncalibrated tests or differences in calibration data used. In contrast to the use of P_g rather than P_{ci}, the use of gap length distorts the true sensitivity scale, particularly in the higher sensitivity (lower P_{ci}) range. For two tests of quite similar dimensions, one would hope both would be affected in the same manner; if so, any distortion would not conceal the relation between the tests when comparing 50% gap values.

LASL has a LSGT, unconfined, of 41 mm dia[23]; this compares to the NOL LSGT, unconfined, of 38 mm dia which correlates well with the standardized LSGT values.* Hence despite different donors and different attenuators some correlation between test results on the same HEs would be expected.

---

[64] Liddiard, T. P., "The Initiation of Burning in High Explosives by Shock Waves," Fourth Symposium (International) on Detonation, ONR ACR-126, U.S. Gov. Print. Office, Washington, D. C., 1967; pp 487-495.

*The correlation holds only for the 50% point gap length L_g; if P_g is used, the data show a jump at x = 35 mm, the point at which rarefactions reach the axis of the PMMA cylinder.

Table 2 contains the reported data for seven cast explosives tested at both LASL and NSWC. All LASL data came from Reference 23; NSWC data are from Reference 28 (Tests made after 8 Mar 1974 are designated by test number in the table.) Differences in composition, density, and, where known, preparation are shown. LASL in testing eight batches of ca cyclotol had a range of 165-180 (average value of 172 ± 8) inches x 10^2; NSWC recorded tests for five batches of cast 50/50 pentolite with a range of 272-284 (average value of 278 ± 6) in. x 10^2. The two laboratories seem comparable in reproducing their values from batch to batch of cast (TNT matrix) HE. Figure 34 shows a plot of the LSGT data. The two sets are definitely related with L_g(NSWC) consistently greater than L_g(LASL). The exact nature of the relationship can only be established with a greater number of explosives of the same composition and preparation tested by both laboratories. For example, the data of Figure 34 might be better fit with a curved than a straight line; the differences in composition and procedures (Table 2) will certainly affect the final result. Even with the present data, there are no reversals in sensitivity ratings. (There is an apparent reversal between Comp B-3 and octol, but these two HE have the same LSGT value, within experimental error, in both sets of data. Hence the apparent reversal is not considered significant.)

The situation for pressed explosives is more complex. Table 3 contains the data which are plotted in Figure 35. With three exceptions, noted in both table and graph, all the explosives were pressed at 25°C. In general, explosives pressed at different temperatures would not be comparable. Figure 35 seems to suggest that there is a relationship between the two sets of test values for six of eight pressed HE. The other two HE are DATB and Comp A-3. The difference of the former might be attributed to the comparison of a cold pressed charge with a hot pressed charge. In the case of Comp A-3, the NSWC charges were prepared from plant production HE which we have found in earlier work gave rather erratic LSGT results. That may also have been the case at LASL; as noted in the table, higher results were reported in Reference 23 for other A-3 charges of nearly the same density.

Although the large departures of DATB and Comp A-3 from the average behavior may be explained as above, the different order of sensitivity ratings cannot be ignored. The ratings are shown in the lower part of Table 3. It is possible that hot pressing of DATB so sensitizes it that it seems equivalent

Table 2

Comparison of LSGT Values for Cast HE

LASL[23]				NSWC[28]				
Material	ρ_o, g/cm^3	%TMD	L_g in. x 10^2	Material	ρ_o, g/cm^3	%TMD	L_g in. x 10^2	
Pentolite				Pentolite				
55.5%PETN	1.702	99.2	255	55% PETN	1.67	97.1	290	
Comp B-3				Comp B-3				
64.0% RDX	1.727	98.6	198	60% RDX	1.71	98.6	209	
75/25 Octol				65/35 Octol				
76% HMX	1.822	99.3	195	65% HMX	1.78	98.9	214	
75/25 Cyclotol				75/25 Cyclotol				
77.7% RDX	1.734	97.8	180					
77.3% RDX	1.714	98.4	177					
77.9% RDX	1.750	98.7	174					
76.9% RDX	1.755	99.1	171					
76.1% RDX	1.757	99.4	170	75% RDX	1.746	99.0	182	(No. 904)
77.0% RDX	1.756	99.1	169					
76.8% RDX	1.756	99.15	167					
76.5% RDX	1.755	99.2	165					
Comp B, Grade A				Comp B				
64% RDX	1.710	97.7	180*	59.4% RDX	1.70	98.8	201	
64.5% RDX	1.714	97.8	170					
TNT	1.615	97.6	111	TNT	1.61	97.3	133	
80/20 Tritonal	1.732	~99	87	80/20 Tritonal	1.73	96.4	120	(No. 884)
					1.73	96.8	101	

*Vacuum cast

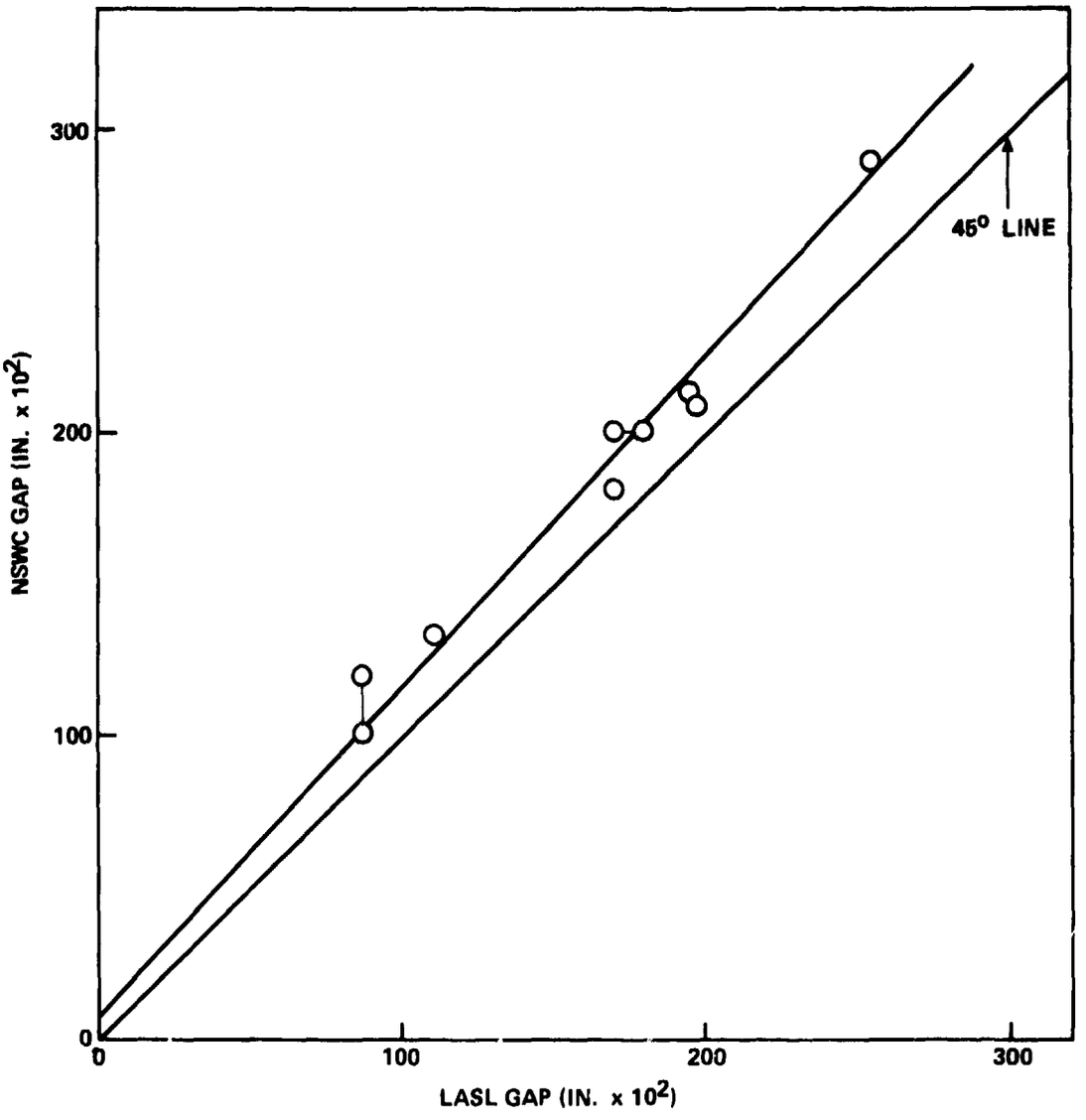

FIGURE 34 COMPARISON OF LSGT VALUES FOR CAST HE

Table 3

Comparison of LSGT Values for Pressed HE (>90%TMD)

	LASL[23]			NSWC[28]			
Material	ρ_o, g/cm^3	%TMD	L_q in. x 10^2	ρ_o, g/cm^3	%TMD	L_g in. x 10^2	
9404	1.771	94.9	237	1.77	94.9	235	
TNT	1.594	96.4	206*	1.60	97.1	183	
	1.637	99.0	168**	1.64	99.0	175	Isostatically pressed; water at 88°C
Tetryl	1.682	97.2	234	Extrapolated		221	
Comp A-3	1.645	97.5	193[a]	1.646	97.8	220	(No. 908)
				1.65	98.0	228	
DATB	1.705	92.8	179[b]	1.70	92.5	132	
	1.786	97.2	164[b]	Extrapolated		116	
Expl. D	1.604	93.4	169	1.60	93.2	160	
	1.64	95.4	168*	1.64	95.1	156	
	1.668	97.1	167	Extrapolated		151	
NQ	1.609	90.4	20	1.61	90.6	47	

Order of Decreasing Sensitivity

9404, Tetryl	9404
TNT	A3, Tetryl
A-3	TNT
DATB, Expl. D, TNT (hot pressed)	TNT (hot pressed)
NQ	Expl. D
	DATB
	NQ

*Average of two
**Pressed at 72°C

a. Values at 96.7 and 97.1%TMD are 208 and 215, respectively.
b. Hot-pressed.

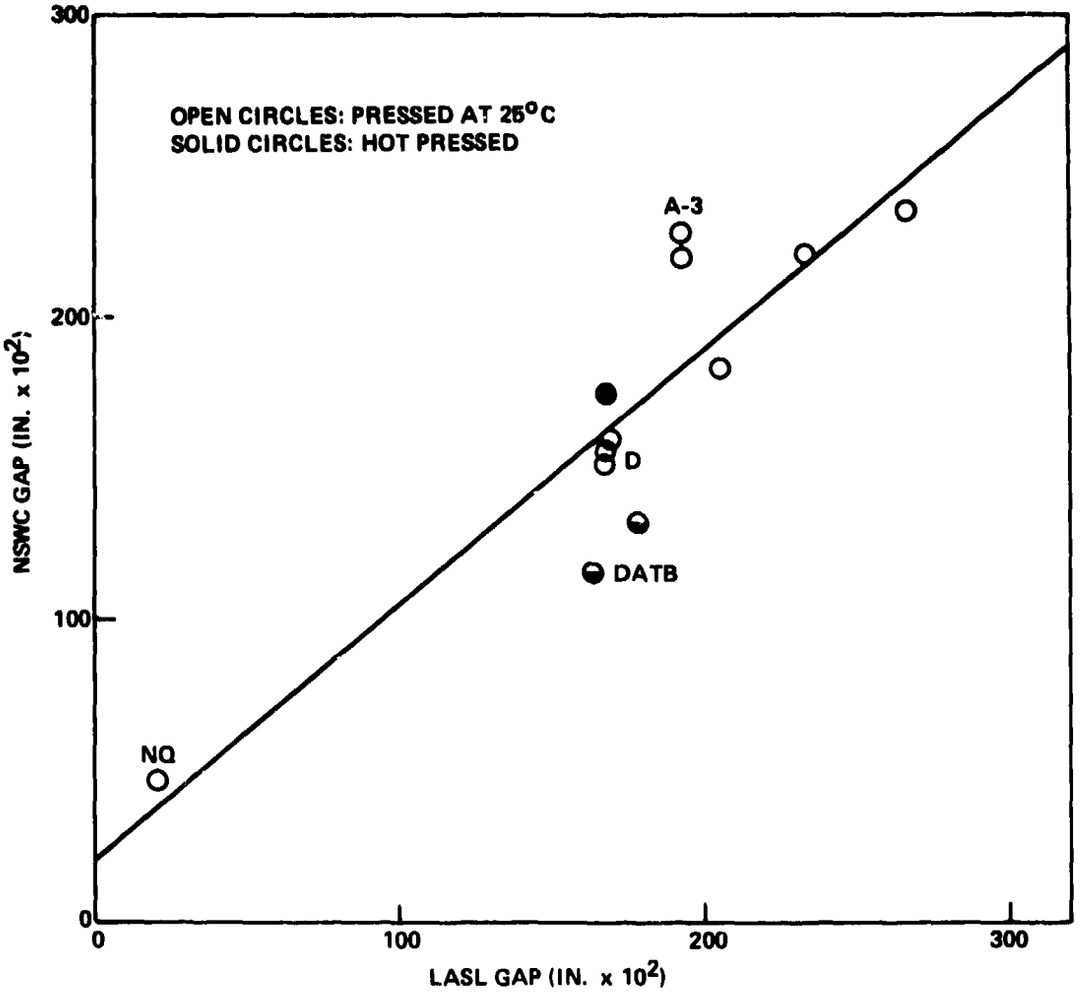

FIGURE 35 COMPARISON OF LSGT VALUES FOR PRESSED HE (>90% TMD)

to Explosive D. It is also possible that an atypical value for Comp A-3 is responsible for the inversion of the TNT/A3 values in the LASL data compared to those of NSWC. The large difference between hot and cold pressed TNT, seen in the LASL data, does not appear in the NSWC data. That might well be because little of the heat from the water medium of the isostatic press was transmitted thru the rubber mold to the TNT. In addition to all these possibilities, initial particle size also has an effect on LSGT values. At the present time, it does not seem warranted to assume a reliable relation between the two sets of test values for pressed HE. This view is reinforced by the definite lack of correlation in the case of porous TNT (pressed at 25^{o}C). The data are listed in Table 4 and plotted in Figure 36.

Table 4

LSGT Data for Porous TNT

LASL [23]				NSWC [28]
ρ_o, g/cm^3	%TMD	L_g in. x 10^2	Average plotted	Interpolated Data L_g, in. x 10^2
1.024	61.9	242		300 (extrapolated)
1.220	73.8	221		249
1.355	81.9	215	216	232
1.356	82.0	217		
1.435	86.8	214		219
1.502	90.8	215	216	209
1.505	91.0	216		
1.551	93.8	214		198
1.594	96.4	207	206	190
1.595	96.4	204		

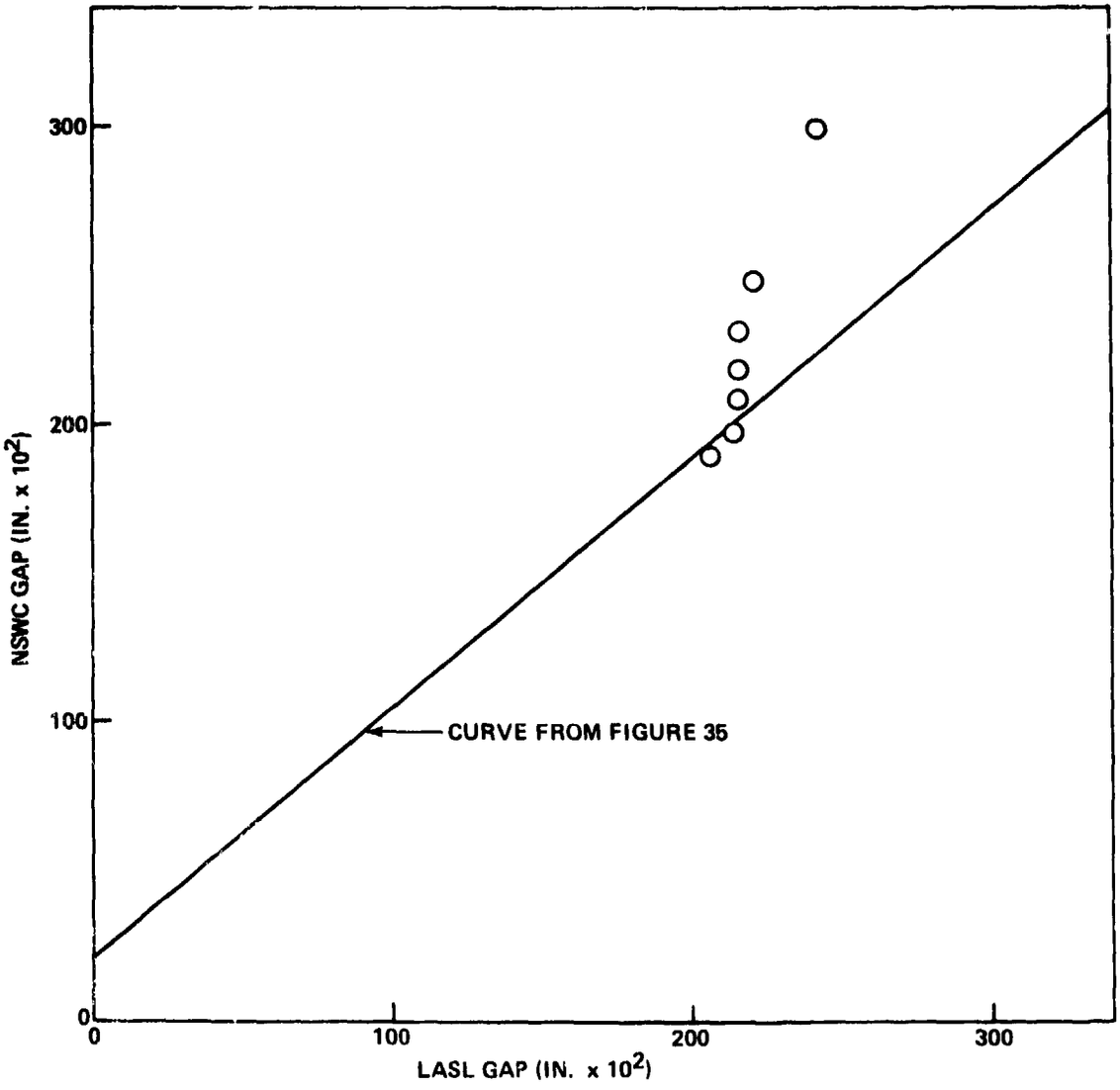

FIGURE 36 COMPARISON LSGT VALUES FOR POROUS TNT (CHARGES PRESSED AT 25°C)

INTERDEPENDENCE OF d_c AND P_{ci}

From the information now available on critical diameter for detonation and critical pressure for initiation it seems evident that the value of either of these quantities is one of the factors determining the other. However, it is not the dominating factor; hence no general relationship between only d_c and P_{ci} exists.

Fig. 37 illustrates the qualitative effects on d_c and P_{ci} of increasing the value of a number of variables defining the experimental conditions. As it shows, confinement, temperature, and dilution with wax cause parallel effects. Porosity causes similar effects in Group 2 HE (e.g., AP) but opposite effects in Group 1 HE (e.g., TNT). Particle size causes similar effects in voidless HE, but opposite ones in porous HE. Addition of Al also seems to cause opposite effects over most of the range. Out of 11 pair comparisons, there were four reversals; this fact alone rules out a general relationship between only these two critical parameters.

On the other hand, a continuous variation of d_c with P_{ci} exists for a single material in various forms. Fig. 38 for TNT is a good illustration of this because this material is castable. From very porous granular charges through hot pressed charges to various forms of castings offers a large variety of physical states as well as introducing the variable of physical heterogeneity not previously mentioned. Although this quantity cannot be measured precisely, we know that it is greatest at the left of Fig. 38 and least at the right. Moreover, we see the trend of the curve d_c vs P_{ci} reverse itself as the porous charges are replaced by voidless ones. Thereafter the critical values vary in the same way: increasing with decreasing heterogeneity (increasing homogeneity). The effect of degree of heterogeneity is attributed to its effect on hot spot formation.

Fig. 39 shows the relations d_c vs P_g for various granular Group 1 HE - all pure explosives. The dashed lines connect all the values at 85% TMD

VARIABLE INCREASED	EFFECT ON		NOTES
	d_c	P_{ci}	
CONFINEMENT	–	–	
TEMPERATURE	–	–	
POROSITY	+ –	– –	GROUP 1 GROUP 2
PARTICLE SIZE	+ +	– +	POROUS HE VOIDLESS, GR 1
% WAX	+ –	+ –	GROUP 1 AP
% Al	– NI – –	+ + – +	CAST TNT GRANULAR TNT AP AT ≥ 80% TMD AP AT ≤ 74% TMD

KEY
+ INCREASES
– DECREASES
NI NO INFORMATION

FIGURE 37 EFFECT OF VARIABLE CHANGE ON VALUES OF d_c AND P_g

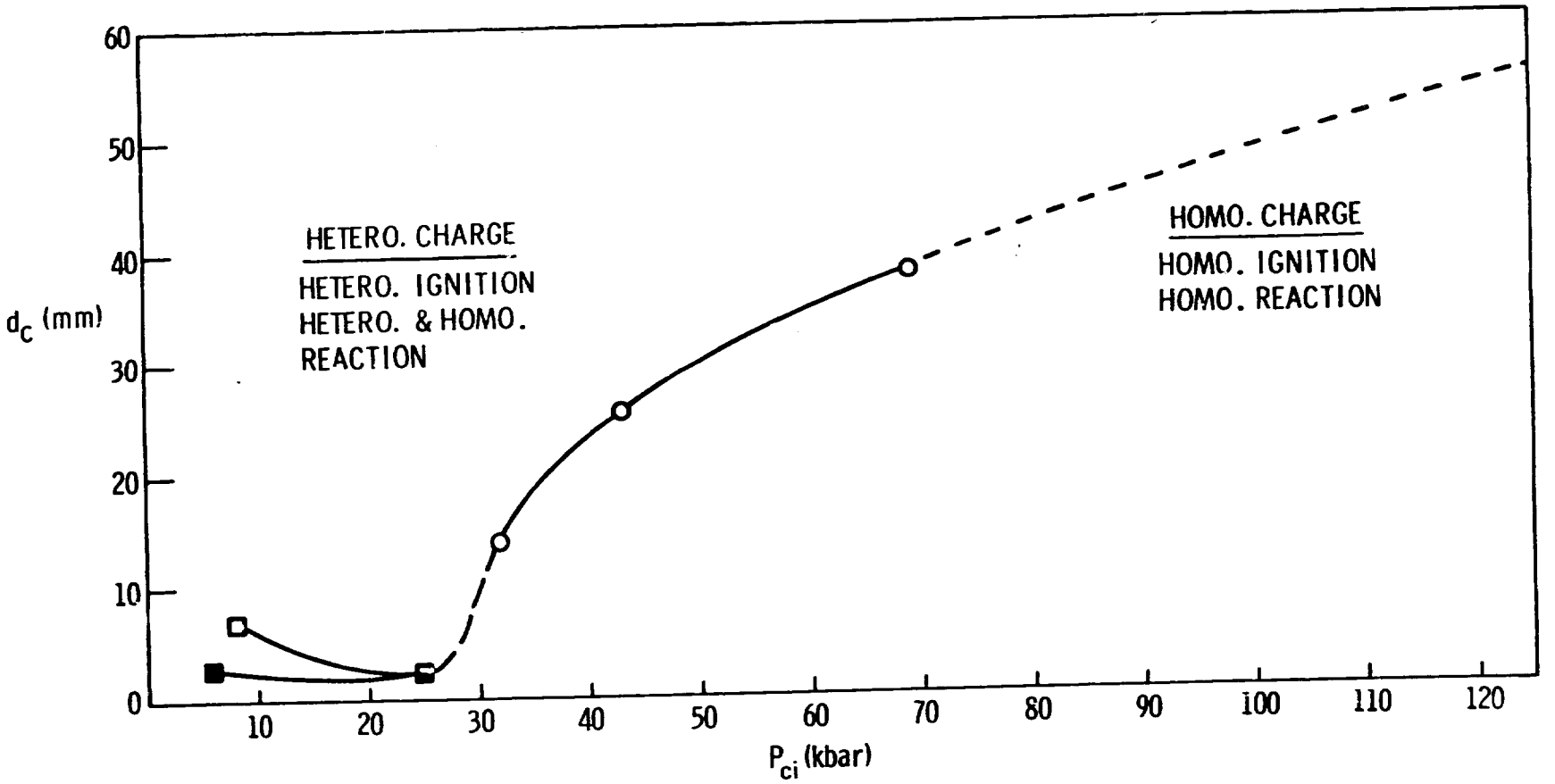

FIGURE 38 VARIATION OF CRITICAL DIAMETER WITH CRITICAL INITIATING PRESSURE FOR SEVERAL FORMS OF TNT. (REF. 1)
(COLD PRESSED CHARGES: □ COARSE, ■ FINE;
HOT PRESSED CHARGES ——; CAST CHARGES O ; EXTRAPOLATION – – –)

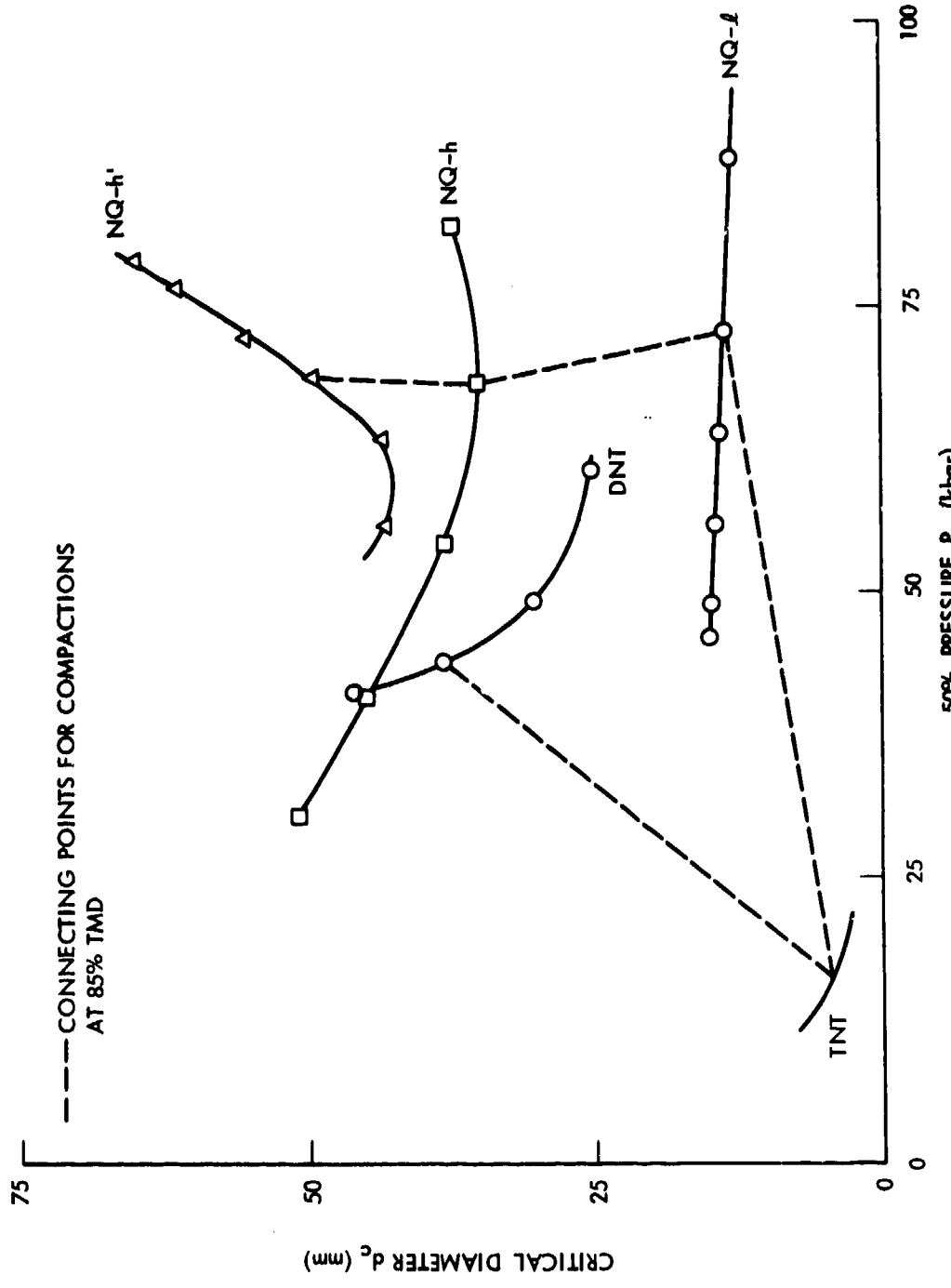

FIGURE 39 RELATIONS d_c VS P_g FOR GROUP 1 HE. (REF. 28)

to demonstrate that there is no smooth curve (at constant porosity) for all explosives although the curves for single explosives are certainly smooth. The dashed line also illustrates that the physical form of NQ (low bulk density, and two different lots of high bulk density material) had very little effect on the P_g value at 85% TMD compared to a relatively large effect on d_c.

Fig. 40 shows comparable d_c vs P_g relations for various granular Group 2 HE, AP and some of its mixtures. In this case, the 80% TMD points are marked to demonstrate again that there is no single curve encompassing all the HE, despite the fact that each one has a smooth curve. Here the particle size of AP at ~ 55% TMD (initial points) has more effect on d_c than on P_g, but at 80% TMD the relative effects are reversed.

So far, the relations considered have been for porous HE. Ref. 28 contains some data for cast and highly pressed explosives, i.e. essentially voidless HE. No correlation between P_{ci} and d_c was found for these materials although it is general knowledge that systematic variation of component concentration in multicomponent, voidless HE frequently results in such a correlation, but only for each series; it is therefore much like the single curves of Figs. 39 and 40.

Recently it was suggested that a linear relationship exists between ln d_c and L_g for voidless charges[24]. In view of the relations found earlier between the NSWC and LASL LSGT values, the suggestion was investigated for each set of values separately. The LASL and NSWC data are given in Tables 5 and 6, respectively.

The d_c values of Table 5 are for the most part, LASL values. One exception is that for TNT. As discussed in Ref. 21, Cybulski et. al.[36] chose unfortunate names for the various TNT castings they prepared and tested. To quote them:

"(1) Poured-clear...

"(2) Poured-cloudy. The molten TNT is allowed to cool to the region of its set-point with continuous stirring until a slurry is formed which is then poured into molds.

"(3) Creamed. The cooling melt is agitated with a mixer of the perforated disk type; when the slurry has formed, 10% by weight of powdered TNT of such fineness that all passed through a no. 52 BSS sieve (300 μ opening) is added slowly; after further agitation, the thickened melt is poured,"

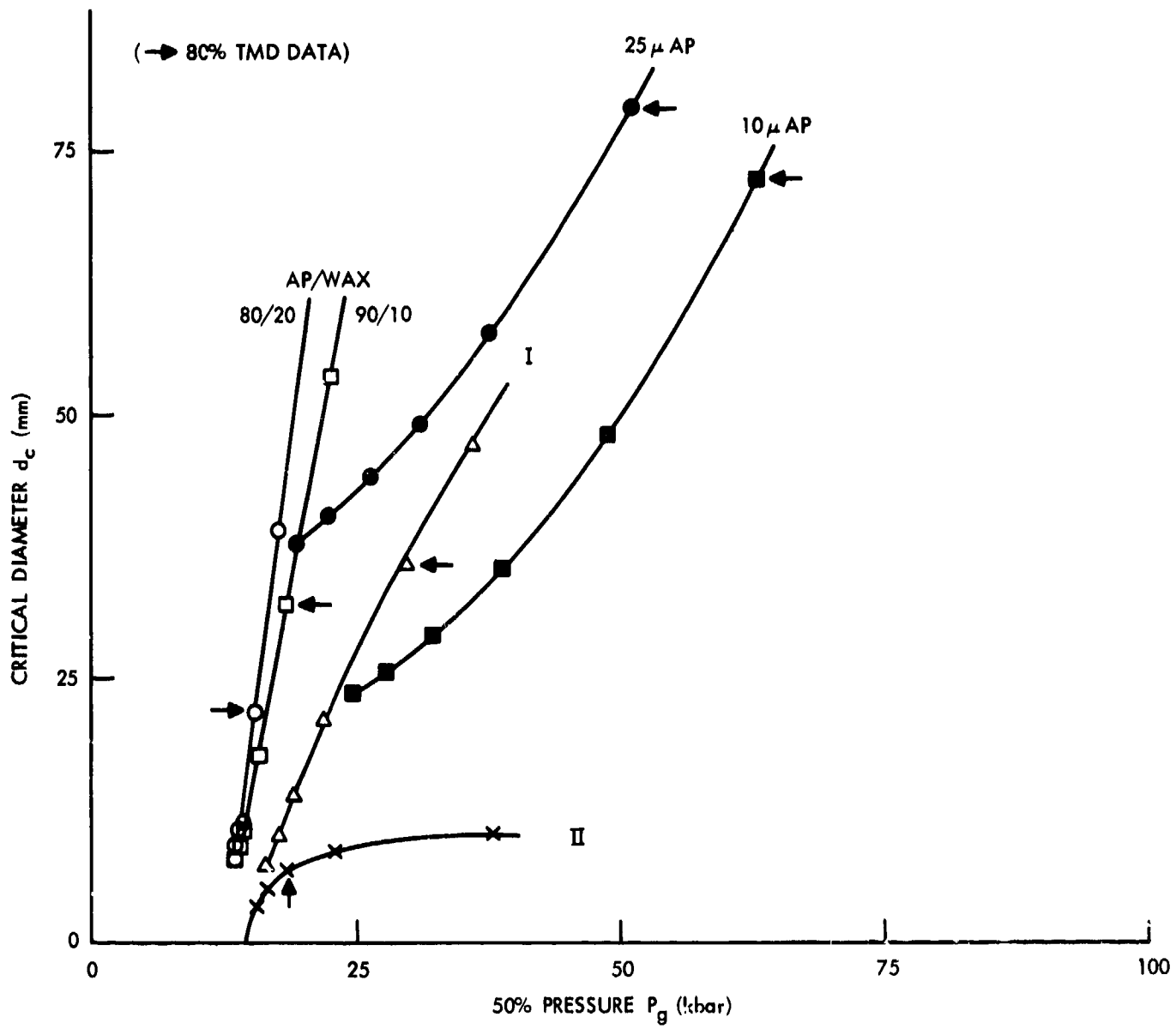

FIGURE 40 RELATIONS d_c VS P_g FOR GROUP 2 HE. (REF. 28)
(I AP/Aℓ /WAX, 62.5/18.75/18.75; II AP/Aℓ /WAX/HMX, 50/15/15/20)

Table 5

Critical Diameter and LASL LSGT Data for Essentially Voidless Charges

HE	ρ_o g/cm^3	%TMD	d_c, mm	Ref.	ρ_o g/cm^3	%TMD	L in. x ...
c-Comp B 63/36/1 RDX/TNT/Wax	1.700/ 1.742	97.6	4.28 ±0.06	14	1..10 1.714	97.7 97.8	180* 170 64.5%RDX
PBX9404 94/3/3 HMX/NC/CEF	1.846/ 1.865	99.0	1.18 ±0.02	14	1.847	99.0	220
c-Cyclotol 77/23 RDX/TNT	1.740/ 1.755	99.1	6.0 ±1.2	14	1.734- 1.756	97.8- 99.2	172 see Table 2 ±8
c-Baratol 24/76 TNT/$Ba(NO_3)_2$	2.619/ 2.63	99.6	43.2 ±5	14	2.597	98.6	107
X-0219 90/10 TATB/Kel F 800	1.9..3/ 1.946	98.4	15.0 ±1.0	14	1.920 1.920		60-62 58±2 Ref. 65
p-TNT	1.62/ 1.654	97.9	2.62 ±0.56	14	1.595 1.627	96.4 98.4	204 pressed at 25°C 194 pressed at 75°C
c-TNT	1.625	98.2	22.0- 25.4	36,38	1.615	97.6	111
			26.9 ±0.1	21			
c-Tritonal 80/20 TNT/Al	~1.73	96.5	18.3 ±1.1	21	1.792	100	87

*64%RDX, vac. cast.

c cast
p pressed

Table 6

Critical Diameter and NSWC LSGT Data for Essentially Voidless Charges

Material	d_c, mm	Ref.	ρ_o g/cm^3	%TMD	L_g in.x10^2	
Cast HE						
TNT	22. -25.4, 26.6±0.1	36,21	1.61	97.3	133	
Tritonal 80/20	18.3±1.1	21	~1.73	96.8	120	
Cyclotol 75/25	8.1±0.3	21	1.75	99.0	182	No. 904
60/40	6.2±0.2	21	1.71	98.6	209*	
Octol 65/35	6.1±0.1	21	1.78	98.9	214	
Pentolite 50/50	6.7±0.5	21	1.67	97.7	278±6	
Picratol 52/48 Ammonium picrate/TNT	13.9	21	-	-	148	
Amatex-20, 40/40/20 TNT/AN/RDX	17.0±1.0	14	1.60	93.6	185±2	No. 889
HBX-1, 40/38/17/5 RDX/TNT/Al/Wax	>6.4	30	~1.72	95.9	154	
PBX-3 AP/Al/NC/METN/TEGD	14.0/16.5	66	1.86	-	89±1	
-5 AP/Al/HEX	38.1/44.5	66	1.86	-	108±3	
OIO d. b. propellant	50/58	67	--	-	16	

Pressed HE

	ρ_o, g/cm^3	%TMD	d_c, mm	Ref.	ρ_o g/cm^3	%TMD	L_g in.x10^2	
DATB	1.800	97.9	5.3	25	1.80	97.9	136	
TATB	1.802	92.7	13	25	1.82	94.6	78	
TNT	1.62	97.9	2.62±0.56	29,14	Interpolated		181	
PBX9404-03	1.865	99.0	1.18±0.02	14	1.77	94.9	235	
DNT (10μ)	1.510	99.3	25.4	2	1.50	98.7	24	(150μDNT)**
NQ (HBD)	1.62	91.0	36.5/38.1	68	Interpolated		42	

*Comp B, 60/40/1 at 1.70 g/cm^3 (98.8%TMD) had value of 201.
**Value therefore high for smaller particle sized DNT.

Procedure No. 2 is that which NSWC uses to produce "creamed cast TNT", its customary cast TNT. Consequently, in Table 4 Cybulski's value for "poured-cloudy" TNT is used instead of the value of his so-called "creamed" TNT. Unfortunately, Campbell & Engelke[14], after treating the data for the latter, labeled it "creamed" without any explanation. It is not surprising that the value of d_c they obtained was about the same as that they derived from the Stesik and Akimova data obtained from TNT cast in water-cooled molds (hence, rapidly cooled to produce very small grains); it is also about a third of the values for creamed cast TNT quoted in Table 4.

In Figure 41, the data of Table 5 are plotted ln d_c vs LSGT value L_g. Squares are used for pressed charges, of which there were three, and circles for cast charges. It is evident that no single line fits all the data. If the points for tritonal and X0219 are omitted, a straight line fits the six remaining data points moderately well. However, there is no justification for omitting two points.

When all NSWC LSGT values are used for a similar comparison, the results are somewhat different -- possibly because the data are more extensive. Table 6 contains the available data which are plotted in Fig. 42. Interestingly enough, a single line would encompass (with moderate scatter) all six pressed charges as well as two plastic bonded castings. However, all of the TNT based castings would require another quite distant parallel line and even then have several points off by an appreciable amount. Hence, neither LASL nor NSWC data indicate a general relationship between ln d_c and L_g.

For some time now a group at Ballistics Research Laboratories, studying initiation of explosives by projectile impact, have treated ignition (first flash of light observed) and buildup of reaction to propagation (monitored by pressure-time and velocity-time data at the fronts) as separable phenomena[69-71].

[69] Frey, R., Howe, P., Timble, J., and Melani, G., "Initiation of Explosive Charges by Projectile Impact," ARBRL-TR-02176, Jun 1979.

[70] Taylor, B. C. and Ervin, L. H., "Separation of Ignition and Buildup to Detonation in Pressed TNT," Sixth Symposium (International) on Detonation, ONR ACR-221, Gov. Print. Office, Washington, D.C., 1978, pp 3-10.

[71] Howe, P., Frey, R., Taylor, B., and Boule, V., "Shock Initiation and the Critical Energy Concept," ibid, pp 11-19.

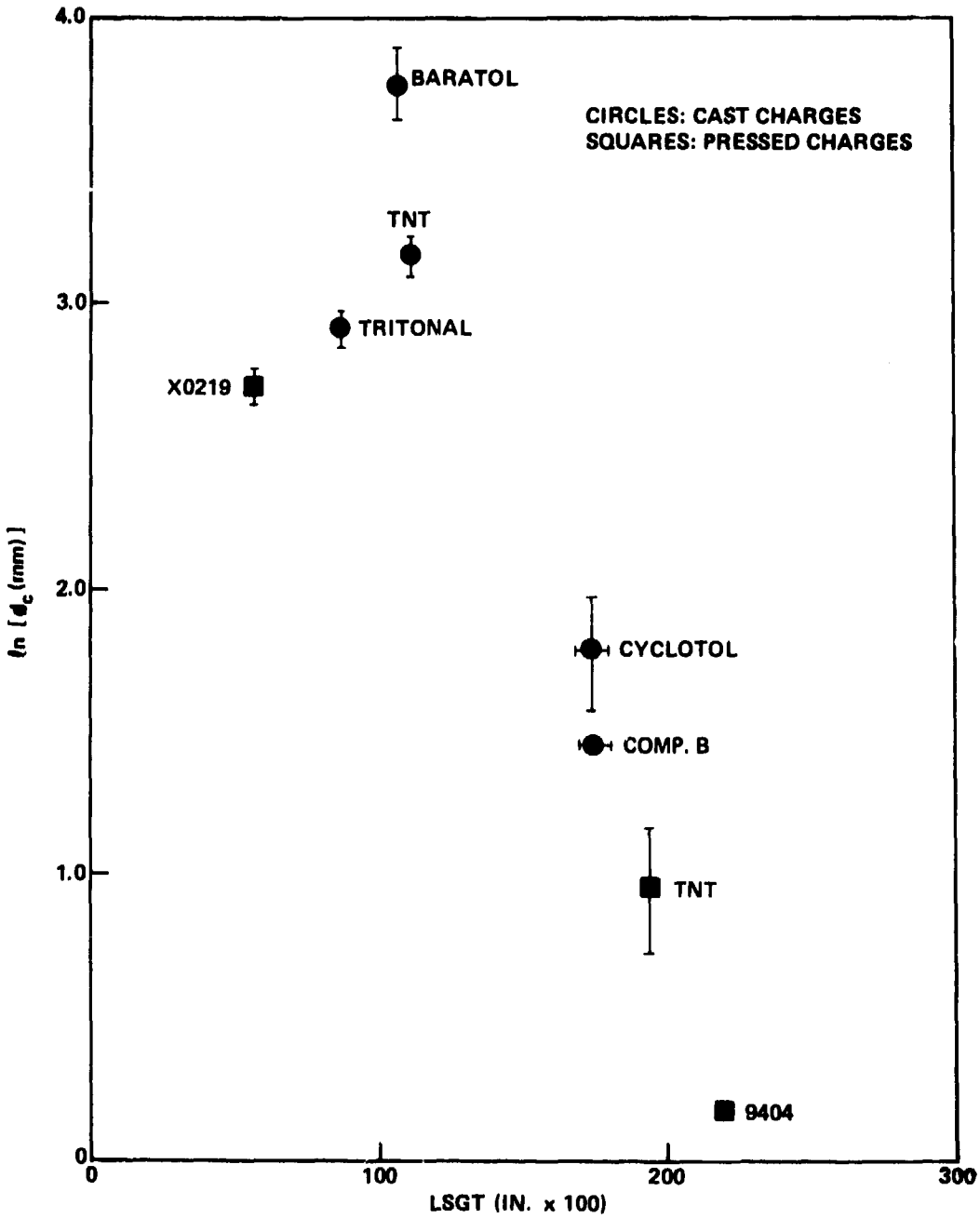

FIGURE 41 Ln d_c VS. L_g WITH LASL LSGT VALUES

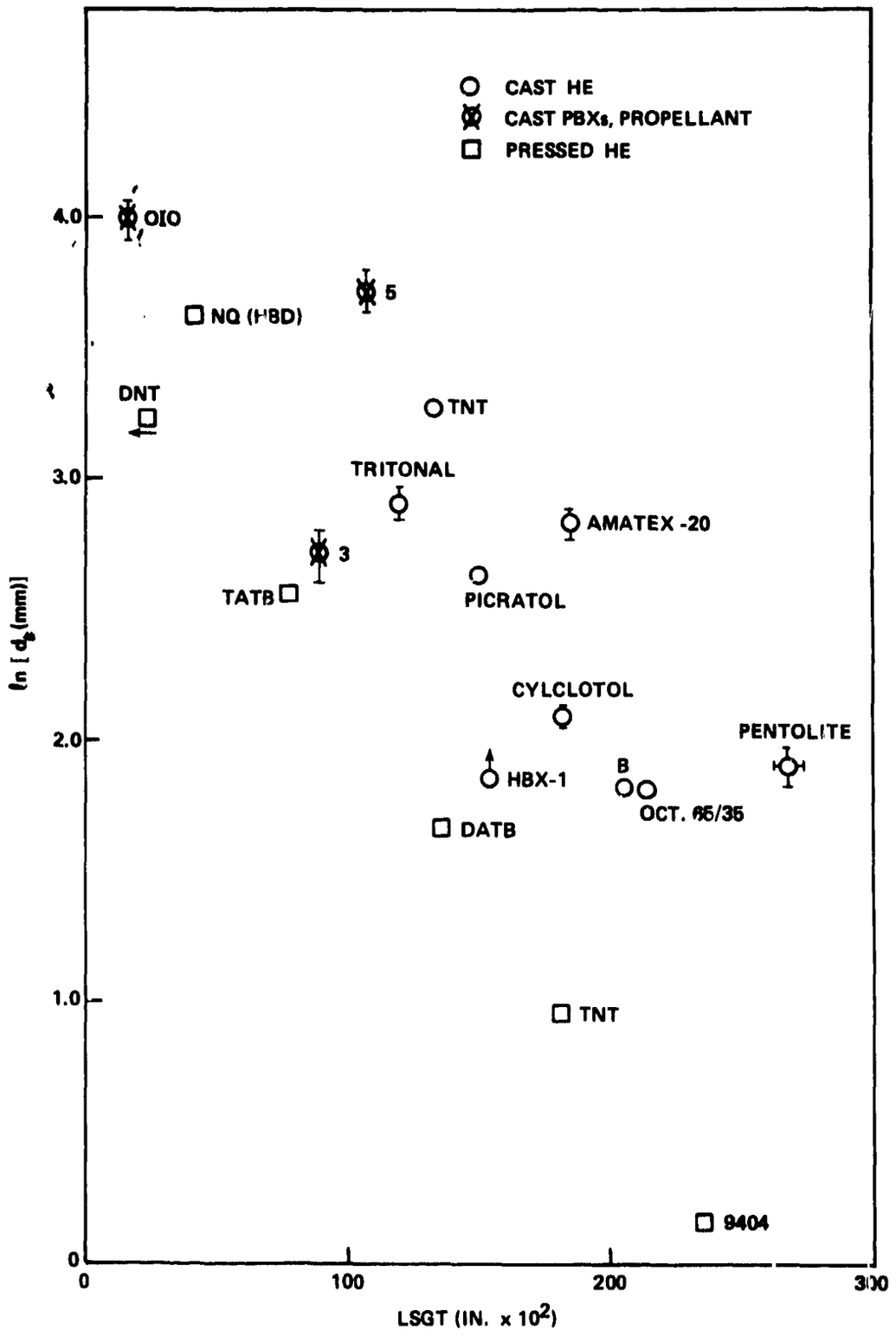

FIGURE 42 Ln d_c VS. L_g WITH NSWC LSGT VALUES

They have shown that some variables have opposite effects on the two, e.g. a large particle size increases the ease of ignition but decreases the ability of the reaction to build up. E. Lee et al.[72] have treated initiation of heterogeneous explosives theoretically as an ignition followed by growth of combustion at the ignited "hot spots". They have had success with PBX 9404, a voidless plastic bonded HE, in quantitative agreement between predicted and experimental values of P-t, u-t in the growth region[73].

If the gap test is carried out at $d \geq 3d_c$, it will be under experimental conditions so favorable to reaction growth and propagation that it can be considered a test of ignitability under shock. Similarly, if critical diameter measurements are made with a donor considerably more energetic than the test explosive to assure ignition under shock, the determination of d_c can be considered a qualitative inverse measure of the ease of reaction build up and propagation. The above is an oversimplified picture, of course. If ignition is by hot spot formation, as is currently believed, then the more hot spots formed, the stronger the ignition and the buildup and propagation. But that assumes the usual transport processes operating throughout. Obviously, if detonation is achieved, the propagation will be hydrodynamic and independent of the initial density of preformed hot spots. Thus hydrodynamic propagation in Group 1 HE vs high pressure burning surface reactions in Group 2 HE could explain the porosity reversal of trends of d_c vs P_{ci} in Fig. 37. Hot spot formation in porous HE could explain the reversal of the particle size effect in Fig. 37 as well as that caused by addition of Al.

---

[72] Green, L., Nidick, E., Lee, E., and Tarver, C., "Reactions in PBX-9404 from Low Amplitude Shocks," Behavior of Dense Media Under High Dynamic Pressures, CEA Paris, 1978; pp 115-126.

[73] Lee, E., "Initiation of Explosives and Propellants," presentation at NSWC/WOL, 5 Jun 1980.

SUMMARY

The value of the critical diameter d_c is determined by charge temperature, initial particle size, density, confinement, composition, and the nature of the HE -- particularly its C-J and von Neumann pressures. Since detonation must be achieved in measuring d_c, a shock must be formed and the shock sensitivity of the material must have a role.

The value of the critical initiating pressure P_{ci}, an inverse measure of shock sensitivity, is a function of charge temperature, initial particle size, density, test dimensions, confinement, composition and the nature of the material -- particularly its d_c and function d/d_c.

The "shock sensitivity" of an explosive cannot be described by a single value such as P_{ci}. Shock sensitivity encompasses all of the complex reactions of the explosive to many different shock conditions. Such reactions are manifested by the phenomenon of failure diameter for propagation of detonation as well as by the critical initiation pressures for shock to detonation transition observed in the numerous gap, booster, projectile, and wedge experiments. A complete description of an explosive's sensitivity to shock should encompass, therefore, not only the thresholds for initiation under transient conditions but also the threshold for propagation under steady state conditions. Moreover, it should account for the large effect of the physical state of the explosive on both thresholds. The relationships between these many aspects of shock sensitivity are complex and cannot be simply stated.

When P_{ci} is measured in two different gap tests, the two sets of values obtained from a group of the same HE charges, identically prepared, correlate well provided geometry and conditions of the two tests are similar. Wedge test results and shock-to-detonation transition studies on cylindrical charges of cast DINA showed strong similarities. It appears that the standard LSGT values lie on the low pressure end of the curve, reciprocal run length vs initiating pressure, defined by the wedge test data.

Although d_c and P_{ci} are obviously interdependent, this fact does not dominate the effects of other variables to produce a general relation between only these two parameters. Instead of d_c, it is sometimes more convenient to use critical density at a given diameter for porous explosives. The emphasis on d_c and P_{ci} is such that other critical parameters (e.g. critical density, particle size and temperature) are apt to be ignored.

REFERENCES

1. Price, D., "Shock Sensitivity, A Property of Many Aspects," 5th Symposium (International) on Detonation, ONR ACR-184, U.S. Gov. Printing Office, Washington, D. C., 1972; pp 207-217.
2. Price, D., Erkman, J. O., Clairmont, Jr., A. R., and Edwards, D. J., "Explosive Characterization of Dinitrotoluene," Combust. Flame, Vol. 14, 1970, pp 145-148.
3. Price, D., Clairmont, Jr., A. R., and Jaffe, I., "Explosive Behavior of Ammonium Perchlorate," Combust. Flame, Vol. 11, No. 5, 1967, pp 415-425. Also ibid. Vol. 13, No. 1, 1969, pp 104-108.
4. Coleburn, N. L. and Liddiard, Jr., T. P., "Hugoniot Equations of State of Several Unreacted Explosives," J. Chem. Phys., Vol. 44, No. 5, 1966, pp 1929-1936.
5. Khariton, Yu. B. and Rozing, V. O., Dokl AN SSSR, Vol. 26, 1940, p. 360. Through Ref. 7 and 8.
6. Khariton, Yu. B., Collection: "Problems of the Theory of Explosives," Izd-vo AN SSSR, Moscow, 1947. Through Ref. 7 and 8.
7. Dremin, A. N., Savrov, S. D., Trofimov, V. S., and Shvedov, K. K., "Detonation Waves in Condensed Media," Izd-vo Nauka, Moscow, 1970. Translation AD 751417.
8. Dremin, A. N. and Trofimov, V. S., "Nature of the Critical Detonation Diameter of Condensed Explosives," Combustion, Explosion, and Shock Waves, Vol. 5, No. 3, 1969, pp. 208-12.
9. Rybanin, S. S., "Effect of Inhomogeneties in an Explosive on the Critical Detonation Diameter," PMTF, Vol. 10, No. 4, 1969, pp 141-144. Through a translation journal.
10. Kravtsov, V. V. and Silvestrov, V. V., "Effect of Low Temperature on Detonation Parameters of Cast Trotyl," Combustion, Expl. and Shock Waves, Vol. 15, No. 3, 1979, pp 387-390.

REFERENCES (Cont.)

11. Jones, H., "The Theory of the Dependence of the Rate of Detonation of Solid Explosives on the Diameter of the Charge," Proc. Roy. Soc., Vol. A189, 1947, p. 415.
12. Eyring, H., Powell, R. E., Duffey, G. H., and Parlin, R. H., "The Stability of Detonation ", Chem. Revs., Vol. 45, 1949, p. 69.
13. Malin, M. E., and Campbell, A. W., "Particle-Size Effects in Explosives at Finite and Infinite Diameters," J. Appl. Phys. Vol. 28, 1957, pp 63-69. Also Malin, Campbell and Mautz, "Particle Size Effect in One- and Two-Component Explosives," 2nd ONR Symposium on Detonation, 1955, pp 360-381.
14. Campbell, A. W. and Engelke, R., "The Diameter Effect in High Density Heterogeneous Explosives," Sixth Symposium (International) on Detonation, ACR 221, ONR, U.S. Gov. Printing Office, Washington, 1978; pp 642-663.
15. Wood, W. W. and Kirkwood, J. G., "Diameter Effect in Condensed Explosives. The Relation between Velocity and Radius of Curvature of the Detonation Wave," J. Chem. Phys., Vol. 22, No. 11, 1954, pp 1920-23.
16. Cook, M. A., "The Science of High Explosives," Reinhold, New York, 1958.
17. Dubnov, L. V., "Losses in a Detonation Wave," Russian J. Chem. Phys., Vol. 30, No. 10, 1960, pp 1124-25.
18. Evans, M. W., "Detonation Sensitivity and Failure Diameter in Homogeneous Condensed Materials," J. Chem. Phys., Vol. 36, No. 1, 1962, p. 193.
19. Rempel, G. G., collection: "Explosives," No. 52/9, 39, through Ref. 7.
20. Chaiken, R. F. and Edwards, John C., "A Kinetic Lattice Approach to Detonation in Heterogeneous Explosives," Sixth Symposium (International) on Detonation, ACR 221, ONR, U.S. Gov. Print. Office, Washington, D.C., 1978, pp 344-351.
21. Jaffe, I. and Price, D., "Determination of the Critical Diameter of Explosive Materials," ARS Journal, Vol. 32, 1962, pp 1060-1065.
22. Belyaev, A. F. and Sukoyan, M. K., "Detonability of Some Explosives with Increase in External Pressure," Comb., Expl., and Shock Waves, Vol. 3, No. 1, 1967, pp 11-13.
23. Urizar, M. J., Peterson, S. W., and Smith, L. C., "Detonation Sensitivity Tests," LA-7193-MS, April 1978.

REFERENCES (Cont.)

24. Walton, J. and Weston, A., Lawrence Livermore Lab., private communication, Oct 1979.
25. Coleburn, N. L. and Drimmer, B. E., "The Explosive Properties of the Amino-Substituted Symmetrical Trinitrobenzenes," NOLTR 63-81, May 1963.
26. Bobolev, V. K., "Limiting Diameters of Charges of Chemically Homogeneous Substances,", Dokl. Akad. Nauk SSSR, JPRS: 4026, Vol. 57, 1947, p. 789.
27. Price, D., "Contrasting Patterns in the Behavior of High Explosives," Eleventh Symposium (International) on Combustion, Combustion Inst., Pittsburgh, 1967, pp 693-702.
28. Price, D., Clairmont, A. R., Jr., and Erkman, J. O., "NOL Large Scale Gap Test III," NOLTR 74-40, 8 Mar 1974.
29. Stesik, L. N. and Akimova, L. N., "An Indirect Method of Estimating Reaction Zone Width of a Detonation Wave," Russ. J. Phys. Chem., Vol. 33, No. 8, 1959, pp 148-151.
30. Roslund, L. A., and Coleburn, N. L., "Hydrodynamic Behavior and Equation of State of Detonation Products Below the Chapman-Jouguet State," Fifth Symposium (International) on Detonation, ONR Rept. ACR 184, U.S. Gov. Print. Office, Washington, D. C., 1972, p. 523.
31. Price, D., Liddiard, T. P., Jr., and Drosd, R. D., "The Detonation Behavior of Hydrazine Mononitrate," NOL TR 66-31, April 1966.
32. Yakovleva, G. S., Kurbangalina, R. Kh., and Stesik, L. N., "Detonation Properties of Ammonium Azide," Combust., Expl., and Sh. Waves, Vol. 13, No. 3, 1977, pp 405-7.
33. Yakovleva, G. S., Kurbangalina, R. Kh., and Stesik, L. N., "Rate of Detonation of Hydrazonium Azide, ibid, Vol. 10, No. 2, 1974, pp 270-4.
34. Gor'kov, V. A. and Kurbangalina, R. Kh., "Some Data Concerning the Detonation Ability of Ammonium Perchlorate," Combust., Explosions, and Shock Waves, Vol. 2, No. 2, 1966, p. 12.
35. Akimova, L. N. and Stesik, L. N., "Detonation Capacity of Perchlorate Explosives," Combust. Expl. and Shock Waves, Vol. 12, No. 2, 1976, pp 247-251.
36. Cybulski, W. B., Payman, W., and Woodhead, D. W., "Explosion Waves and Shock Waves VII. The Velocity of Detonation in Cast TNT," Proc. Roy. Soc. (London), Vol. 197A, 1949, pp 51-72.

REFERENCES (Cont.)

37. Belyaev, A. F. and Kurbangalina, R. Kh., "Effect of Initial Temperature on Critical Diameter of Nitorglycerin and Trinitrotoluene," Russian J. Phys. Chem., Vol. 34, No. 3, 1960, pp 285-9.

38. Price, D., Jaffe, I., and Roberson, G. E., "Shock Sensitivity of Solid Explosives and Propellants," Ind. chim. Belge, 1967, No. 32 (Spec. No.), pp. 506-510.

39. Price, D., and Clairmont, Jr., A. R., "Explosive Behavior of Simplified Propellant Models," Combust. Flame, Vol. 29, 1977, pp 87-93.

40. Dimza, G. V., "Critical Detonation Diameter for an Explosive Containing an Inert-Additive," Comb., Expl. and Shock Waves, Vol, 12, No. 2, 1976, pp 244-47.

41. Apin, A. Ya. and Stesik, L. N., "The Chemical Reaction Mechanism in the Detonation of Explosives," J. Practical Mechanics & Tech. Physics, No. 2, 1965, pp 142-145.

42. Shvedov, K.K., Aniskin, A. I., Il'in, A. N., and Dremin, A. N., "Detonation of Highly Diluted Porous Explosives I. Effect of Inert Additives on Detonation Parameters," Comb., Expl. and Shock Waves, Vol. 16, No. 3, 1980, pp 324-331.

43. Kurbangalina, R. Kh. and Patronova, L. I., "Effect of a Steel Sheath on the Critical Detonation Diameter of Condensed Explosives," Comb., Expl., and Shock Waves, Vol. 12, No. 4, 1976, pp 587-90.

44. Hubbard, H. W. and Johnson, M.H., "Initiation of Detonations." J. Appl. Phys., Vol. 30, No. 5, 1959, pp 765-69.

45. Brown, S. M. and Whitbread, E. G., "The Initiation of Detonation by Shock Waves of Known Duration and Intensity," Les Ondes de Detonation, Edition du Centre National de la Recherche Scientifique, Paris, 1962, pp 69-80.

46. Jacobs, S. J., Liddiard, T. P., and Drimmer, B. E., "The Shock-to-Detonation Transition in Solid Explosives," Ninth Symposium (International) on Combustion, Academic Press, N.Y.C., 1963, pp 517-529.

47. Price, D. and Petrone, F. J., "Detonation Initiated by High-Pressure Gas Loading of a Solid Explosive," J. App. Phys., Vol. 35, No. 3, 1964, pp 710-714.

48. Afanasenkov, A. N. and Voskoboinikov, I. M., "Shock-Ignition Sensitivity of Ballistite," Comb. Expl. Shock Waves, Vol. 9, No. 2, 1973, pp 331-332.

REFERENCES (Cont.)

49. Erkman, J. O., Edwards, D. J., Clairmont, A. R., Jr., and Price, D., "Calibration of the NOL Large Scale Gap Test; Hugoniot Data for Polymethyl Methacrylate," NOLTR 73-15, Apr 1973.
50. Price, D., "Large Scale Gap Test: Interpretation of Results for Propellants," NAVWEP 7401, Mar 1961.
51. Jaffe, I., Toscano, J., and Price, D., "Behavior of Plexiglass under Shock Loading by a Tetryl Donor," NOLTR 64-66, 2 Jul 1964.
52. Walker, F. E., and Wasley, R. J.,"Critical Energy for Shock Initiation of Heterogeneous Explosives," Explosivstoffe, Vol. 17, No. 1, 1969, p. 9.
53. Kamegai, M. and Erkman, J. O., "Numerical Analysis of a Diverging Shock Wave in Cylinders of Plexiglas," Fifth Symposium (International) on Detonation, ONR ACR-184, U.S. Gov. Print. Office, Washington, D.C., 1972, pp 477-485.
54. Jaffe, I. and Clairmont, A. R., Jr., "The Effect of Configuration and Confinement on Booster Characteristics," NOLTR 65-33, 13 Apr 1965.
55. Price, D., Toscano, J. P., and Jaffe, I., "Development of the Continuous Wire Method. Progress Report III, "Measurements in Cast DINA," 20 Apr 1967.
56. Moulard, H., "Critical Conditions for Shock Initiation of Detonation by Small Projectile Impact," Preprints of the Seventh Symposium (International) on Detonation, Vol. 1, 1981, pp 182-189.
57. Bowman, A. L., Kershner, J. D. and Mader, C. L., "A Numerical Model of the Gap Test," LA-8408, Oct 1980.
58. Piacesi, D., Jr., "Numerical Hydrodynamic Calculations of the Flow of the Detonation Products from a Point-Initiated Explosive Cylinder," NOLTR 66-150, Jan 1967.
59. Edwards, D. J., Erkman, J. O. and Price, D., "The Measurement of Particle Velocity in Pressed Tetryl," NOLTR 72-83, Aug 1972.
60. de Longueville, Y., Fauquignon, C., and Moulard, H., "Initiation of Several Condensed Explosives by a Given Duration Shock Wave," Sixth Symposium (International) on Detonation, ONR ACR-221, U.S. Gov. Print. Office, Washington, D. C., 1978, pp 105-114.

REFERENCES (Cont.)

61. Jackson, R. K., Green, L. G., Bartlett, R. H., Hofer, W. W., Kramer, P. E., Lee, R. S., Nidick, E. J., Jr., Shaw, L. L., and Weingart, R. C., "Initiation and Detonation Characteristics of TATB," ibid. pp 755-765.

62. Ramsay, J. B. and Popolato, A., "Analysis of Shock Wave and Initiation Data for Solid Explosives," Fourth Symp. (Int.) on Detonation, ONR, ACR-126, U.S. Gov. Print. Office, Washington, D. C., 1967, pp 233-238.

63. Seely, L. B., "A Proposed Mechanism for Shock Initiation of Low Density Granular Explosives," Proc. Fourth Elec. Initiation Symposium, Franklin Institute, Phila. 1963, Paper 27 of Rept. EIS-A-2357.

64. Liddiard, T. P., "The Initiation of Burning in High Explosives by Shock Waves," Fourth Symposium (Int.) on Detonation, ONR ACR-126, U.S. Gov. Print. Office, Washington, D. C., 1967, pp 487-495.

65. Dobratz, B. M., et al., "The Sensitivity of Triaminotrinitrobenzene (TATB) and TATB Formulations: Summary Report," Table C4, UCID-17808, Sep 1978.

66. Toscano, J., Lee, T., and Jaffe, I., "Some Explosive Characteristics of Two PBXW Charges," NOLTR 66-7, May 1966.

67. Jaffe, I., and Roberson, G. E., "The Critical Diameter and Detonation Velocity of Double Base Propellants," NOLTR 65-112, Aug 1965.

68. Price, D. and Clairmont, A. R., Jr., "Explosive Behavior of Nitroguanidine," 12th Symposium (Int.) on Combustion, The Combustion Institute, Phttsburgh, 1969, pp 761-770.

69. Frey, R., Howe, P., Timble, J., and Melani, G., "Initiation of Explosive Charges by Projectile Impact," ARBRL-TR-02176, June 1979.

70. Taylor, B. C. and Ervin, L. H., "Separation of Ignition and Buildup to Detonation in Pressed TNT," Sixth Symposium (Int.) on Detonation, ONR ACR-221, Gov. Print. Office, Washington, D. C., 1978, pp 3-10.

71. Howe, P., Frey, R., Taylor, B., and Boyle, V., "Shock Initiation and the Critical Energy Concept," ibid, pp 11-19.

72. Green, L., Nidick, E., Lee, E., and Tarver, C., "Reactions in PBX-9404 from Low Amplitude Shocks," Behavior of Dense Media Under High Dynamic Pressures, CEA Paris, 1978, pp 115-126.

73. Lee, E., "Initiation of Explosives and Propellants," presentation at NSWC/WOL, 5 June 1980.

DISTRIBUTION

	Copies
Chief of Naval Material Washington, DC 20360	
Commander Naval Air Systems Command Attn: AIR-350 AIR-330 Department of the Navy Washington, DC 20361	
Commander Naval Sea Systems Command Attn: SEA-09G32 SEA-03B SEA-62R SEA-62R2 SEA-62R3 SEA-62R32 SEA-64E Department of the Navy Washington, DC 20362	2
Director Strategic Systems Project Office (PM-1) Attn: SP-2731 (E. L. Throckmorton, Jr.) John F. Kincaid Department of the Navy Washington, DC 20376	
Office of Naval Research Attn: Rear Admiral L. S. Kollmorgen ONR-473 (R. Miller) ONR-741 (Technical Library) Department of the Navy Arlington, VA 22217	

DISTRIBUTION (Cont.)

Copies

Office of Naval Technology
Attn: MAT-07P (J. Enig)
Department of the Navy
Arlington, VA 22217

Commander
Naval Weapons Center
Attn: Technical Library
Code 3264
Code 3205 (C. Thelin)
Code 32052 (L. Smith)
Code 388 (R. L. Derr, T. Boggs)
Code 383 (H. D. Mallory)
Code 3835 (K. Graham)
China Lake, CA 93555

Director
Naval Research Laboratory
Attn: Technical Information Section 2
Washington, DC 20375

Office of Chief of Naval Operations
Operations Evaluation Group (OP03EG)
Washington, DC 20350

Director
Office of the Secretary of Defense
Advanced Research Projects Agency
Washington, DC 20301

Commanding Officer
Naval Weapons Station
Attn: R&D Division
Code 50
Yorktown, VA 23691

Commanding Officer
Naval Propellant Plant
Attn: Technical Library
Indian Head, MD 20640

Commanding Officer
Naval Explosive Ordnance Disposal Facility
Attn: Information Services
Indian Head, MD 20640

DISTRIBUTION (Cont.)

Copies

[illegible]ell Aircraft Company
[illegible] M. [illegible]chimmel
[illegible]ox 516
[illegible]uis, MO 63166

Commanding Officer
Naval Ammunition Depot
Crane, IN 47522

Commanding Officer
Naval Underwater Systems Center
Attn: LA 151-Technical Library
Newport, RI 02840

Commanding Officer
Naval Weapons Evaluation Facility
Attn: Code AT-7
Kirtland Air Force Base
Albuquerque, NM 87117

Commanding Officer
Naval Ammunition Depot
Attn: QEL
Concord, CA 94522

Superintendent Naval Academy
Attn: Library
Annapolis, MD 21402

Naval Plant Representative Office
Strategic Systems Project Office
Lockheed Missiles and Space Company
Attn: SPL-332 (R. H. Guay)
P. O. Box 504
Sunnyvale, CA 94088

Hercules Incorporated
Allegany Ballistics Laboratory
Attn: Library
P. O. Box 210
Cumberland, MD 21502

AMCRD
5001 Eisenhower Avenue
Alexandria, VA 22302

DISTRIBUTION (Cont.)

	Copies
Redstone Scientific Information Center U. S. Army Missile Command Attn: Chief, Documents Redstone Arsenal, AL 35809	2
Commanding Officer Army Armament Research and Development Command Energetic Materials Division Attn: Louis Avrami, DRDAR-LCE Dover, NJ 07801	
Commanding General Attn: BRL Library DRDAR-BLT (P. Howe) Aberdeen Proving Ground, MD 21005	
Commanding Officer Harry Diamond Laboratories Attn: Library Keith Warner 2800 Powder Mill Road Adelphi, MD 20783	
Armament Development & Test Center DLOSL/Technical Library Eglin Air Force Base, Florida 32542	
Commanding Officer Naval Ordnance Station Louisville, KY 40124	
Director Applied Physics Laboratory Attn: Library Johns Hopkins Road Laurel, MD 20810	
U. S. Department of Energy Attn: DMA Washington, DC 20545	
Research Director Pittsburgh Mining and Safety Research Center Bureau of Mines 4800 Forbes Avenue Pittsburgh, PA 15213	

DISTRIBUTION (Cont.)

	Copies
Director Defense Technical Information Center Cameron Station Alexandria, VA 22314	12
Goddard Space Flight Center, NASA Glenn Dale Road Greenbelt, MD 20771	
Lawrence Livermore National Laboratory University of California Attn: M. Finger E. James E. Lee P. Urtiew C. Tarver P. O. Box 808 Livermore, CA 94550	
Sandia National Laboratories Attn: R. J. Lawrence, Div. 5166 P. O. Box 5800 Albuquerque, NM 87115	
Director Los Alamos National Laboratory Attn: Library R. L. Rabie B. G. Craig H. Flaugh C. Forest P. O. Box 1663 Los Alamos, NM 87544	
Chairman DOD Explosives Safety Board Attn: Dr. T. A. Zoker 2461 Eisenhower Avenue Alexandria, VA 22331	
Aerojet Ordnance and Manufacturing Company 9236 East Hall Road Downey, CA 90241	

DISTRIBUTION (Cont.)

	Copies
Hercules Incorporated Research Center Attn: Technical Information Division B. E. Clouser Wilmington, DE 19899	
Thiokol/Huntsville Division Attn: Technical Library Huntsville, AL 35807	
Shock Hydrodynamics Division Whittaker Corporation Attn: Dr. L. Zernow 4716 Vineland Avenue North Hollywood, CA 91706	2
Stanford Research Institute Attn: D. Curran 333 Ravenswood Avenue Menlo Park, CA 94025	
Thiokol/Wasatch Division Attn: Technical Library P. O. Box 524 Brigham City, UT 84302	
Thiokol/Elkton Division Attn: Technical Library P. O. Box 241 Elkton, MD 21921	
Teledyne McCormick Selph P. O. Box 6 Hollister, CA 95023	
Lockheed Missiles and Space Co., Inc. P. O. Box 504 Sunnyvale, CA 94086	
R. Stresau Laboratory, Inc. Star Route Spooner, WI 54801	
Rohm and Haas Huntsville, Defense Contract Office Attn: H. M. Shuey 723-A Arcadia Circle Huntsville, AL 35801	

DISTRIBUTION (Cont.)

Copies

U. S. Army Foreign Service
and Technology Center
220 7th Street, N.E.
Charlottesville, VA 22901

Princeton Combustion Research Laboratories, Inc.
1041 U. S. Highway One North
Attn: M. Summerfield
N. Messina
Princeton, NJ 08540

Pennsylvania State University
Department of Mechanical Engineering
Attn: K. Kuo
University Park, PA 16802

Ballistic Research Laboratories
Attn: N. Gerri
P. Howe
R. Frey
D. Kooker
Aberdeen Proving Ground, MD 21005

Paul Gough Associates
1048 South Street
Portsmouth, NH 03801

Hercules Incorporated, Bacchus Works
Attn: B. Hopkins
Library 100-H
D. Caldwell 2
P. O. Box 98
Magna, UT 84044

Professor H. Krier
A & A Engineering Department
101 Transportation Building
University of Illinois
Urbana, IL 61801

Chemical Propulsion Information Agency
The Johns Hopkins University
Applied Physics Laboratory
Johns Hopkins Road
Laurel, MD 20810

DISTRIBUTION (Cont.)

	Copies
ITT Research Institute Attn: H. S. Napadensky 10 West 35th Street Chicago, IL 60616	
Erion Associates, Inc. Attn: W. Petray 600 New Hampshire Avenue, Suite 870 Washington, DC 20037	
Brigham Young University Department of Chemical Engineering Attn: Dr. M. W. Beckstead Provo, UT 84601	
Library of Congress Attn: Gift and Exchange Division Washington, DC 20540	4

NSW-NSWC(W)-5605/1 (Rev. 5/79)

TO AID IN UPDATING THE DISTRIBUTION LIST FOR NAVAL SURFACE WEAPONS CENTER, WHITE OAK TECHNICAL REPORTS PLEASE COMPLETE THE FORM BELOW:

TO ALL HOLDERS OF NSWC TR 80-339

By Donna Price, Code R10

DO NOT RETURN THIS FORM IF ALL INFORMATION IS CURRENT

A. FACILITY NAME AND ADDRESS *(OLD) (Show Zip Code)*

NEW ADDRESS *(Show Zip Code)*

B. ATTENTION LINE ADDRESSES:

C.

☐ REMOVE THIS FACILITY FROM THE DISTRIBUTION LIST FOR TECHNICAL REPORTS ON THIS SUBJECT.

D.

NUMBER OF COPIES DESIRED _____

GPO 000-704